Aus dem Institut für Neurophysiologie
der Medizinischen Fakultät Charité – Universitätsmedizin Berlin

DISSERTATION

Dissecting the functions of Synaptotagmin-1 and Synaptotagmin-7 in synaptic transmission

Untersuchung der Funktionen von Synaptotagmin-1 und Synaptotagmin-7 in der Synaptischen Transmission

zur Erlangung des akademischen Grades
Doctor of Philosophy (PhD)

vorgelegt der Medizinischen Fakultät
Charité – Universitätsmedizin Berlin

von

BORIS BOUAZZA AROSTEGUI

Datum der Promotion: 30.11.2023

Table of Contents

List of tables

List of figures

List of abbreviations

AP	Action potential
AZ	Active Zone
Ca^{2+}	Calcium ion
DIV	Days *in vitro*
EPSC	Excitatory postsynaptic current
GABA	γ-Aminobutyric acid
HF	High frequency
ICC	Immunocytochemistry
mEPSC	“miniature” excitatory postsynaptic current
Munc13	Mammalian uncoordinated-13
NA	Numerical aperture
NBQX	2,3-dihydroxy-6-nitro-7-sulphamoyl-benzo(F)quinoxaline
Norm.	Normalized
NT	Neurotransmitter
PL	Phospholipid
PM	Plasma membrane
Pvr	Vesicular release probability
RIM	Rab3-interacting molecule
RIM-BP	RIM-binding protein
RNAi	RNA interference
RRP	Readily releasable pool
RT-PCR	Reverse transcription–polymerase chain reaction
SEM	Standard error of the mean
shRNA	short hairpin RNA
SNARE	Soluble N-ethylmaleimide-sensitive factor attachment protein receptor
SNAP25	Synaptosomal-associated protein, 25kDa
SV	Synaptic vesicle
SYT1	Synaptotagmin-1 protein
Syt1	Synaptotagmin-1 gene
SYT2	Synaptotagmin-2 protein
SYT5/9	Synaptotagmin-5/Synaptotagmin-9 protein
SYT7	Synaptotagmin-7 protein
Syt7	Synaptotagmin-7 gene
VAMP	Vesicle-associated membrane protein
VGLUT1	Vesicular glutamate transporter 1

Abstract

The underlying mechanisms that govern neuronal communication through synaptic transmission have been the object of study for decades. Neurotransmission requires of a presynaptic bouton where specialized secretory organelles, synaptic vesicles (SVs), reside. In the SV secretory pathway, neurotransmitter-filled vesicles are actively localized at specialized zones of the presynaptic plasma membrane and subsequently primed in a fusion ready state. These ready-to-fuse SVs form the readily releasable pool, and their spatial organization is carried out by a set of docking/priming factors that spatially couple calcium-channels and SVs. The fusion step of the SVs with the plasma membrane is tightly controlled by an exocytotic fusion machinery composed by SNARE proteins and a calcium sensor. The neuronal calcium-sensing protein Synaptotagmin-1 (SYT1) is responsible for the temporal precision of fast synchronous fusion in response to local calcium entry through voltage-gated calcium-channels. Upon Ca^{2+}-binding SYT1 reduce the energy barrier between SVs and the plasma membrane, coupling calcium-influx with SV fusion. Experiments performed with genetically modified neurons suggested that SYT1 might play two additional roles, regulating spontaneous neurotransmitter release, clamping the SNARE complex in the absence of an action potential, and priming SVs. In this study, we perform electrophysiological recordings on primary mouse hippocampal glutamatergic neurons to explore how the absence of SYT1 affects neurotransmitter release and how this mechanism evolves during the development of synapses. Furthermore, by the systematic genetic manipulation using lentiviral vectors and immunocytochemistry quantification of SYT1 protein expression levels, we dissect its triple synaptic function, gaining insights into their mechanisms. Recently, another isoform of the synaptotagmin family, Synaptotagmin-7 (SYT7), has been suggested to be involved in neurotransmitter release. Due to the overlapping yet partially independent functions of SYT1 and SYT7, the direct contribution of SYT7 to neurotransmission in the absent of SYT1 is unclear. We report that SYT1 and SYT7 have both redundant and antagonistic roles in different aspects of the SV exocytotic pathway. Finally, this study not only deepens in our understanding on how those two presynaptic proteins operate but also provides with insights into how presynaptic malfunction could be the underlying cause of the cellular pathophysiology of neurodevelopmental disorders.

Zusammenfassung

Die zugrundeliegenden Mechanismen, die die neuronale Kommunikation durch synaptische Übertragung steuern, werden seit Jahrzehnten in zahlreichen Studien untersucht. Die Neurotransmission erfolgt im präsynaptischen Bouton, in dem sich spezialisierte sekretorische Organellen, die synaptischen Vesikel (SVs), befinden. Diese Vesikel, welche mit Neurotransmittern gefüllt sind, werden an spezialisierten Zonen der präsynaptischen Plasmamembran lokalisiert und anschließend in einen fusionsbereiten Zustand gebracht. Diese fusionsbereiten SVs bilden den leicht freisetzbaren Pool, und ihre räumliche Organisation erfolgt durch eine Reihe von Docking/Priming-Faktoren, wodurch Kalziumkanäle und SVs räumlich gekoppelt werden. Der Fusionsschritt der SVs mit der Plasmamembran wird durch eine exozytotische Fusionsmaschinerie, bestehend aus SNARE-Proteinen und einem Kalziumsensor, genauestens kontrolliert. Das neuronale Kalzium-Sensorprotein Synaptotagmin-1 (SYT1) ist für die zeitliche Präzision der schnellen synchronen Fusion als Reaktion auf den lokalen Kalziumeinstrom durch spannungsabhängige Kalziumkanäle verantwortlich. Nach der Kalziumbindung verringert SYT1 die Energiebarriere zwischen SVs und der Plasmamembran und koppelt den Kalziumeinstrom mit der SV-Fusion. Experimente mit genetisch veränderten Neuronen deuten darauf hin, dass SYT1 zwei weitere Rollen haben könnte: es reguliert die spontane Freisetzung von Neurotransmittern, sorgt für die Klemmung des SNARE-Komplexes in Abwesenheit eines Aktionspotenzials und kontrolliert das "Priming" der SVs. In dieser Studie führen wir elektrophysiologische Ableitungen an primären glutamatergen Neuronen des Hippocampus der Maus durch, um zu erforschen, wie sich das Fehlen von SYT1 auf die Freisetzung von Neurotransmittern auswirkt und wie sich dieser Mechanismus während der Entwicklung von Synapsen entwickelt. Durch die systematische genetische Manipulation mit lentiviralen Vektoren und die immunzytochemische Quantifizierung der SYT1-Proteinexpression untersuchen wir die synaptische Funktion von SYT1 und erhalten so Einblicke in ihre Mechanismen. Kürzlich wurde eine weitere Isoform der Synaptotagmin-Familie, Synaptotagmin-7 (SYT7), mit der Freisetzung von Neurotransmittern in Verbindung gebracht. Aufgrund der sich überschneidenden, aber teilweise unabhängigen Funktionen von SYT1 und SYT7 ist der direkte Beitrag von SYT7 zur Neurotransmission in Abwesenheit von SYT1 unklar. Wir berichten, dass SYT1 und

SYT7 sowohl redundante als auch antagonistische Funktionen in verschiedenen Aspekten des exozytotischen Weges der SV haben. Schließlich vertieft unsere Studie nicht nur unser Verständnis der Funktionsweise dieser beiden präsynaptischen Proteine, sondern liefert auch Erkenntnisse darüber, wie eine präsynaptische Fehlfunktion die zugrundeliegende Ursache für die zelluläre Pathophysiologie von neurodegenerativen Erkrankungen sein könnte.

1. Introduction

1.1. Synaptic transmission is exquisitely controlled by a presynaptic molecular machinery

Neuronal communication through synaptic transmission is a rapid and highly regulated process. It requires an efficient fusion of neurotransmitter (NT)-containing synaptic vesicles (SVs) with the presynaptic plasma membrane (PM) (Südhof & Rizo, 2011). The fundamental pathway of synaptic transmission starts with the arrival of an action potential (AP) at the axon terminal that induces the opening of voltage-gated Ca^{2+}-channels (Catterall, 2011; Katz, 1969). The influx of calcium ions (Ca^{2+}) into the neuron triggers the exocytosis of the SVs, releasing their content to the synaptic cleft. Then, neurotransmitters bind to a variety of receptors located at the postsynaptic PM producing a postsynaptic signal (Katz, 1969). This Ca^{2+}-triggered pathway happens in less than one millisecond (Sabatini & Regehr, 1996).

Prior to fusion, SVs are actively located near the PM at specialized release sites, known as active zones (AZs) (Südhof, 2012), and subsequently docked and primed to form the readily releasable pool (RRP) (Kaeser & Regehr, 2017). A SV is considered docked when determined in electron micrographs, is attached to the PM (Hammarlund *et al.*, 2007; Harris & Sultan, 1995; Schikorski & Stevens, 2001), and primed when, functionally assessed, is in a ready-to-fuse state (Rosenmund & Stevens, 1996). The Ca^{2+}-channels must be in the proximity to docked SVs for coupling Ca^{2+}'s inward current with fast exocytosis. An evolutionarily conserved protein complex, formed by RIM (Rab3-interacting molecule), RIM-BP (RIM-binding protein) and Munc13, is probably the main molecular organizer of the AZs by mediating the docking/priming of SVs, recruiting Ca^{2+}-channels next to release sites and, ultimately, controlling NT-release (Augustin *et al.*, 1999; Han *et al.*, 2011; Südhof, 2012; Brockmann *et al.*, 2020; Zarebidaki *et al.*, 2020; Camacho *et al.*, 2021). The formation of a fusiogenic complex integrated by SNARE (soluble *N*-ethylmaleimide sensitive factor (NSF) attachment protein receptor) proteins is essential to overcome the energy barrier that a SV must break before it fuse with the PM (Jahn & Scheller, 2006). The *trans*-SNARE complex consists of four long helical bundle that are aligned in a parallel fashion, one α-helix contributed by Synaptobrevin (also known as VAMP, vesicle-associated membrane protein), one from Syntaxin and two SNAP-25, that during fusion zippers and leads to NT-release (Jahn & Scheller, 2006). Importantly, additional layers of control over the

fusion process are set by molecules such as Complexin (Trimbuch & Rosenmund, 2016).

NT-release occurs synchronously and asynchronously (Kaeser & Regehr, 2014). The synaptic vesicular protein Synaptotagmin-1 (SYT1), first identified as p65 in a monoclonal antibody screen for synaptic proteins (Matthew *et al.*, 1981), orchestrates the fast synchronous release of the NT (Brunger *et al.*, 2018). Functionally, SYT1 is a low-affinity Ca^{2+} sensor that acts in a Ca^{2+}-dependent manner as a phospholipid-binding machine and interacts with SNAREs leading to synchronous NT-release (Fernández-Chacón *et al.*, 2001; Geppert *et al.*, 1994; Zhou *et al.*, 2015, 2017). From a structural point of view, the members of the synaptotagmin family are characterized by an N-terminal transmembrane region, a variable linker and two C-terminal C2 domains with strong similarity to the Ca^{2+}-binding C2 domains of Protein Kinase C (Perin *et al.*, 1990, 1991; Südhof, 2002; Südhof & Rizo, 1996). The two cytosolic C2 domains of SYT1, namely C2A and C2B, are composed of eight-stranded β-sandwiches with three flexible loops emerging on top, where Ca^{2+} ions bind, and four loops at the bottom that interacts with the phospholipids (PL) of the PM (Fernandez *et al.*, 2001; Shao *et al.*, 1996, 1998; Sutton *et al.*, 1995). Although the intrinsic Ca^{2+}-affinity of the protein is low, it is markedly increased by phospholipidic membranes (Radhakrishnan *et al.*, 2009). In fact, when the Ca^{2+} is present, the C2 domains form a ternary complex in which Ca^{2+} is simultaneously ligated by the top loops and the PL headgroups (Fernández-Chacón *et al.*, 2001).

Evidence of SYT1 as the major sensor responsible for synchronous NT-release is extensive. For instance, in *C. elegans, Drosophila* and mammalian synapses in the absence of the *Syt1* gene, AP-evoked synchronous NT-release is drastically impaired (Broadie *et al.*, 1994; Geppert *et al.*, 1994; Maximov & Südhof, 2005; Nishiki & Augustine, 2004b, 2004a; Nonet *et al.*, 1993; Xue *et al.*, 2008; Yoshihara & Littleton, 2002). When a point mutation (R233Q) was introduced into the endogenous *syt1* gene in mice without affecting its three-dimensional structure, it selectively decreased its apparent Ca^{2+}-affinity and caused a corresponding decrease in the Ca^{2+}-sensitivity of NT-release (Fernández-Chacón *et al.*, 2001). Therefore, Ca^{2+}-binding to SYT1 directly determines Ca^{2+}-dependent exocytosis. Whereas it is universally accepted that SYT1 regulates synchronous NT-release, it's under intensive investigation what other synaptic functions SYT1 might perform and how they are mechanistically related to each other.

1.2. Synaptotagmin-1 roles in spontaneous NT-release and docking/priming SVs

In addition to evoked transmission, synapses spontaneously release neurotransmitter quanta at a low frequency (Fatt & Katz, 1952; Kavalali, 2015). Several presynaptic proteins are involved in the regulation of this form of NT-release. For instance, suppression of Complexin increased spontaneous release (Reim *et al.* 2001; Xue *et al.* 2007; Jorquera *et al.* 2012). Likewise, blocking SYT1 or SYT2 isoforms, but not SYT7, functions caused an increase in spontaneous release (Maximov & Südhof, 2005; Pang *et al.*, 2006; Sun *et al.*, 2007; Xu *et al.*, 2009; Lee *et al.*, 2013). In fact, structure/function analysis of the SYT1's C2B domain have suggested that it might act as a "clamp" suppressing the spontaneous release of SVs (DiAntonio & Schwarz, 1994; Littleton *et al.*, 1994; Chicka *et al.*, 2008; Xu *et al.*, 2009; Bacaj *et al.*, 2013). Although the specific mechanism by which SYT1 influences spontaneous NT-release needs to be elucidated, and some contradictory results from *drosophila* to mammalian preparations have to be resolved (Broadie *et al.*, 1994; Geppert *et al.*, 1994; Okamoto *et al.*, 2005; Pang *et al.*, 2006; Yoshihara & Littleton, 2002), it is likely that SYT1 is a regulatory element of this mode of release.

Different studies have suggested that SYT1 might have another role upstream to Ca^{2+}-triggered exocytosis. By using electron microscopy has been reported a decrease in the number of docked vesicles of *Syt1* mutants in different preparations (Jorgensen *et al.*, 1995; Reist *et al.*, 1998; de Wit *et al.*, 2009; Chang *et al.*, 2018; Chen *et al.*, 2021). However, those defects in vesicle docking were suggested to be caused by an overall reduction in the total vesicle number at the synapse (Imig *et al.*, 2014). In relation to the priming function, electrophysiological recordings of SYT1-lacking synapses have reported contradictory results (Bacaj *et al.*, 2015; Geppert *et al.*, 1994; Huson *et al.*, 2020; Liu *et al.*, 2009; Maximov & Südhof, 2005). Besides culturing conditions (Liu et al., 2009), the difficulty in revealing the role of SYT1 in priming SVs also reside in the functional redundancy that exists among the distinct synaptotagmin isoforms (Bacaj *et al.*, 2015; Chen & Jonas, 2017).

1.3. Synaptotagmin-7 roles in synaptic function

The mammalian genome encodes 17 synaptotagmin isoforms and their expression is regulated in a cell-type-specific manner (Chen & Jonas, 2017). Due to its biochemical

properties and cellular localization, SYT7 has been proposed to be the Ca^{2+}-sensor for the slow asynchronous release mode in neurons (Bacaj *et al.*, 2013; Chen & Jonas, 2017; Li *et al.*, 1995). SYT7 shows ~40% sequence identity with SYT1, SYT2 or SYT5/9 isoforms (Maximov *et al.*, 2008), and, while SYT1 and SYT2 are on the SV membrane, SYT7 is aboundingly expressed and located at the PM (Li *et al.*, 2017). This isoform binds Ca^{2+} with high affinity (Sun *et al.*, 2007; Maximov *et al.*, 2008), has the slowest Ca^{2+}-kinetics (Hui *et al.*, 2005), and a stronger membrane affinity than SYT1 (Tran *et al.*, 2019). Supporting the role of SYT7 in exocytosis are experiments performed on non-neuronal cells where deletion of *syt7,* or inactivation of Ca^{2+}-binding to its C2B domain, impairs Ca^{2+}-induced chromaffin granule exocytosis (Schonn *et al.*, 2008), or insulin-containing vesicles exocytosis in pancreatic cells (Gustavsson *et al.*, 2008). At the central nervous system, first experiments performed on inhibitory neurons displayed normal synaptic response properties when *syt7* gene was deleted, arguing against a role in SV exocytosis (Maximov *et al.*, 2008). But a number of recent studies have showed that SYT7 could be a regulator of different forms of synaptic plasticity (Chen *et al.*, 2017; Fujii *et al.*, 2021; Jackman *et al.*, 2016; Turecek & Regehr, 2018; Wen *et al.*, 2010). In addition, while experiments blocking SYT7 expression didn't show an effect in spontaneous NT-release, when SYT7 was overexpressed in SYT1-lacking neurons, the enhanced spontaneous release phenotype was reduced (Bacaj *et al.*, 2013; Liu *et al.*, 2014), remaining unsolved what role SYT7 plays in spontaneous NT-release. Interestingly, the double deletion of *syt1* and *syt7* genes in neurons led to a strong reduction in the number of primed vesicles (Bacaj *et al.*, 2015). Those results suggest that SYT7 may be able to prime or clamp SVs, although how it may perform such functions remain unknown.

1.4. Research Question

We aim to clarify whether SYT1 plays a triple role in the SV exocytotic pathway and how those roles relate to each other. To dissect SYT1's functions and better understand their underlaying molecular mechanisms we studied the relation of SYT1 expression levels at the presynaptic terminal and each SYT1 synaptic function. Also, we will reconcile contradictory results previously reported by studying how synaptic responses of SYT1-lacking neurons during the development of synapses and investigate whether the SYT1's functions are distinctly essential at different culture stages. Furthermore, we investigate whether SYT7 is involved in exocytosis, priming

and/or clamping of SVs by manipulating its expression levels. In general, we intent to understand how the interplay between SYT1 and SYT7 may regulate synaptic function and examine whether they have a similar or different roles in NT-release and priming of SVs.

2. Methods

2.1. Animal maintenance and mouse lines

This work used SYT1 knock-out mice line, obtained from Dr. Thomas Südhof (Stanford University School of Medicine, USA). Since the *Syt1*$^{-/-}$ animals die shortly after birth, the embryos *Syt1*$^{+/+}$, *Syt1*$^{+/-}$ and *Syt1*$^{-/-}$ at day 18-19 (E18-19) on C57BL/6 background of either sex generated by interbreeding *Syt1* heterozygous mice were used for the experiments. For the embryonic culture preparation, upon anaesthetization and cervical dislocation of the pregnant mice, embryos were extracted via caesarean section, genotyped by polymerase chain reaction (PCR), and then sacrificed to prepare hippocampal neurons. Also, we used postnatal (P) 0-2 C57BL/6N mice to obtain astrocytes for autaptic cultures. Procedures used to maintain and use these animals followed all regulations of the Directive 2010/63/EU of the European Parliament on the protection of animals used for scientific purposes and approved by the Berlin state authorities under the license number G-Project 106/20 and the animal welfare committee of Charité – Universitätsmedizin.

2.2. Lentivirus constructs

Lentiviruses were generated and produced by the Viral Core Facility of Charité – Universitätsmedizin Berlin. To silence targeted gene expression via RNA interference (*RNAi*), we used two different short hairpin RNA (*shRNA*) molecules. To knock-down SYT1 protein levels, we used an *shRNA* cassette containing a 19bp target oligonucleotide sequence of *Syt1* (5'AGTCTTCCTGCTGCCCGAC-3') and, to knock-down SYT7 protein levels, we used an *shRNA* cassette containing a 21bp targeting sequence KD607 from (Bacaj *et al.*, 2013). Each construct was cloned downstream of a U6 promotr expression cassette within a lentivirus that also contained a human synapsin1 promoter (for SYT7's *shRNA*) or ubiquitin promotor (for SYT1's *shRNA*), and to monitor neuronal infection, a nuclear RFP expression cassette (NLS-RFP). The control groups were infected with a scramble RNA (*scRNA*) sequence instead of the *shRNA* cassette (Watanabe *et al.*, 2014). For SYT1 or SYT7 rescue and overexpression experiments, we used a lentiviral *Syt1* construct generated from mouse *Syt1* cDNA (NCBI reference sequence: NM_001252341) or a lentiviral *Syt7* construct generated from rat *Syt7* cDNA (NCBI reference sequence: NM_021659). The cDNA was cloned into a lentiviral vector (*FUGW*) with a human synapsin1

promoter and a nuclear localization signal (NLS)-RFP-P2A expression cassette for identification of infected cells. A lentivirus expressing only NLS-RFP-P2A controlled by the human synapsin1 promoter served as control. We cultured hippocampal neurons and calculated the lentiviral titer by quantification of neurons expressing a fluorescent marker after DIV 7.

2.3. Neuronal culture and viral infection

For both electrophysiology recordings and immunocytochemistry experiments, we took advantage of using autaptic cultures. We prepared the neuronal culture as previously reported (Bekkers & Stevens, 1991). Briefly, we plated hippocampal neurons derived from embryonic (E18-19) or postnatal (P0-2) mice of either sex at a density of 300 cells/cm^2 on 30 mm coverslips containing single-layer astrocytic microislands of a few tens of microns across. Astrocytes were obtained from cerebral cortices of postnatal day (P) 0-2 C57BL/6N mice and plated at a density of 5000 cells/cm^2 on the micropattern coverslips 1 week before the preparation of the neurons. Neurons were infected with the appropriate lentiviral construct 24–48 h after plating and maintained at 37 °C and 5 % CO_2.

2.4. Electrophysiology

We performed whole-cell patch-clamp recordings in autaptic neurons after 11-21 days *in vitro* (DIV). All electrophysiological recordings were done at room temperature with a Multiclamp 700B amplifier (Molecular Devices) controlled by Clampex 10 software (Molecular Devices). Data were digitally sampled at 10 kHz and were filtered using a low-pass Bessel filter at 3 kHz. Series resistance was compensated up to 70%. Neurons were clamped at -70 mV during recordings. Exclusion criteria were established for patched cells with a leak current higher than -200 pA. Single APs were evoked by a 2 ms depolarization step to 0 mV. The bath solution in which cultures were immersed while recording was composed by (in mM): 140 NaCl, 2.4 KCl, 10 HEPES, 10 glucose, 2 $CaCl_2$ and 4 $MgCl_2$. We filled borosilicate glass patch pipettes with a solution containing (in mM): 136 KCl, 17.8 HEPES, 1 EGTA, 4.6 $MgCl_2$, 4 ATP-Na_2, 0.3 GTP-Na_2, 12 creatine phosphate, and 50 U/ml phosphocreatine kinase. Solutions were adjusted for osmolarity (300 mOsm) and pH (7.4). We used a multistep puller (P-1000, Sutter Instruments) to produce pulled glass pipettes and used those with an adequate resistance (3-5 MOhms). A series of electrophysiological parameters

were measured. We recorded excitatory postsynaptic currents (EPSCs) induced by 2 ms somatic depolarization from -70 to 0 mV producing an axonal AP, “mini” excitatory postsynaptic currents (mEPSCs), the readily releasable pool (RRP) of synaptic vesicles and short-term plasticity characteristics by the application a train stimulation of 10 APs at 20 Hz or two consecutive pulses at 40Hz. We functionally measured the RRP size by the application of external solution for 5 s containing 500 mM sucrose (Rosenmund & Stevens, 1996), and we integrated the area of the evoked-sucrose current with the steady-state current set as the baseline. Then, we computed the vesicular release probability (Pvr) as the ratio between the charge of the EPSC and the evoked-sucrose current. To analyze mEPSC, electrophysiological traces were filtered at 1 kHz and the range of parameters for inclusion of selected events using a conventionally defined template algorithm in Axograph X (Axograph Scientific) were 5-200 pA, 0.15-1.5 ms rise-time and 0.5-5 ms half-width. False-positive events were excluded by subtracting events detected from traces in the presence of the AMPA receptor antagonist, NBQX (3μM). The spontaneous release rate was calculated by dividing the mEPSC frequency by the number of synaptic vesicles in the RRP. The number of synaptic vesicles was calculated by dividing the RRP size by the mEPSC charge. We calculated the paired-pulsed ratio (PPR) by dividing the second EPSC amplitude (EPSC2) by the first (EPSC1). The synaptic responses from the train of APs were normalized to the first EPSC peak amplitude.

2.5. Immunocytochemistry and confocal imaging

Neurons were fixed with 4% paraformaldehyde (PFA; Sigma-Aldrich) for 10 min at 11-21DIV and immunostained as previously reported by (Xue *et al.*, 2007). The primary antibodies used were monoclonal mouse anti-Synaptotagmin-1 (1:1000; Synaptic System), polyclonal guinea pig anti-VGLUT1 (1:4000; Synaptic System), and polyclonal rabbit anti-Synaptotagmin-7 (1:500; Synaptic System). The secondary antibodies (1:500) conjugated with Alexa Fluor 405, 488, or 647 (Jackson ImmunoResearch). Images were acquired by using a Nikon Scanning Confocal A1Rsi+ with a 60×, 1.4 NA oil-immersion objective with identical acquisition settings for each group. Overexposure and photobleaching were avoided by checking the fluorescence signal saturation in synaptic boutons. Z stacks of neurons were set with a 0.3 μm inter-stack interval and total z axis range of 5–6 μm, and a sum of intensity projection was further used for analyses. Quantification of SYT1 or SYT7 signals over

VGLUT1 signals was performed using ImageJ software (US National Institutes of Health). Excitatory synapses (region of interest, ROI) were defined as VGLUT1 positive signals, and the fluorescence intensity of SYT1 or SYT7 was then measured in the defined ROI. Approximately the same number of autaptic neurons were collected per condition per culture.

2.6. Data collection and statistical analysis

We collected approximately the same number of neurons from each experimental group each day to reduce data variability. Also, to minimize culture-culture variation, we acquired images from at least three independent hippocampal cultures from three different litters. For Figure 1 we chose the nonlinear regression model standard Hill equation. We did not constrain any parameter of the model to a constant value. We performed a global nonlinear regression; we specify that parameters are shared to fit all data sets. All data points are weighted equally in the model. To perform all statistical analysis and to generate all graphs we used Prism 8 (GraphPad) software. Data were tested for normality distribution by the application of a Pearson omnibus K2 normality test. Statistical significance was assessed using Two-tailed unpaired t test or one-way ANOVA test for normally distributed data and Mann-Whitney test or Kruskal-Wallis ANOVA test for non-normally distributed data followed by Tukey-Kramer's *post hoc* multiple comparison methods where appropriate. The significance and P values for all statistical tests are define as: *$p < 0.05$, **$p < 0.01$, ***$p < 0.001$ and ****$p < 0.0001$. No method was used to determine if the data met the assumptions of the statistical approach.

3. Results

Here, I present a selection of relevant findings of my PhD project. Data from Figures 1 and 2 can be found in Bouazza-Arostegui *et al.* 2022 (attached manuscript). Data from Figure 3 has not been published yet. Data from Figures 4 and 5 can be found in Bouazza-Arostegui *et al.* 2022, except data regarding SYT7 overexpression experiments in Figures 4 and 5 that have not been published yet. Data from Figure 6 have not been published yet. Finally, data from Table 1 can be found in Bouazza-Arostegui *et al.* 2022.

3.1. Distinct sensitivity of Synaptotagmin-1's synaptic functions to its expression levels at the presynaptic compartment

First, we performed a quantitative analysis of the relationship between SYT1 expression levels at the presynaptic terminal of hippocampal glutamatergic autaptic neurons and the measured values of priming and fusion of SVs by applying a dose-response model (**Figure 1**). We used our previously obtained values of SYT1 endogenous expression (from Figure 5 in Bouazza-Arostegui *et al.* 2022), overexpression (from Figure 6 in Bouazza-Arostegui *et al.* 2022) and knock-down (from Figure 7 in Bouazza-Arostegui *et al.* 2022) experiments performed at DIV15-21 as source data to apply a nonlinear regression analysis (**Figure 1**). We found that the number of fusion-competent vesicles, as measured by sucrose application (Rosenmund & Stevens, 1996), was only significantly reduced when SYT1 was almost absent from the synapse, which indicated that the function of SYT1 in synaptic vesicle priming was least sensitive to protein loss (**Figure 1B**). On the other hand, SYT1's function as a regulator of spontaneous NT-release showed a moderate sensitivity to protein levels, leading to increased spontaneous release activity when the expression levels were reduced by 50% or more. The gradual reduction in SYT1 expression levels led to the progressive unclamping of SVs, reaching a ~3-fold increase in the spontaneous release rate when SYT1 levels were close to those of *Syt1*$^{-/-}$ neurons (**Figure 1C**). Ca^{2+}-dependent evoked release displayed the highest sensitivity to SYT1 expression changes of all synaptic functions (**Figure 1D and E**). The similarity between the fitting-curves that define the EPSC charge (**Figure 1D**) and Pvr (**Figure 1E**) in relation to variations in SYT1 expression was not surprising since both reflect SYT1's role as Ca^{2+} sensor. Remarkably, in our study of heterozygous neurons for SYT1 we examined the sensitivity of SYT1 to the two forms of NT-release and priming.

From the analysis of the dose-response functions we elucidated that SYT1 haploinsufficiency affects the efficiency of the evoked synaptic transmission and the spontaneous neurotransmitter release mode, while the RRP size of SVs is similar to those neurons with two copies of the *Syt1* gene (**Figure 1, Table 1**).

Overall, our sensitive manipulation of SYT1 expression revealed that Ca^{2+}-dependent and priming functions have distinct sensitivity to SYT1 presence with different thresholds. This result suggests that at low concentrations, SYT1 is a rate-limiting factor for release efficiency but not for SV priming. These different sensitivities are also indicative of at least two different molecular mechanisms of action. Moreover, our fittings indicated that genetic modification of SYT1 expression associated with allelic loss or gene duplication may lead to a more pronounced impact on evoked NT-release compared to SYT1 function in SV priming.

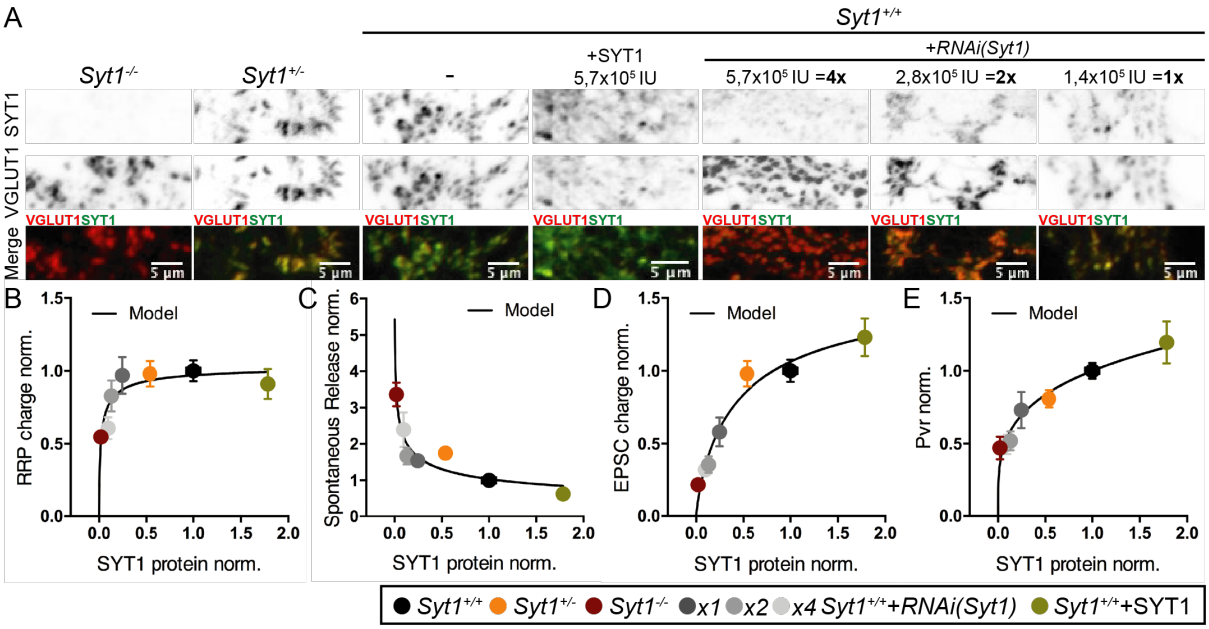

Figure 1. Different sensitivity of SYT1's synaptic functions to its expression at the presynaptic terminal.

(**A**) Representative images of VGLUT1 and SYT1 expression at hippocampal glutamatergic autaptic synapses from *Syt1*$^{+/+}$, *Syt1*$^{+/-}$, *Syt1*$^{-/-}$, *Syt1*$^{+/+}$ with overexpression of SYT1 and *Syt1*$^{+/+}$ infected with a lentiviral vector expressing an increasing amount of *RNA interference* (*RNAi*) targeting *Syt1*. Plots of RRP size (**B**), spontaneous release rate (**C**), EPSC charge (**D**) and Pvr (**E**) normalized to *Syt1*$^{+/+}$ against the normalized SYT1/VGLUT1 fluorescence intensity ratios obtained from the titration of SYT1 in autaptic neuronal cultures. To calculate SYT1 expression at synapses: *Syt1*$^{+/+}$ (black), *Syt1*$^{+/-}$ (orange), and *Syt1*$^{-/-}$ (burgundy) data (Bouazza-Arostegui *et al.* 2022: Figure 5) were normalized to *Syt1*$^{+/+}$ and subtracting the *Syt1*$^{-/-}$ expression levels in the different experiments. For *Syt1*$^{+/+}$ infected with the different amounts of *Syt1 RNAi* (1x dark grey, 2x grey, 4x light grey) and *Syt1*$^{+/+}$ + SYT1 (olive drab) data (from Bouazza-Arostegui *et al.* 2022: Figures 6 and 7), SYT1 expression levels were normalized to *Syt1*$^{+/+}$. All cells used for the model were from DIV15-21. Continuous black-line represent the curve-fitting of the Hill function. Scale bars: 5 µm. All data shown represent mean +/- SEM. Adapted from Bouazza-Arostegui *et al.* 2022: Figures 5, 6, and 7. Order and layout of graphs are different from the paper.

B		SYT1 expression norm.		RRP norm.		C		SYT1 expression norm.		Spontaneous Release norm.	
Syt1+/+		1,00	0,08	1,000	0,072	*Syt1+/+*		1,00	0,08	1,000	0,079
Syt1+/-		0,54	0,04	0,9808	0,087	*Syt1+/-*		0,54	0,04	1,749	0,205
Syt1-/-		0,02	0,02	0,5469	0,047	*Syt1-/-*		0,02	0,02	3,363	0,326
Syt1+/+	1x *RNAi (Syt1)*	0,25	0,04	0,9697	0,127	*Syt1+/+*	1x *RNAi (Syt1)*	0,25	0,04	1,539	0,163
	2x *RNAi (Syt1)*	0,13	0,02	0,8282	0,107		2x *RNAi (Syt1)*	0,13	0,02	1,666	0,230
	4x *RNAi (Syt1)*	0,10	0,01	0,6067	0,075		4x *RNAi (Syt1)*	0,10	0,01	2,391	0,474
Syt1+/+	1x SYT1	1,78	0,06	0,9109	0,103	*Syt1+/+*	1x SYT1	1,78	0,06	0,622	0,088
D		**SYT1 expression norm.**		**EPSC charge norm.**		**E**		**SYT1 expression norm.**		**Pvr norm.**	
Syt1+/+		1,00	0,08	1,000	0,076	*Syt1+/+*		1,00	0,08	1,000	0,054
Syt1+/-		0,54	0,04	0,9808	0,087	*Syt1+/-*		0,54	0,04	0,808	0,059
Syt1-/-		0,02	0,02	0,2176	0,023	*Syt1-/-*		0,02	0,02	0,470	0,078
Syt1+/+	1x *RNAi (Syt1)*	0,25	0,04	0,5809	0,099	*Syt1+/+*	1x *RNAi (Syt1)*	0,25	0,04	0,731	0,124
	2x *RNAi (Syt1)*	0,13	0,02	0,3553	0,056		2x *RNAi (Syt1)*	0,13	0,02	0,520	0,065
	4x *RNAi (Syt1)*	0,10	0,01	0,3208	0,05		4x *RNAi (Syt1)*	0,10	0,01	0,495	0,066
Syt1+/+	1x SYT1	1,78	0,06	1,23	0,129	*Syt1+/+*	1x SYT1	1,78	0,06	1,196	0,144

Table 1. Values corresponding to Figure 1. All data shown represent mean +/- SEM. Adapted from Figure 7-1 Bouazza-Arostegui *et al.* 2022.

3.2. Synaptotagmin-1-lacking neurons phenotype changes over time

Next, we aim to further clarify the roles of SYT1 in NT-release and priming of SVs and analyze whether the phenotype of SYT1's loss is sensitive to the neuronal culture stage. For that, we proceed to voltage-clamp recordings in autaptic hippocampal neurons derived from *Syt1*$^{+/+}$ or *Syt1*$^{-/-}$ mice at early (11-12 DIV) and later (15-16 DIV) culture stages. Recent works have suggested that SYT7 may have functional redundancy in the priming of SVs (Bacaj *et al.*, 2015). Therefore, we also investigated whether SYT7 contributes to the phenotype of SYT1 loss by knocking-down SYT7 protein expression in *Syt1*$^{-/-}$ neurons at the two time periods (**Figure 2**). By using the VGLUT1 fluorescence signal we defined presynaptic compartments and measured SYT1 and SYT7 expression at both stages. We showed that both VGLUT1 and SYT1 but not SYT7 expression increased overtime at synapses and that our lentiviral infection containing *shRNA* targeting *Syt7* induced an average reduction of the fluorescence signal of 75% at both culture stages (from Figure 3 in Bouazza-Arostegui *et al.* 2022; (VGLUT1 norm.): *Syt1*$^{+/+}_{DIV11}$ 1±0.12, n=21/3 and *Syt1*$^{+/+}_{DIV16}$ 3.2±0.4, n=21/3, p<0.0001; Two-tailed unpaired t test; (SYT1 norm.): *Syt1*$^{+/+}_{DIV11}$ 1±0.10, n=21/3 and *Syt1*$^{+/+}_{DIV16}$ 2.9±0.4, n=21/3, p<0.0001; Two-tailed unpaired t test; (SYT7 norm.): *Syt1*$^{+/+}_{DIV11}$ 1±0.14, n=21/3 and *Syt1*$^{+/+}_{DIV16}$ 1.3±0.2, n=21/3, p=ns; Mann-Whitney test; (VGLUT1 norm.): *Syt1*$^{-/-}_{DIV11}$ 1±0.12, n=27/3 and *Syt1*$^{+/+}_{DIV16}$ 2.3±0.36, n=28/3, p<0.001; Mann-Whitney test; (VGLUT1 norm.): *Syt1*$^{-/-}_{+RNAi(Syt7)DIV11}$ 1±0.14, n=21/3 and *Syt1*$^{-/-}_{+RNAi(Syt7)DIV16}$ 3.5±0.47, n=17/3, p<0.0001; Mann-Whitney test; (SYT7DIV11 norm.): *Syt1*$^{-/-}$ 1±0.21, n=27/3 and *Syt1*$^{-/-}_{+RNAi(Syt7)}$ 0.30±0.15, n=21/3, p<0.001; Mann-Whitney test; (SYT7DIV16 norm.): *Syt1*$^{-/-}$ 1±0.13, n=28/3 and *Syt1*$^{-/-}_{+RNAi(Syt7)}$ 0.34±0.09, n=17/3, p<0.001; Mann-Whitney test).

While the RRP charge of *Syt1*$^{+/+}$ and *Syt1*$^{-/-}$ autaptic neurons at DIV11-12 was indistinguishable, at later culturing stage (DIV15-16) we detected a significant ~40-50% reduction in the RRP charge in the *Syt1*$^{-/-}$ group. Also, reduction of SYT7 protein expression in *Syt1*$^{-/-}$ autaptic neurons reduced the RRP size of SVs (**Figure 2A**; (RRP, pC): DIV11-12: *Syt1*$^{+/+}$ 165±23, n=48/4, Syt1$^{-/-}$ 170±21, n=40/4, p=ns and *Syt1*$^{-/-}_{+RNAi(Syt7)}$ 34±6, n=40/4, p<0.0001/0.0001; DIV15-16: *Syt1*$^{+/+}$ 567±69, n=44/4, *Syt1*$^{-/-}$ 279±43, n=41/4, p<0.01 and *Syt1*$^{-/-}_{+RNAi(Syt7)}$ 50±9, n=30/4, p<0.0001/0.0001; Kruskal-Wallis test).

Interestingly, we observed that loss of SYT1 didn't lead to significant changes in spontaneous release rates for the early synaptic responses group, while spontaneous release rate was enhanced in the older synaptic responses. Furthermore, reduction of SYT7 protein expression in *Syt1*$^{-/-}$ autaptic neurons increased spontaneous release rates at all culture stages (**Figure 2B**; (Spontaneous release rate, s^{-1}): DIV11-12: *Syt1*$^{+/+}$ 0.003±0.0004, n=48/4, *Syt1*$^{-/-}$ 0.0043±0.0005, n=33/4, p=ns and *Syt1*$^{-/-}$$_{+RNAi(Syt7)}$ 0.012±0.0015, n=38/4, p<0.0001/0.01; DIV15-16: *Syt1*$^{+/+}$ 0.0016±0.0002, n=44/4, *Syt1*$^{-/-}$ 0.0054±0.0012, n=41/4, p<0.01 and *Syt1*$^{-/-}$$_{+RNAi(Syt7)}$ 0.013±0.001, n=24/4, p<0.0001/0.01; Kruskal-Wallis test).

We concluded that the impact of SYT1 loss on spontaneous release, like the impact on RRP size, could be dependent on the maturation state of the neuron. Furthermore, these results suggest that SYT7 is capable of compensating for the loss of SYT1-dependent phenotypes in SV priming and clamping SVs (**Figure 2A and B**). In contrast, both the EPSC charge and the Pvr, as calculated by dividing the EPSC charge by the RRP charge, were reduced in *Syt1*$^{-/-}$ neurons regardless of culture age. While knocking-down SYT7 expression levels in *Syt1*$^{-/-}$ neurons had an impact on the ESPC charge at both stages, the changes were proportional to the observed RRP size, and thus did not impact the Pvr of the *Syt1*$^{-/-}$ group in any of the stages tested (**Figure 2C**; (EPSC charge, pC): DIV11-12: *Syt1*$^{+/+}$ -11.1±1.5, n=47/4, *Syt1*$^{-/-}$ -3.8±0.5, n=43/4, p<0.01 and *Syt1*$^{-/-}$$_{+RNAi(Syt7)}$ -1.1±0.2, n=40/4, p<0.0001/0.001; DIV15-16: *Syt1*$^{+/+}$ -36±5, n=40/4, *Syt1*$^{-/-}$ -5.3±1, n=44/4, p<0.0001 and *Syt1*$^{-/-}$$_{+RNAi(Syt7)}$ -1.4±0.3, n=32/4, p<0.0001/0.01; **Figure 2D**; (Pvr, %): DIV11-12: *Syt1*$^{+/+}$ 8.5±1, n=47/4, *Syt1*$^{-/-}$ 3.2±0.5, n=40/4, p<0.0001 and *Syt1*$^{-/-}$$_{+RNAi(Syt7)}$ 3.3±0.6, n=39/4, p<0.0001/ns; DIV15-16: *Syt1*$^{+/+}$ 7.4±0.8, n=38/4, *Syt1*$^{-/-}$ 3.5±0.6, n=38/4, p<0.001 and *Syt1*$^{-/-}$$_{+RNAi(Syt7)}$ 2.9±0.8, n=30/4 , p<0.0001/ns; Kruskal-Wallis test).

These results demonstrated that SYT1 is essential for evoked NT-release at all culture stages. In contrast, SYT1's roles in clamping spontaneous release and priming of SVs are essential in more mature hippocampal glutamatergic neurons. Moreover, SYT7 redundantly with SYT1 promotes priming of SVs and negatively regulates spontaneous NT-release, which likely contributes to the differences in the phenotype exhibited by SYT1-lacking neurons at different culture stages.

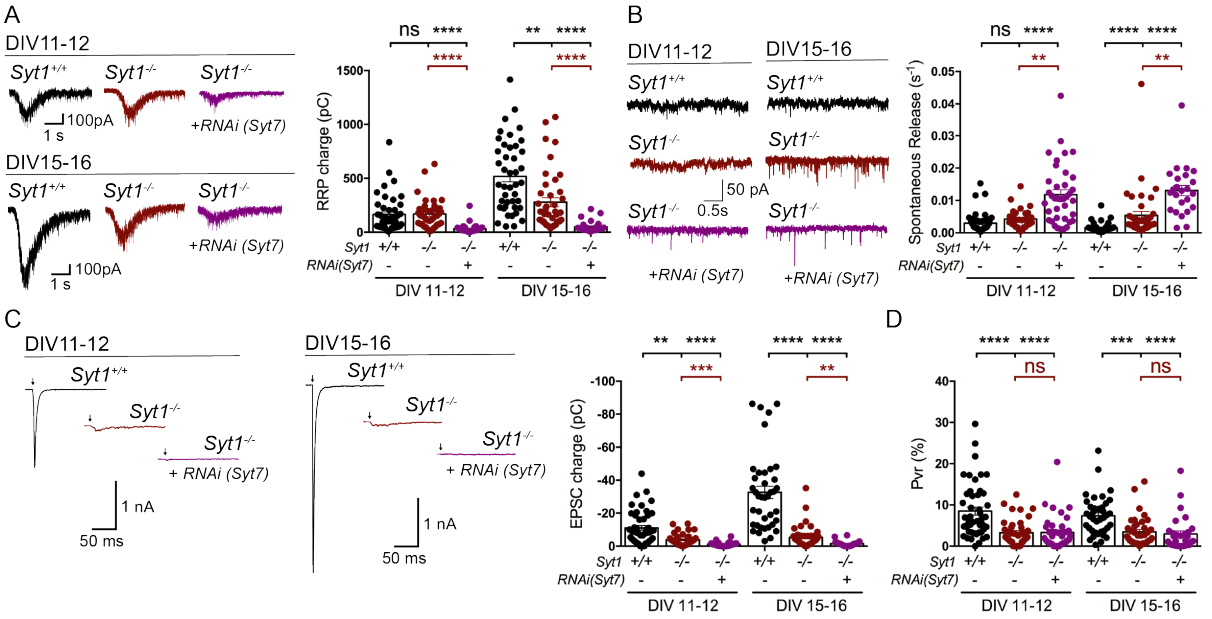

Figure 2. Phenotype of *Syt1*$^{-/-}$ hippocampal glutamatergic neurons at different neuronal stages and SYT7 synaptic functions. (**A**) Representative traces at early (DIV11-12) and intermediate (DIV15-16) autaptic neuronal stages (left) and summary bar graphs (right) of the charge of sucrose evoked NT-release of *Syt1*$^{+/+}$ (black), *Syt1*$^{-/-}$ (burgundy) and *Syt1*$^{-/-}$ neurons infected with lentivirus containing *RNA interference* (*RNAi*) for silencing SYT7 (purple). (**B**) Example traces of spontaneous release events (left) and summary bar graphs of spontaneous release rate (right) at the two different neuronal stages. (**C**) Representative EPSC traces (left) and summary bar graphs of total EPSC charge measured over an interval of 1s (right). (**D**) Summary bar graphs of average vesicular release probability (Pvr). Data are mean +/- SEM. Statistical significance and p values were estimated by a Kruskal-Wallis test (*p≤0.05, **p≤0.01, ***p≤0.001, ****p≤0.0001, ns = not significant). Adapted from Bouazza-Arostegui *et al.* 2022 (Figure 4). Order and layout of graphs are different from the paper.

3.3. Synaptotagmin-1 and Synaptotagmin-7 redundant functions in clamping and priming SVs

To further demonstrate that SYT1 is a priming and clamping factor and to study SYT7 functional redundancy, we performed rescue experiments on SYT1-lacking neurons by infecting them with lentiviral particles containing either SYT1 or SYT7 and performed patch-clamp recordings at DIV15-21. First, we showed the restoration of SYT1 expression levels at the presynaptic compartment of *Syt1*$^{-/-}$ neurons (from Figure 2 in Bouazza-Arostegui *et al.* 2022; (VGLUT1 norm.): *Syt1*$^{+/+}$ 1±0.06, n=29/3, *Syt1*$^{-/-}$ 1.07±0.06, n=23/3, p=ns and *Syt1*$^{-/-}$$_{+SYT1}$ 0.89±0.04, n=26/3, p=ns/ns; (SYT1/VGLUT1 norm.): *Syt1*$^{+/+}$ 1±0.05, n=29/3, *Syt1*$^{-/-}$ 0.16±0.01, n=23/3 , p<0.0001 and *Syt1*$^{-/-}$$_{+SYT1}$ 1.02±0.05, n=26/3, p=ns/<0.0001; Kruskal-Wallis test). Next, by introducing SYT7 we induced its strong overexpression in both *Syt1*$^{+/+}$ and *Syt1*$^{-/-}$ neurons (**Figure 3A-D**; (VGLUT1 norm.): *Syt1*$^{+/+}$ 1±0.06, n=58/3, *Syt1*$^{+/+}$$_{+SYT7}$ 1.03±0.13, n=22/3, p=ns, *Syt1*$^{-/-}$ 1.21±0.15, n=35/3, p=ns and *Syt1*$^{-/-}$$_{+SYT7}$ 1.16±0.13, n=20/3, p=ns/ns; (SYT1/VGLUT1 norm.): Syt1$^{+/+}$ 1±0.05, n=58/3, *Syt1*$^{+/+}$$_{+SYT7}$ 1.06±0.11, n=22/3, p<0.0001, *Syt1*$^{-/-}$ 0.07±0.01, n=35/3, p<0.0001 and *Syt1*$^{-/-}$$_{+SYT7}$ 0.07±0.02, n=20/3, p<0.0001/<0.0001; (SYT7/VGLUT1 norm.): *Syt1*$^{+/+}$ 1.01±0.11, n=58/3, *Syt1*$^{+/+}$$_{+SYT7}$ 5.92±0.51, n=22/3, p<0.0001, *Syt1*$^{-/-}$ 0.89±0.08, n=35/3, p=ns and Syt1$^{-/-}$$_{+SYT7}$ 5.51±0.59, n=20/3, p<0.0001/<0.0001; Kruskal-Wallis test).

We showed that while reintroducing SYT1 in *Syt1*$^{-/-}$ neurons fully restored SV priming, spontaneous and evoked NT-release, exogenous overexpression of SYT7 restored the RRP size and repressed spontaneous release to wild-type levels but not evoked release, which was significantly reduced (**Figure 4A-C**; (RRP norm.): *Syt1*$^{+/+}$ 1±0.07, n=68/6, *Syt1*$^{-/-}$ 0.43±0.04, n=65/6, p<0.0001, *Syt1*$^{-/-}$$_{+SYT1}$ 0.93±0.15, n=29/3, p=ns/<0.05 and *Syt1*$^{-/-}$$_{+SYT7}$ 0.71±0.08, n=27/3, p=ns/<0.05; (Spontaneous rate norm.): *Syt1*$^{+/+}$ 1±0.09, n=66/6, *Syt1*$^{-/-}$ 2.31±0.27, n=62/6, p<0.0001, *Syt1*$^{-/-}$$_{+SYT1}$ 0.96±0.12, n=26/3, p=ns/<0.05 and *Syt1*$^{-/-}$$_{+SYT7}$ 1.03±0.05, n=25/3, p<0.01/ns; (EPSC charge norm.): *Syt1*$^{+/+}$ 1±0.1, n=74/6, *Syt1*$^{-/-}$ 0.2±0.02, n=72/3, p<0.0001, *Syt1*$^{-/-}$$_{+SYT1}$ 1.05±0.2, n=29/3, p=ns/<0.0001 and *Syt1*$^{-/-}$$_{+SYT7}$ 0.11±0.01, n=29/3, p<0.0001/<0.0001; Kruskal-Wallis test). These results indicated that the loss of function phenotype of SYT1 was due to the loss of the protein, and, remarkably, we provide evidence of SYT7 function as a priming factor as well as proof of its capability

to arrest spontaneous NT-release. We also analyzed evoked release efficacy by computing the Pvr and by measuring changes in short-term plasticity by applying a pair-pulse stimulation at 40Hz. As expected, lentiviral expression of SYT1 rescued the Pvr to wild-type levels and, interestingly, overexpressing SYT7 significantly reduced the Pvr (**Figure 4D**; (Pvr norm.): *Syt1*$^{+/+}$ 1±0.08, n=66/6, *Syt1*$^{-/-}$ 0.54±0.07, n=59/6, p<0.0001, *Syt1*$^{-/-}$$_{+SYT1}$ 1.21±0.15, n=28/3, p=ns/<0.0001 and *Syt1*$^{-/-}$$_{+SYT7}$ 0.22±0.03, n=27/3, p<0.0001/<0.0001; Kruskal-Wallis test). Short-term plasticity experiments showed similar results. Lentiviral infection with SYT1 of *Syt1*$^{-/-}$ neurons reduced the facilitation of the responses to the wild-type group, and overexpression of SYT7 further increased the faciliatory phenotype of *Syt1*$^{-/-}$ neurons (**Figure 4E**; (PPR 40Hz, norm.): *Syt1*$^{+/+}$ 1±0.04, n=53/6, *Syt1*$^{-/-}$ 2.45±0.20, n=57/6, p<0.0001, *Syt1*$^{-/-}$$_{+SYT1}$ 0.97±0.07, n=24/3, p=ns/<0.0001 and *Syt1*$^{-/-}$$_{+SYT7}$ 4.4±0.63, n=23/3, p<0.0001/<0.01; Kruskal-Wallis test).

All together, these results further demonstrated that SYT1's absence is responsible for the phenotype displayed by *Syt1*$^{-/-}$ neurons and that both SYT1 and SYT7 are redundantly capable of priming and clamping SVs. Interestingly, these data indicate that SYT1 and SYT7 may have opposing roles in evoked NT-release and short-term plasticity.

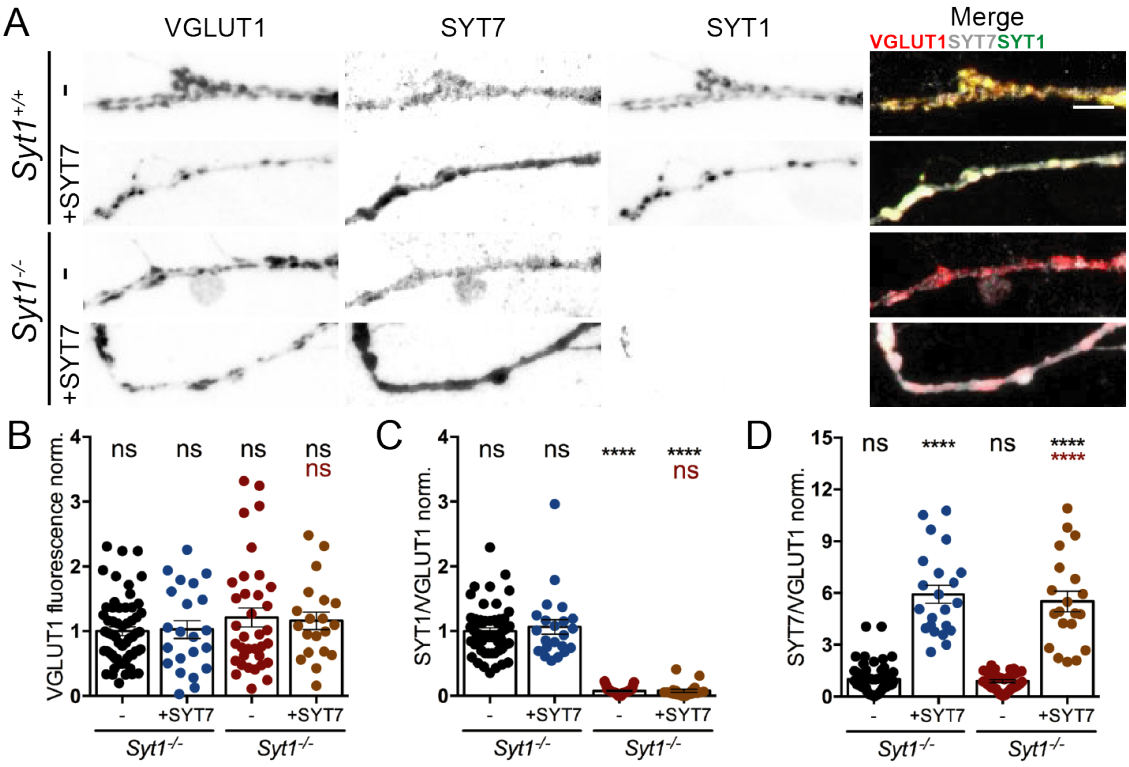

Figure 3. Lentiviral overexpression of SYT7 in *Syt1*$^{+/+}$ and *Syt1*$^{-/-}$ neurons. (**A**) Representative images of hippocampal glutamatergic autaptic neurons (DIV15-21) of *Syt1*$^{+/+}$ and *Syt1*$^{-/-}$ infected with a lentivirus containing a nuclear RFP vector (-) or *Syt7*. Summary bar graphs showing VGLUT1 (**B**), SYT1/VGLUT1 (**C**), SYT7/VGLUT1 (**D**) fluorescence intensity normalized to *Syt1*$^{+/+}$. Scale bar: 5 µm. Data are mean +/- SEM. Statistical significance and p values were estimated by a Kruskal-Wallis test (*p≤0.05, **p≤0.01, ***p≤0.001, ****p≤0.0001, ns = not significant). Data from this figure were not published before.

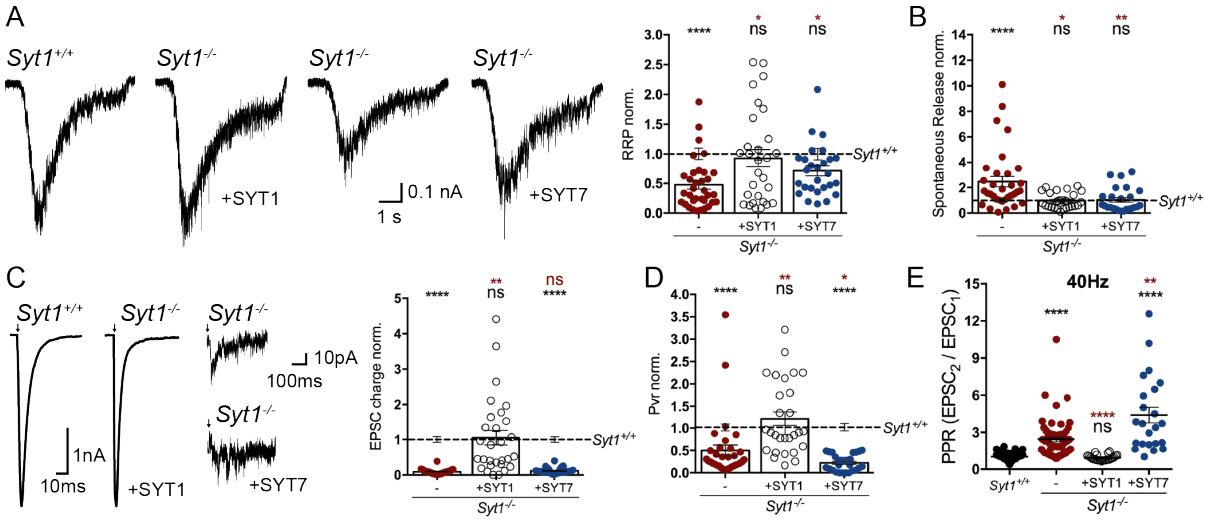

Figure 4. Impact on synaptic properties of lentiviral expression of SYT1 or SYT7 in *Syt1*$^{-/-}$ neurons. All electrophysiological experiments were done on hippocampal glutamatergic autaptic neurons at DIV15-21. (**A**) Representative traces (left) and normalized summary bar graphs (right) of the charge of sucrose-evoked release of *Syt1*$^{+/+}$ (black), *Syt1*$^{-/-}$ (burgundy), and *Syt1*$^{-/-}$ neurons infected with lentivirus containing SYT1 (white) or SYT7 (marine blue). (**B**) Summary bar plot of spontaneous release rate from *Syt1*$^{-/-}$ neurons rescued with either SYT1 or SYT7 normalized to the *Syt1*$^{+/+}$control (black). (**C**) Representative EPSC traces (left) and normalized summary bar graphs of total EPSC charge measured over an interval of 1s (right). (**D**) Normalized summary bar graphs of vesicular release probability of evoked release induced by a single AP. (**E**) Graph of paired-pulse ratio (PPR) at 40Hz (left). Artifacts and/or action potentials were blanked and substituted by arrows in **C**. Data shown represent mean +/- SEM. Statistical significance and p values were estimated by a Kruskal-Wallis test (*p≤0.05, **p≤0.01, ***p≤0.001, ****p≤0.0001, ns = not significant). Data for SYT1 rescue experiments were adapted from Bouazza-Arostegui *et al.* 2022 (Figure 2). The order and layout of the graphs are different from the paper.

3.4. Synaptotagmin-1 and Synaptotagmin-7 functions in NT-release

Our results from the experiments performed on *Syt1*$^{-/-}$ neurons suggested that SYT7 might be involved not only upstream to the Ca^{2+}-dependent release pathway but also directly in NT-release. In addition, our evidence describing how SYT1 expression levels fundamentally determine release efficacy (Bouazza-Arostegui *et al.*, 2022) led us to investigate how the interplay between SYT1 and SYT7 regulates NT-release. For this purpose, we extended our analysis to lentiviral overexpression of SYT1 or SYT7 in *Syt1*$^{+/+}$ neurons (**Figure 3**) and performed patch-clamp recordings of autaptic glutamatergic neurons at DIV15-21 (**Figure 5 and 6**).

First, sucrose-induced SVs fusion experiments showed that neither increasing the number of SYT1 or SYT7 molecules significantly changed the RRP size of SVs (**Figure 5A**; (RRP norm.): *Syt1*$^{+/+}$ 1.00±0.08, n=76/6, *Syt1*$^{+/+}{}_{+SYT1}$ 0.95±0.09, n=36/3, p=ns and *Syt1*$^{+/+}{}_{+SYT7}$ 0.84±0.08, n=43/3, p=ns; Mann-Whitney test). Similarly, we assessed the effect of overexpressing SYT1 or SYT7 in the spontaneous fusion of SVs, and we could not detect significant differences between *Syt1*$^{+/+}$ and SYT1- or SYT7-overexpressing neurons (**Figure 5B**; (Spontaneous release rate norm.): *Syt1*$^{+/+}$ 1.00±0.13, n=75/6, *Syt1*$^{+/+}{}_{+SYT1}$ 0.62±0.08, n=36/3, p=ns and *Syt1*$^{+/+}{}_{+SYT7}$ 0.84±0.13, n=43/3, p=ns; Mann-Whitney test). Interestingly, while overexpressing SYT1 in *Syt1*$^{+/+}$ neurons showed a not significant increase in the EPSC charge or the computed Pvr, overexpressing SYT7 significantly decreased both parameters (**Figure 5C-D**; (EPSC charge norm.): *Syt1*$^{+/+}$ 1.00±0.1, n=80/6, *Syt1*$^{+/+}{}_{+SYT1}$ 1.23±0.12, n=35/3, p=ns and *Syt1*$^{+/+}{}_{+SYT7}$ 0.64±0.08, n=49/3, p=ns; (Pvr, %): *Syt1*$^{+/+}$ 1.00±0.1, n=76/6, *Syt1*$^{+/+}{}_{+SYT1}$ 1.19±0.14, n=35/3, p=0.19 and *Syt1*$^{+/+}{}_{+SYT7}$ 0.68±0.09, n=43/3, p=ns; Mann-Whitney test). To further analyze the SYT1 and SYT7 effect on evoked release, we performed paired-pulse experiments at 40Hz. While overexpressing SYT1 induced a significant decrease in the pair-pulse ratio, overexpressing SYT7 significantly increased the ratio when compared to *Syt1*$^{+/+}$ (**Figure 5E**; (PPR at 40Hz): *Syt1*$^{+/+}$ 1.04±0.04, n=42/3, *Syt1*$^{+/+}{}_{+SYT1}$ 0.98±0.04, n=33/3, p=0.000519 and *Syt1*$^{+/+}{}_{+SYT7}$ 1.40±0.07, n=42/3, p=ns; Mann-Whitney test).

To further explore the role of SYT7 in short-term plasticity, we applied repetitive stimulation at 20Hz on *Syt1*$^{+/+}$ or *Syt1*$^{-/-}$ neurons with or without overexpression of SYT7 (**Figure 3 and 6**). We showed that overexpression of SYT7 in wild-type neurons led to a facilitatory phenotype (**Figure 6A**; ($EPSC_{10}/EPSC_1$): *Syt1*$^{+/+}$ 0.74±0.05, n=35/3

and *Syt1*$^{+/+}$$_{+SYT7}$ 1.13±0.1, n=39/3, p=0.0008; Mann-Whitney test). and in *Syt1*$^{-/-}$ neurons exacerbated the already strong facilitatory phenotype of the SYT1-lacking synaptic responses (**Figure 6B**; ($EPSC_{10}/EPSC_1$): *Syt1*$^{+/+}$ 0.62±0.04, n=27/3, *Syt1*$^{-/-}$ 5.63±0.46, n=27/3 p<0.0001 and *Syt1*$^{-/-}$$_{+SYT7}$ 9.58±1.51, n=26/3, p<0.0001/ p=0.048; Mann-Whitney test).

All together, these results indicated that neither SYT1 nor SYT7 are a limiting factor for the RRP size or the spontaneous release rate of SVs. Importantly, we showed that SYT1 is a limiting factor for evoked release efficacy and induces depression of synaptic responses during high-frequency stimulation. In contrast, SYT7 may impair the overall NT release and is a limiting factor for the facilitation of synaptic responses during repetitive stimulation.

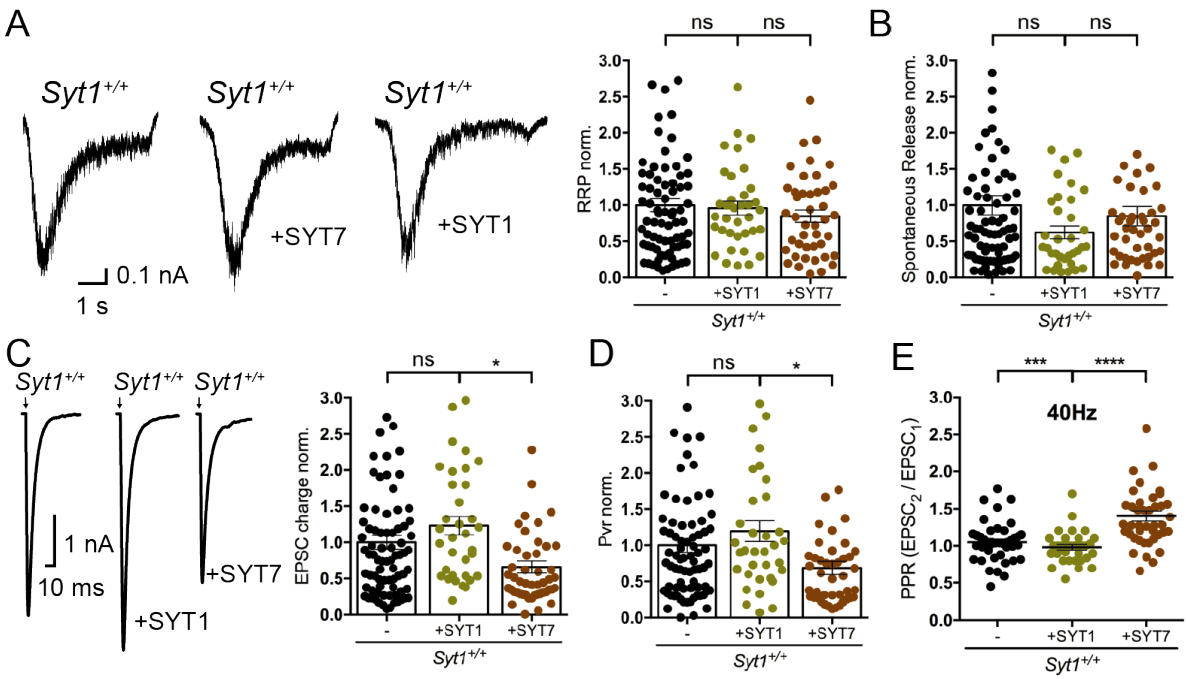

Figure 5. Impact on synaptic properties of overexpressing SYT1 or SYT7 in *Syt1*$^{+/+}$ neurons. All electrophysiological experiments were performed on hippocampal glutamatergic autaptic neurons at DIV15-21. (**A**) Representative sucrose-evoked current traces (left) and normalized summary bar plot of the RRP size of SVs (right). (**B**) Summary bar graph of normalized spontaneous release rate**.** (**C**) Sample EPSC traces (left) and bar plot of normalized EPSC charge (right). (**D**) Summary bar graph of computed Pvr. (**E**) Bar graph of paired-pulse ratio (PPR) at 40Hz. Artifacts and/or action potentials were blanked and substituted by arrows in **C**. All data shown represent mean +/- SEM. Statistical analysis was applied Mann-Whitney *U* test (*p≤0.05, **p≤0.01, ***p≤0.001, ****p≤0.0001, ns = not significant). Data for SYT1 overexpression experiments was adapted from Bouazza-Arostegui *et al.* 2022 (Figure 6). The order and layout of the graphs are different from the paper.

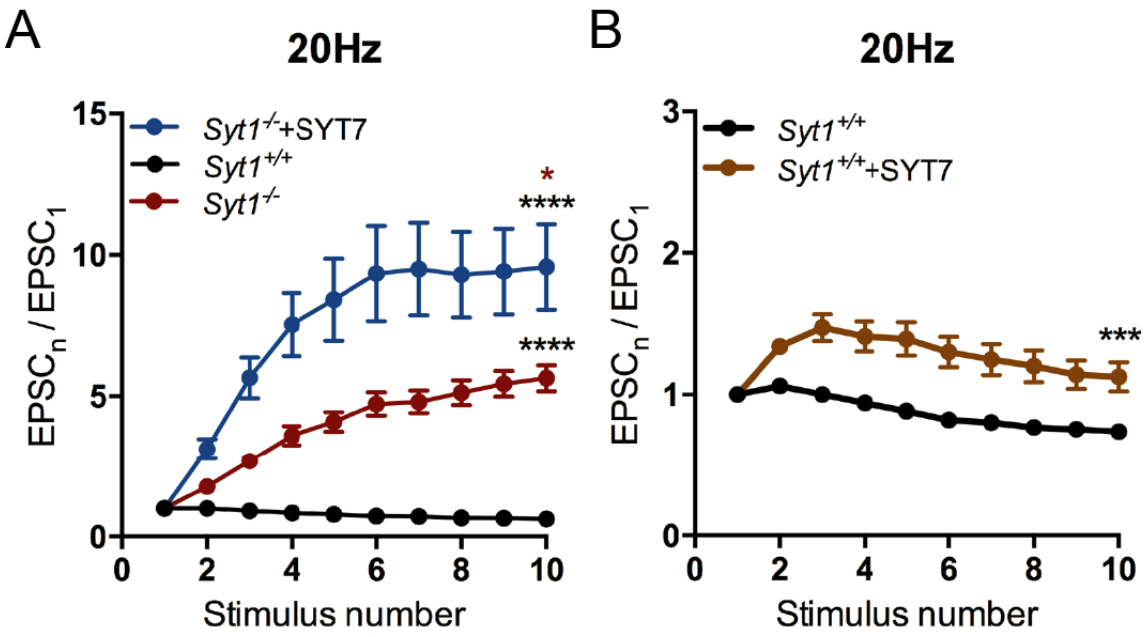

Figure 6. SYT1 and SYT7 function in short-term plasticity. All experiments were performed on hippocampal glutamatergic autaptic neurons at DIV15-21. Synaptic responses during stimulation of 10 consecutive APs separated by 50ms. (**A**) Plots of mean EPSC amplitudes normalized to the first EPSC of *Syt1*$^{+/+}$ (black), *Syt1*$^{-/-}$ (burgundy), and *Syt1*$^{-/-}$ infected with lentivirus containing SYT7 (marine blue) during train stimulation. (**B**) Plots of mean EPSC amplitudes normalized to the first EPSC of *Syt1*$^{+/+}$ (black) and *Syt1*$^{+/+}$ infected with lentivirus containing SYT7 (brown) during train stimulation. All data shown represent mean +/- SEM. Statistical significance and p values were estimated by a Kruskal-Wallis test (*p≤0.05, **p≤0.01, ***p≤0.001, ****p≤0.0001, ns = not significant). Data from this figure were not published before.

4. Discussion

In summary, here we demonstrated that SYT1 plays a triple function at the presynaptic terminal by performing genetic deletion, knock-down, and rescue experiments. Indeed, we showed that the SYT1 knock-out phenotype develops over time in excitatory autaptic neurons. Our time-sensitive experiments revealed that SYT1's role in evoked NT-release was essential at all culture stages, while SYT1 functions as a clamp of spontaneous SV-release, and priming factor of SVs is just detected in autaptic preparations when the synaptic responses are fully developed. Which could partly explain seemingly disparate results reported in previous works. Also, we provided direct evidence of SYT7 role in SV-priming and clamping of spontaneous release by rescuing the phenotype of SYT1-lacking neurons. In general, upstream of Ca^{2+}-triggered release SYT1 and SYT7 redundantly contribute to form and maintain the RRP of SVs and to clamp their spontaneous release. In contrast, during evoked NT-release SYT1 and SYT7 presence have opposite effects, increasing or reducing the probability of SV release, respectively. Therefore, in this work we provided with novel evidence of how two presynaptic proteins from the same family, by sharing similar and disparate roles, set balance in synaptic transmission. Finally, our careful titration of SYT1 expression at the presynaptic compartment shed light on the distinct sensitivity to STY1 expression of its different synaptic functions, being the priming function the least sensitive and the evoked Ca^{2+}-release the most sensitive. Importantly, our results from SYT1-deficient synapses demonstrated that changes in SYT1 expression could lead to aberrant synaptic function.

4.1. Interpretation of results in relation to similar works

As expected, we recapitulated previous results over SYT1's role as the Ca^{2+}-sensor for synchronous NT-release (Geppert *et al.*, 1994; Yoshihara & Littleton, 2002; Bacaj *et al.*, 2013; Brunger *et al.*, 2018; Bouazza-Arostegui *et al.*, 2022). Whether its specific role was to accelerate and synchronize Ca^{2+}-triggered release or, also, contributed to the total amount of exocytosis has been a matter of debate (Chapman, 2008; Liu *et al.*, 2009). While some works using autaptic cultures didn't detect differences in the total amount of NT-released (Nishiki & Augustine, 2004b, 2004a; Liu, *et al.*, 2009), most studies, including our quantitative experiments, demonstrated that deletion of SYT1 not only completely abolished synchronous NT-release but also reduced the total amount of NT-released (Bacaj *et al.*, 2013; Bouazza-Arostegui *et al.*, 2022; Liu *et*

al., 2009; Maximov & Südhof, 2005). Moreover, works using cultured neurons have also reported conflicting results regarding SYT1 functions regulating spontaneous release and priming of SVs. While in some studies SYT1-lacking neurons showed an increased spontaneous NT-release (DiAntonio & Schwarz, 1994; Littleton *et al.*, 1994; Pang *et al.*, 2006; Chicka *et al.*, 2008; Xu *et al.*, 2009), others didn't detect those differences in mini frequency (Geppert *et al.*, 1994). Similarly, early works of experiments performed in cultured SYT1-lacking neurons didn't detect a reduction in the RRP size of SVs (Bacaj et al., 2015; Geppert *et al.*, 1994; Liu *et al.*, 2009; Nagy *et al.*, 2006), but more recent studies have shown that SYT1 is likely involved in the constitution of the RRP of SVs (Huson *et al.*, 2020; Bouazza-Arostegui *et al.*, 2022). Our results confirms that SYT1 functions as a clamp of spontaneous-SV fusion and in the formation and maintenance of the RRP of SVs (Bouazza-Arostegui *et al.*, 2022). We showed that at early synaptic responses of autaptic neurons the spontaneous release mode and the RRP was unaffected, which suggests that those studies that didn't report such increase or decrease, respectively, might be influenced by the time-point those experiments were performed and/or the pooling of early and late synaptic responses. Moreover, redundancy between different SYT isoforms at different neuronal types could also account for such discrepancies in the results. Here, similar to previous reports (Bacaj *et al.*, 2013, 2015), we showed that SYT7 redundantly with SYT1 prime SVs and is involved in NT-release. Remarkably, we showed that SYT7 not only conditions the phenotype of the SYT1-lacking neurons but corroborates (Jackman *et al.*, 2016; Turecek & Regehr, 2018) that modulates synaptic plasticity.

4.2. Synaptotagmin-1 performs a triple synaptic function

Classically, mammalian and invertebrate loss-of-function mutants were generated to study synaptic function (Deng *et al.*, 2011; Geppert *et al.*, 1994; Schulze *et al.*, 1995). However, a more thorough control of protein amount is a powerful approach to uncover differences in molecular stoichiometry or signaling pathways. For instance, the titration of the SNARE protein Syntaxin-1 (Stx1) expression revealed that is involved in priming and vesicle fusion by highly related mechanisms (Arancillo *et al.*, 2013). Similarly, the detailed examination of the relation protein expression-priming function for the scaffold protein Munc13-1, revealed that a different degree of cooperativity of Munc13 molecules is needed to perform either docking or priming of SVs (Zarebidaki *et al.*, 2020). Continuing these works, we showed that exist clear differences in the sensitivity

of SYT1's functions to its presynaptic expression, obtaining a quantitative understanding of how SYT1 is differently involved at least in three consecutive and independent pathways of synaptic transmission.

SYT1 mediates fast synchronous NT-release through the interaction of its C2 domains with the acidic phospholipids of the PM and SNAREs (Fernández-Chacón *et al.*, 2001; Zhou *et al.*, 2015; Brunger *et al.*, 2018). Structural studies of SYT1 indicated that the acidic amino acid side chains at the C2A domain bind three Ca^{2+} ions and two at the C2B (Cheng *et al.*, 2004; Fernandez *et al.*, 2001; Ubach *et al.*, 1998). Ca^{2+}-binding causes hydrophobic residues at the tips of the Ca^{2+}-binding loops to insert into the membrane, generating curvature and triggering fusion of the SV with the PM (Martens *et al.*, 2007; Lynch *et al.*, 2008; Hui *et al.*, 2009). SYT1-mediated bending of the PM is a fundamental step to facilitate the opening of the initial fusion pore by bringing the two membranes into close proximity and initiating lipid exchange between them (Chernomordik & Kozlov, 2008; Kozlov *et al.*, 2010; Wu *et al.*, 2021). Furthermore, the membrane-bending activity of SYT1 might also contribute to pore expansion (Lynch *et al.*, 2008). However, the specific mechanism of how Ca^{2+}-binding to SYT1 leads to fusion is still unclear. We showed that the Ca^{2+}-evoked fusion pathway is highly sensitive to SYT1 presynaptic expression, where varying its presence affects vesicular release probability and short-term plasticity characteristics more than any other parameters. We argue that small changes in the number of SYT1 molecules might disrupt the formation and stoichiometry of functional SYT1-SNARE complexes necessary to overcome the energy barrier. Indeed, disruption of SYT1 function may allow another isoform to dominate fusion pore dynamics (Rao *et al.*, 2014; Wu *et al.*, 2021).

Besides SYT1 positive role in triggering release, SYT1 serves as a Ca^{2+}-sensitive fusion clamp, blocking SNARE-catalyzed fusion until the arrival of a Ca^{2+} signal (Popov & Poo, 1993; Ramakrishnan *et al.*, 2020; Söllner *et al.*, 1993). The supporting evidence of the clamp model came from how the disruption of SYT1 function led to higher rates of spontaneous SV exocytosis (DiAntonio & Schwarz, 1994; Littleton *et al.*, 1994; Chicka *et al.*, 2008; Xu *et al.*, 2009). In a recent model, SYT1 oligomerization would provide the molecular basis for SYT1 control of spontaneous release. Upon Ca^{2+} influx, a SYT1 multimeric structure would undergo a conformational change from a SV clamping mode to one that induces synchronous release (Bello *et al.*, 2018; Tagliatti *et al.*, 2020). SYT1 oligomerization has been proposed to occur either *via* its

N-terminal region (Bai *et al.*, 2000; Brose *et al.*, 1992; Perin *et al.*, 1991) or *via* its cytoplasmatic C2B domain (Chapman *et al.*, 1996; 1998; Hui *et al.*, 2011; Bello *et al.*, 2018). EM data showing ring-like structures of SYT1 (Wang et al., 2014), that are Ca^{2+}-sensitive (Bello et al., 2018; Tagliatti et al., 2020; Wang et al., 2014, 2017; Zanetti *et al.*, 2016), supported the cytoplasmatic model. In a recent work (Courtney *et al.*, 2021), a cluster of lysine residues in the juxtamembrane linker region was shown to govern homo-multimerization in an anionic lipid-dependent meaner. Moreover, mutations that neutralized the positively charged region not only disrupted SYT1 self-association but induced defects in clamping spontaneous SV release and evoked release (Courtney *et al.*, 2021). Considering the estimation that SVs contain approximately 15 copies of SYT1 (Takamori *et al.*, 2006), which in turn are the number of molecules that may form the ring-like structures (Wang *et al.*, 2014), could explain the sensitivity of this SYT1 function to a moderate decrease in SYT1 expression. Reductions in the number of SYT1 copies per SV could result in both defects in the formation of the oligomeric clamp and deficiencies of in its clamping function. Interestingly, we showed that overexpression of SYT7 rescued the enhanced spontaneous release phenotype that SYT1 knock-out neurons exhibit, and when both proteins are missing the phenotype is enhanced. This may indicate that SYT7 clamp spontaneous SV fusion independently from the formation of the SYT1 multimeric clamp.

Analysis of *Drosophila Syt1* mutants (Reist *et al.*, 1998) and *C. elegans Syt1*-null mutants (Jorgensen *et al.*, 1995) revealed a decrease in the number of SVs docked, suggesting also a role for SYT1 in this step of the exocytotic pathway. Similarly, in mouse embryonic chromaffin *Syt1*-null cells a strong docking defect was reported (de Wit *et al.*, 2009). It was suggested that SYT1 interactions with the anionic lipids on the PM, phosphatidylserine and phosphatidylinositol 4, 5-bisphosphate, mediate the docking of vesicles (Honigmann *et al.*, 2013; Parisotto *et al.*, 2012; Park *et al.*, 2012). Recent studies that combined high-pressure freezing and EM showed SV-docking defects in SYT1-knockout murine synapses and have come to support that pathway (Liu *et al.*, 2009; Chang *et al.*, 2018; Chen *et al.*, 2021). Conversely, defects in SV docking were suggested to be due to a reduction in the total number of SVs, related to developmental defects (Imig *et al.*, 2014). When functionally addressed, some studies showed that individual deletion of SYT1 had no detectable effect on the RRP size (Bacaj et al., 2015; Geppert et al., 1994; Maximov & Südhof, 2005), while others showed a reduction in the number of primed vesicles (Bouazza-Arostegui *et al.*, 2022;

Huson *et al.*, 2020). It was proposed that differences in the culture preparation might account for differences in the phenotype (Liu *et al.*, 2009), but works using the same autaptic system have reported contrary results (Bacaj *et al.*, 2015; Bouazza-Arostegui *et al.*, 2022; Geppert *et al.*, 1994; Huson *et al.*, 2020; Liu *et al.*, 2009). Importantly, we showed that a reduction in the RRP size only became detectable at mature synapses in autaptic cultures (Bouazza-Arostegui *et al.*, 2022). Furthermore, SYT1 priming activity was relatively insensitive to changes in SYT1 expression, and the additional suppression of SYT7 expression levels drastically reduced the number of primed SVs at all stages. Therefore, besides culturing conditions, conflicting results over detecting SYT1 function in priming might reside in the functional redundancy between synaptic protein isoforms. The fact that SV priming was impaired only after a major drop in SYT1 concentration shows that low SYT1 expression was sufficient to preserve maximum priming activity, suggests an independent pathway for priming than for regulating NT-release.

4.3. Synaptotagmin-1 synaptic disfunction and neurodevelopmental disorders

An increasing number of neurodevelopmental disorders are associated with mutations in genes encoding synaptic proteins (Claes *et al.*, 2001; McTague *et al.*, 2016; Bonnycastle *et al.*, 2020; Alten *et al.*, 2021). The substantial phenotypic heterogeneity observed in SYT1-associated disorders (Baker *et al.*, 2015, 2018) suggests that allelic expressivity plays an important role in determining disease severity (Bradberry *et al.*, 2020). Therefore, is relevant to investigate how SYT1 wild-type and mutant alleles vary in expression across neuronal subtypes and brain regions in the patient. Although the titration of $SYT1_{D304G}$, $SYT1_{D366E}$, or $SYT1_{I368T}$ mutants resulted in a ponent dominant-negative inhibition of SV exocytosis (Bradberry *et al.*, 2020), a loss-of-function phenotype is not excluded. At least one of the variants ($SYT1_{M303K}$) is dysfunctional in its level of expression and retention at the nerve terminals *(Baker et al.*, 2018). Furthermore, $SYT1_{D304G}$ and $SYT1_{D366E}$ variants failed to re-localize to nerve terminals following stimulation, indicative of impairments in endocytic retrieval and trafficking of SYT1 (Baker *et al.*, 2018). In our study, we showed that haploinsufficiency of SYT1 resulted in an aberrant spontaneous release phenotype and decreased release probability with additional consequences in short-term plasticity characteristics. If patients with heterozygous SYT1 mutations have deficiencies in SYT1 expression/localization could lead to synaptic inefficacy and,

ultimately, contribute to network disfunction. While allelic expressivity may not explain the whole pathophysiology, it could exacerbate synaptic manifestations of individual SYT1 variants (Baker *et al.*, 2018; Bradberry *et al.*, 2020). In fact, a recent article showed that an aberrant spontaneous NT-release phenotype, due to SNAP25 mutations, could result in developmental and epileptic encephalopathies (Alten *et al.*, 2021). Conversely, our findings indicate that the patient's pathophysiology that could derive from changes in the SYT1 expression levels are unlikely to be related to SYT1's priming activity.

4.4. Synaptotagmin-7 and Synaptotagmin-1 redundant and antagonistic roles

SYT7 has similar Ca^{2+}-dependent binding and tilting properties to SYT1, but with a lower Ca^{2+}-sensing threshold and stronger membrane binding affinity (Hui *et al.*, 2005; Chon *et al.*, 2015; Tran *et al.*, 2019). This isoform has been shown to be involved in exocytosis in chromaffin and pancreatic cells (Sugita *et al.*, 2001; Shin *et al.*, 2002; Schonn *et al.*, 2008; Bendahmane *et al.*, 2020), suggesting a role in asynchronous release; a form of NT-release that is characterized by a variable delay following a stimulus (Kaeser & Regehr, 2014). However, initial electrophysiological recordings of SYT7-lacking neurons didn't show changes in this release mode (Maximov *et al.*, 2008). Posterior studies did describe a role in asynchronous release during high-frequency (HF) stimulation at the zebrafish neuromuscular junctions (Wen *et al.*, 2010) and hippocampal murine neurons (Bacaj *et al.*, 2013). Currently, SYT7 has been consistently reported to regulate two forms of plasticity at various types of synapses (Huson & Regehr, 2020; Silva *et al.*, 2021). First, it has been implicated in SV-replenishment in response to HF repetitive stimulation (Chen *et al.*, 2017; Liu *et al.*, 2014; Vevea *et al.*, 2021). Second, it was shown that Ca^{2+}-binding at its C2A domain was required for synaptic facilitation (Jackman *et al.*, 2016), as reported in diverse neuronal types (Jackman *et al.*, 2016; Chen *et al.*, 2017; Turecek *et al.*, 2017; Turecek & Regehr, 2018; Fujii *et al.*, 2021; Vevea *et al.*, 2021). When we overexpress SYT7 in either wild-type or SYT1-null synapses a strong facilitatory phenotype of the synaptic responses appeared or was exacerbated, respectively. Which contrasts with SYT1's role in increasing release probability and necessary for depression of synaptic responses during repetitive stimulation. Therefore, we interpret that SYT7 antagonizes SYT1 function during short-term plasticity. SYT7 may promote facilitation through two mechanisms. First, as facilitation may involve enhanced docking, SYT7 could function

as a Ca^{2+}-dependent docking factor, similar to Munc13-1 presynaptic protein (Lipstein *et al.*, 2021). During repetitive stimulation SYT7 would function as a SV-replenishment machine by interacting with PM and vesicle membrane upon binding Ca^{2+} (Liu *et al.*, 2014; Silva *et al.*, 2021), so more SVs would be available to be released. Second, putative competition between SYT1 and SYT7 may contribute to the modulation of NT-release. SYT7 may be interfering with SYT1's activity during triggered release, removing the number of effective SYT1 molecules that bind to SNAREs to form fusion-competent SYT1-SNARE complexes. In fact, both SYT1 and SYT7 bind to SNARE complexes, which is impaired by the top-loop Ca^{2+}-binding sequence mutations of the C2-domains (Bacaj *et al.*, 2015). But there are critical differences between their Ca^{2+}-binding domains since SYT7-C2B domain when transplanted into SYT1 did not rescue SYT1 function (Xue *et al.*, 2010). Interestingly, in neurons expressing the SNAP23 variant SYT7 might regulate asynchronous NT-release (Weber *et al.*, 2014), indicating that differential expression of presynaptic protein isoforms across cell-types and development stages conditions synaptic function. Interestingly, we found that suppressing SYT7 expression in SYT1 knock-out neurons led to a strong increase in spontaneous SV-fusion events. In fact, overexpression of any of the synaptotagmin isoforms in the SYT1 knock-out neurons reduced spontaneous release to wild-type levels, indicating that SYT7 clamping function might be independent of SYT1 presence. As discussed above, SYT1 might clamp spontaneous release via homo-multimerization. Whether the redundant clamping function of SYT7 is a secondary effect as an overall inhibitor of NT-release or is a putative function needs to be resolved. In a compelling model, the SYT1 oligomeric clamp would be augmented by the SYT7 C2B domain bound via the "tripartite" site (Zhou *et al.*, 2017), providing an extremely tight dual clamp (Rothman *et al.*, 2017; Brunger *et al.*, 2018; Grushin *et al.*, 2019). Overall, we conclude that the expression strength and the copy number of SYT1/7 proteins contribute to determine NT-release properties.

Like in forebrain neurons (Bacaj *et al.*, 2015), ablation of SYT1 and SYT7 expression in hippocampal neurons drastically decreased the RRP size of SVs. Previous works showed that for maintaining the RRP size of SVs, SYT1 and SYT7 do not require Ca^{2+} (Bacaj *et al.*, 2015). Our expression- and time-sensitive experiments demonstrated that SYT7 redundantly with SYT1 primes SVs at hippocampal synapses. Furthermore, we showed that none of them are a limiting factor for the RRP size of SVs, but SYT1 function becomes essential over time at glutamatergic synapses. Only at initial culture

stages SYT7 fully compensate for SYT1 loss, while only partially at more mature synapses. Importantly, by overexpressing SYT7 in *Syt1*-null mature neurons, we rescued the RPP size of SVs, suggesting that SYT7 priming activity can be carried-out mechanistically independent to SYT1. Taking together, whether SYT7 redundant/antagonistic roles regulating NT-release upon stimulation and clamping spontaneous SV-fusion are part of the same mechanism needs to be investigated. In contrast, the molecular mechanisms underlying SYT1/7 redundant Ca^{2+}-independent priming activity seem to be independent of each other.

4.5. Strengths and weaknesses of the study and implications for future research

Properly assessing protein expression levels was critical for our assessments and conclusions. Although not fully quantitative, using ratiometric immunocytochemistry (ICC) quantification of the protein expression in autaptic neurons has been consistently shown to be the most reliable and adequate approach (Xue *et al.*, 2007; Weston *et al.*, 2011; Arancillo *et al.*, 2013; Zimmermann *et al.*, 2014; Zarebidaki *et al.*, 2020; Vardar *et al.*, 2021), and consistent with western blot (WB) quantifications (Zarebidaki *et al.*, 2020). ICC has the advantage of quantifying the protein of interest in the functionally relevant compartment. Moreover, utilizing SYT1/SYT7-to-VGLUT1 signal ensures that we do not average expression across glutamatergic and GABAergic neurons, which would not be possible when using bulk analysis methods like WB or RT-PCR. Future studies using the novel patch-seq technique, which combines transcriptome analysis with the electrophysiological and morphological characterization of individual neurons (Cadwell *et al.*, 2016; Lipovsek *et al.*, 2021), could provide complementary results regarding the relation of molecular composition with specific synaptic functions. Indeed, we limited our work to excitatory synapses, which opened the door to further studies analyzing whether SYT1/7 protein exhibit a similar interplay in other types of chemical synapses.

Using autaptic neurons gave us full control of synaptic input and output. While this system has the advantage to provide mechanistic information about a synaptic component, it has the disadvantage of missing its network and homeostatic effects. In fact, network connectivity can regulate synapse phenotype, including the frequency of spontaneous release events, the kinetics of evoked release and release probability in the absence of SYT1 (Liu *et al.*, 2009). Also, our work indicated that future assessments of synaptic responses in autaptic neurons should consider their

developmental stage. By pooling data from differently develop sets over large time windows may lead to missing a phenotypic trait. This work helps others to appreciate how differences in the experimental design may contribute to different outcomes.

From a previous study, it is established that synaptotagmin isoform regulation during development is a mechanisms that fine-tunes the speed, reliability, and plasticity of transmitter release at the calyx of Held synapse (Kochubey *et al.*, 2016). We have further confirmed that SYT1 and SYT7 redundant and antagonistic functions are conditioned by their expression levels. Future studies of aberrant forms of neuronal communication associated with SYT1 or SYT7 mutations will tackle how the SYT1/SYT7 balance changes overtime at different neuronal types. Furthermore, it would be interesting to study whether SYT7 affects SYT1 role in vesicle endocytosis (Poskanzer *et al.*, 2003; Yao *et al.*, 2012; Liang *et al.*, 2017). Finally, this work has thoroughly investigated how the presence SYT1 and SYT7 impacts synaptic function, but whether their functional interplay is translated into morphological changes at synapses remains to be elucidated.

5. Conclusions

- SYT1 is essential for synchronous Ca^{2+}-dependent NT-release and perform at least two additional functions upstream to the evoked Ca^{2+}-triggering step, priming SVs and clamping spontaneous SV exocytosis.
- SYT1's functions have distinct sensitivity to expression levels at the presynaptic compartment, being its priming activity the least sensitive and its regulation of Ca^{2+}-triggered release the most sensitive.
- The first-time electrophysiological characterization of *Syt1* heterozygous neurons phenotype indicated that a deficit in SYT1 expression/localization leads to synaptic malfunction.
- SYT1-laking hippocampal neurons phenotype develops overtime in autaptic cultures. While its function as Ca^{2+} sensor is essential at all stages, the phenotypic traits regarding priming and clamping of SVs are only exhibit at later culture stages of hippocampal neurons.
- SYT7 isoform redundantly with SYT1 is well capable of priming SVs and clamping spontaneous SV fusion.
- While SYT1 is sufficient and necessary for the maintenance of the RRP size of SVs and clamping spontaneous SV fusion, SYT7 becomes only essential in the absence of SYT1.
- Neither SYT1 nor SYT7 are a limiting factor for the RRP size of SVs or the clamping of spontaneous NT-release.
- SYT7 works as an antagonistic force to SYT1 in NT-release during repetitive stimulation. While SYT1 induce depression of the synaptic responses and positively regulates release probability of neurons, SYT7 presence promotes a facilitatory phenotype and, likely, negatively regulates release probability.

Reference list

Alten, B., Zhou, Q., Shin, O. H., Esquivies, L., Lin, P. Y., Ian, K., Sun, R., Chung, W. K., Monteggia, L. M., Brunger, A. T., Ege, T., White, K. I., Sun, R., Chung, W. K., Monteggia, L. M., Brunger, A. T., & Kavalali, E. T. (2021). Role of Aberrant Spontaneous Neurotransmission in SNAP25-Associated Encephalopathies. *Neuron*, *109*(1), 59-72.e5 https://doi.org/10.1016/j.neuron.2020.10.012

Arancillo M, Min SW, Gerber S, Münster-Wandowski A, Wu YJ, Herman M, Trimbuch T, Rah JC, Ahnert-Hilger G, Riedel D, Südhof TC, Rosenmund C. (2013) Titration of Syntaxin1 in mammalian synapses reveals multiple roles in vesicle docking, priming, and release probability. *Journal of Neuroscience, 33*(42):16698-714. https://doi.org/10.1523/JNEUROSCI.0187-13.2013

Augustin I, Rosenmund C, Südhof TC, Brose N. (1999). Munc13-1 is essential for fusion competence of glutamatergic synaptic vesicles. *Nature, 400*(6743):457-61. https://doi.org/10.1038/22768

Bacaj, T., Wu, D., Burré, J., Malenka, R. C., Liu, X., & Südhof, T. C. (2015). Synaptotagmin-1 and -7 Are Redundantly Essential for Maintaining the Capacity of the Readily-Releasable Pool of Synaptic Vesicles. *PLoS Biology*, *13*(10), 1–26. https://doi.org/10.1371/journal.pbio.1002267

Bacaj, T., Wu, D., Yang, X., Morishita, W., Zhou, P., Xu, W., Malenka, R. C., & Südhof, T. C. (2013). Asynchronous Phases of Neurotransmitter Release. *Neuron*, *80*(4), 947–959. https://doi.org/10.1016/j.neuron.2013.10.026

Bai, J., Earles, C. A., Lewis, J. L., & Chapman, E. R. (2000). Membrane-embedded synaptotagmin penetrates cis or trans target membranes and clusters via a novel mechanism. *The Journal of Biological Chemistry*, *275*(33), 25427–25435. https://doi.org/10.1074/JBC.M906729199

Baker, K., Gordon, S. L., Grozeva, D., Van Kogelenberg, M., Roberts, N. Y., Pike, M., Blair, E., Hurles, M. E., Chong, W. K., Baldeweg, T., Kurian, M. A., Boyd, S. G., Cousin, M. A., & Raymond, F. L. (2015). Identification of a human synaptotagmin-1 mutation that perturbs synaptic vesicle cycling. *Journal of Clinical Investigation*, *125*(4), 1670–1678. https://doi.org/10.1172/JCI79765

Baker, K., Gordon, S. L., Melland, H., Bumbak, F., Scott, D. J., Jiang, T. J., Owen, D., Turner, B. J., Boyd, S. G., Rossi, M., Al-Raqad, M., Elpeleg, O., Peck, D., Mancini, G. M. S., Wilke, M., Zollino, M., Marangi, G., Weigand, H., Borggraefe,

I., Haack, T., Stark, Z., Sadedin, Broad Center for Mendelian Genomics, Tan, T.Y., Jiang, Y., Gibbs, R.A., Ellingwood, S., Amaral, M., Kelley, W., Kurian, M.A., Raymond, F.L. (2018). SYT1-associated neurodevelopmental disorder: A case series. *Brain*, *141*(9), 2576–2591. https://doi.org/10.1093/brain/awy209

Bekkers, J. M., & Stevens, C. F. (1991). Excitatory and inhibitory autaptic currents in isolated hippocampal neurons maintained in cell culture. *Proceedings of the National Academy of Sciences of the United States of America*, *88*(17), 7834–7838. https://doi.org/10.1073/pnas.88.17.7834

Bello, O. D., Jouannot, O., Chaudhuri, A., Stroeva, E., Coleman, J., Volynski, K. E., Rothman, J. E., & Krishnakumar, S. S. (2018). Synaptotagmin oligomerization is essential for calcium control of regulated exocytosis. *Proceedings of the National Academy of Sciences of the United States of America*, *115*(32), E7624–E7631. https://doi.org/10.1073/pnas.1808792115

Bendahmane, M., Morales, A., Kreutzberger, A. J. B., Schenk, N. A., Mohan, R., Bakshi, S., Philippe, J. M., Zhang, S., Kiessling, V., Tamm, L. K., Giovannucci, D. R., Jenkins, P. M., & Anantharam, A. (2020). Synaptotagmin-7 enhances calcium-sensing of chromaffin cell granules and slows discharge of granule cargos. *Journal of Neurochemistry*, *154*(6), 598–617. https://doi.org/10.1111/jnc.14986

Bonnycastle, K., Davenport, E. C., & Cousin, M. A. (2020). Presynaptic dysfunction in neurodevelopmental disorders: Insights from the synaptic vesicle life cycle. *Journal of Neurochemistry*, *157*(2):179-207. https://doi.org/10.1111/jnc.15035

Bouazza-Arostegui, B., Camacho, M., Brockmann, M. M., Zobel, S., & Rosenmund, C. (2022). Deconstructing Synaptotagmin-1's Distinct Roles in Synaptic Vesicle Priming and Neurotransmitter Release. *Journal of Neuroscience*, *42*(14):2856-2871. https://doi.org/10.1523/jneurosci.1945-21.2022

Bradberry, M. M., Courtney, N. A., Dominguez, M. J., Lofquist, S. M., Knox, A. T., Sutton, R. B., & Chapman, E. R. (2020). Molecular Basis for Synaptotagmin-1-Associated Neurodevelopmental Disorder. *Neuron*, *107*(1), 52-64.e7. https://doi.org/10.1016/j.neuron.2020.04.003

Broadie, K., Bellen, H. J., DiAntonio, A., Littleton, J. T., & Schwarz, T. L. (1994). Absence of synaptotagmin disrupts excitation-secretion coupling during synaptic transmission. *Proceedings of the National Academy of Sciences of the United States of America*, *91*(22), 10727–10731.

https://doi.org/10.1073/pnas.91.22.10727

Brockmann, M. M., Zarebidaki, F., Camacho, M., Grauel, M. K., Trimbuch, T., Südhof, T. C., & Rosenmund, C. (2020). A Trio of Active Zone Proteins Comprised of RIM-BPs, RIMs, and Munc13s Governs Neurotransmitter Release. *Cell Reports*, *32*(5), 107960. https://doi.org/10.1016/j.celrep.2020.107960

Brose, N., Petrenko, A. G., Sudhof, T. C., & Jahn, R. (1992). Synaptotagmin: A calcium sensor on the synaptic vesicle surface. *Science*, *256*(5059), 1021–1025. https://doi.org/10.1126/science.1589771

Brunger, A. T., Choi, U. B., Lai, Y., Leitz, J., & Zhou, Q. (2018). Molecular Mechanisms of Fast Neurotransmitter Release. *Annual Reviews of Biophysics, 47*:469-497. https://doi.org/10.1146/annurev-biophys-070816-034117

Brunger, A. T., Leitz, J., Zhou, Q., Choi, U. B., & Lai, Y. (2018). Ca2+-Triggered Synaptic Vesicle Fusion Initiated by Release of Inhibition. *Trends in Cell Biology*, *28*(8), 631–645. https://doi.org/10.1016/J.TCB.2018.03.004

Cadwell, C. R., Palasantza, A., Jiang, X., Berens, P., Deng, Q., Yilmaz, M., Reimer, J., Shen, S., Bethge, M., Tolias, K. F., Sandberg, R., & Tolias, A. S. (2016). Electrophysiological, transcriptomic and morphologic profiling of single neurons using Patch-seq. *Nature Biotechnology*, *34*(2), 199–203. https://doi.org/10.1038/nbt.3445

Camacho, M., Quade, B., Trimbuch, T., Xu, J., Sari, L., Rizo, J., & Rosenmund, C. (2021). Control of neurotransmitter release by two distinct membrane- - binding faces of the Munc13- - 1 C 1 C 2 B region. *ELife*, *10*, 1–34. https://doi.org/10.7554/ELIFE.72030

Catterall, W. A. (2011). Voltage-gated calcium channels. *Cold Spring Harbor Perspectives in Biology*, *3*(8), 1–23. https://doi.org/10.1101/cshperspect.a003947

Chang, S., Trimbuch, T., Rosenmund, C. (2018). Synaptotagmin-1 drives synchronous Ca 2+ -triggered fusion by C 2 B-domain-mediated synaptic-vesicle-membrane attachment. *Nature Neuroscience*, *21*(1), 33–42. https://doi.org/10.1038/s41593-017-0037-5

Chapman, E. R. (2008). How does synaptotagmin trigger neurotransmitter release? *Annual Review of Biochemistry*, *77*, 615–641. https://doi.org/10.1146/annurev.biochem.77.062005.101135

Chapman, E. R., An, S., Edwardson, J. M., & Jahn, R. (1996). A novel function for the second C2 domain of synaptotagmin. Ca2+-triggered dimerization. *The Journal of Biological Chemistry*, *271*(10), 5844–5849. https://doi.org/10.1074/JBC.271.10.5844

Chapman, E. R., & Davis, A. F. (1998). Direct interaction of a Ca2+-binding loop of synaptotagmin with lipid bilayers. *Journal of Biological Chemistry*, *273*(22), 13995–14001. https://doi.org/10.1074/jbc.273.22.13995

Chen, C., & Jonas, P. (2017). Synaptotagmins: That's Why So Many. *Neuron*, *94*(4), 694–696. https://doi.org/10.1016/j.neuron.2017.05.011

Chen, C., Satterfield, R., Young, S. M., & Jonas, P. (2017). Triple Function of Synaptotagmin 7 Ensures Efficiency of High-Frequency Transmission at Central GABAergic Synapses. *Cell Reports*, *21*(8), 2082–2089. https://doi.org/10.1016/j.celrep.2017.10.122

Chen, Y., Wang, Y. H., Zheng, Y., Li, M., Wang, B., Wang, Q. W., Fu, C. L., Liu, Y. N., Li, X., & Yao, J. (2021). Synaptotagmin-1 interacts with PI(4,5)P2 to initiate synaptic vesicle docking in hippocampal neurons. *Cell Reports*, *34*(11), 108842. https://doi.org/10.1016/j.celrep.2021.108842

Cheng, Y., Sequeira, S. M., Malinina, L., Tereshko, V., Söllner, T. H., & Patel, D. J. (2004). Crystallographic identification of Ca2+ and Sr2+ coordination sites in synaptotagmin I C2B domain. *Protein Science*, *13*(10):2665–2672. https://doi.org/10.1110/ps.04832604

Chernomordik, L. V., & Kozlov, M. M. (2008). Mechanics of membrane fusion. *Nature Structural and Molecular Biology, 15*(7):675–683. https://doi.org/10.1038/nsmb.1455

Chicka, M. C., Hui, E., Liu, H., & Chapman, E. R. (2008). Synaptotagmin arrests the SNARE complex before triggering fast, efficient membrane fusion in response to Ca2+. *Nature Structural and Molecular Biology*, *15*(8), 827–835. https://doi.org/10.1038/nsmb.1463

Chon, N. L., Osterberg, J. R., Henderson, J., Khan, H. M., Reuter, N., Knight, J. D., Lin, H., Knight, D., Lin, H., Knight, J. D., & Lin, H. (2015). Membrane Docking of the Synaptotagmin 7 C2A Domain: Computation Reveals Interplay between Electrostatic and Hydrophobic Contributions. *Biochemistry*, *54*(37):5696–5711. https://doi.org/10.1021/acs.biochem.5b00421

Claes, L., Del-Favero, J., Ceulemans, B., Lagae, L., Van Broeckhoven, C., & De

Jonghe, P. (2001). De Novo Mutations in the Sodium-Channel Gene SCN1A Cause Severe Myoclonic Epilepsy of Infancy. *American Journal of Human Genetics*, *68*(6), 1327. https://doi.org/10.1086/320609

Courtney, K. C., Vevea, J. D., Li, Y., Wu, Z., Zhang, Z., & Chapman, E.R. (2021). Synaptotagmin 1 oligomerization via the juxtamembrane linker regulates spontaneous and evoked neurotransmitter release. *Proceedings of the National Academy of Sciences of the United States of America*, *118*(48):e2113859118. https://doi.org/10.1073/pnas.2113859118

de Wit, H., Walter, A. M., Milosevic, I., Gulyás-Kovács, A., Riedel, D., Sørensen, J. B., & Verhage, M. (2009). Synaptotagmin-1 Docks Secretory Vesicles to Syntaxin-1/SNAP-25 Acceptor Complexes. *Cell*, *138*(5), 935–946. https://doi.org/10.1016/j.cell.2009.07.027

Deng, L., Kaeser, P. S., Xu, W., & Südhof, T. C. (2011). RIM proteins activate vesicle priming by reversing autoinhibitory homodimerization of munc13. *Neuron*, *69*(2), 317–331. https://doi.org/10.1016/j.neuron.2011.01.005

DiAntonio, A., & Schwarz, T. L. (1994). The effect on synaptic physiology of synaptotagmin mutations in drosophila. *Neuron*, *12*(4), 909–920. https://doi.org/10.1016/0896-6273(94)90342-5

Fatt, P., & Katz, B. (1952). Spontaenous subthreshold activity at motor nerve endings. *The Journal of Physiology, 117*(1):109-28

Fernández-Chacón, R., Königstorfer, A., Gerber, S. H., García, J., Matos, M. F., Stevens, C. F., Brose, N., Rizo, J., Rosenmund, C., & Südhof, T. C. (2001). Synaptotagmin I functions as a calcium regulator of release probability. *Nature*, *410*(6824), 41–49. https://doi.org/10.1038/35065004

Fernandez, I., Araç, D., Ubach, J., Gerber, S. H., Shin, O. H., Gao, Y., Anderson, R. G. W., Südhof, T. C., & Rizo, J. (2001). Three-dimensional structure of the synaptotagmin 1 C2B-domain: Synaptotagmin 1 as a phospholipid binding machine. *Neuron*, *32*(6), 1057–1069. https://doi.org/10.1016/S0896-6273(01)00548-7

Fujii, T., Sakurai, A., Littleton, J. T., & Yoshihara, M. (2021). Synaptotagmin 7 switches short-term synaptic plasticity from depression to facilitation by suppressing synaptic transmission. *Scientific Reports*, *11*(1), 1–9. https://doi.org/10.1038/s41598-021-83397-5

Geppert, M., Goda, Y., Hammer, R. E., Li, C., Rosahl, T. W., Stevens, C. F., &

Südhof, T. C. (1994). Synaptotagmin I: a major Ca2+ sensor for transmitter release at a central synapse. *Cell*, *79*(4), 717–727. https://doi.org/10.1016/0092-8674(94)90556-8

Grushin, K., Wang, J., Coleman, J., Rothman, J. E., Sindelar, C. V., & Krishnakumar, S. S. (2019). Structural basis for the clamping and Ca2+ activation of SNARE-mediated fusion by synaptotagmin. *Nature Communications*, *10*(1), 1–12. https://doi.org/10.1038/s41467-019-10391-x

Gustavsson, N., Lao, Y., Maximov, A., Chuang, J. C., Kostromina, E., Repa, J. J., Li, C., Radda, G. K., Südhof, T. C., & Han, W. (2008). Impaired insulin secretion and glucose intolerance in synaptotagmin-7 null mutant mice. *Proceedings of the National Academy of Sciences of the United States of America*, *105*(10), 3992–3997. https://doi.org/10.1073/pnas.0711700105

Hammarlund, M., Palfreyman, M. T., Watanabe, S., Olsen, S., & Jorgensen, E. M. (2007). Open Syntaxin Docks Synaptic Vesicles. *PLOS Biology*, *5*(8), e198. https://doi.org/10.1371/JOURNAL.PBIO.0050198

Han, Y., Kaeser, P. S., Südhof, T. C., & Schneggenburger, R. (2011). RIM determines Ca 2+ channel density and vesicle docking at the presynaptic active zone. *Neuron, 69*(2):304-16. https://doi.org/10.1016/j.neuron.2010.12.014

Harris, K. m., & Sultan, P. (1995). Variation in the number, location and size of synaptic vesicles provides an anatomical basis for the nonuniform probability of release at hippocampal CA1 synapses. *Neuropharmacology*, *34*(11), 1387–1395. https://doi.org/10.1016/0028-3908(95)00142-S

Honigmann, A., Van Den Bogaart, G., Iraheta, E., Risselada, H. J., Milovanovic, D., Mueller, V., Müllar, S., Diederichsen, U., Fasshauer, D., Grubmüller, H., Hell, S. W., Eggeling, C., Kühnel, K., & Jahn, R. (2013). Phosphatidylinositol 4,5-bisphosphate clusters act as molecular beacons for vesicle recruitment. *Nature Structural and Molecular Biology*, *20*(6):679-86. https://doi.org/10.1038/nsmb.2570

Hui, E., Bai, J., Wang, P., Sugimori, M., Llinas, R. R., & Chapman, E. R. (2005). Three distinct kinetic groupings of the synaptotagmin family: Candidate sensors for rapid and delayed exocytosis. *Proceedings of the National Academy of Sciences of the United States of America*, *102*(14), 5210–5214. https://doi.org/10.1073/pnas.0500941102

Hui, E., Gaffaney, J. D., Wang, Z., Johnson, C. P., Evans, C. S., & Chapman, E. R.

(2011). Mechanism and function of synaptotagmin-mediated membrane apposition. *Nature Structural and Molecular Biology*, *18*(7), 813. https://doi.org/10.1038/NSMB.2075

Hui, E., Johnson, C. P., Yao, J., Dunning, F. M., & Chapman, E. R. (2009). Synaptotagmin-Mediated Bending of the Target Membrane Is a Critical Step in Ca2+-Regulated Fusion. *Cell*, *138*(4), 709–721. https://doi.org/10.1016/J.CELL.2009.05.049

Huson, V., Meijer, M., Dekker, R., Veer, M. Ter, Ruiter, M., van Weering, J., Verhage, M., & Cornelisse, L. N. (2020). Post-tetanic potentiation lowers the energy barrier for synaptic vesicle fusion independently of synaptotagmin-1. *ELife*, *9*, 1–56. https://doi.org/10.7554/ELIFE.55713

Huson, V., & Regehr, W. G. (2020). Diverse roles of Synaptotagmin-7 in regulating vesicle fusion. *Current Opinion in Neurobiology*, *63*, 42–52. https://doi.org/10.1016/j.conb.2020.02.006

Imig, C., Min, S. W., Krinner, S., Arancillo, M., Rosenmund, C., Südhof, T. C., Rhee, J. S., Brose, N., & Cooper, B. H. (2014). The Morphological and Molecular Nature of Synaptic Vesicle Priming at Presynaptic Active Zones. *Neuron*, *84*(2), 416–431. https://doi.org/10.1016/j.neuron.2014.10.009

Jackman, S. L., Turecek, J., Belinsky, J. E., & Regehr, W. G. (2016). The calcium sensor synaptotagmin 7 is required for synaptic facilitation. *Nature*, *529*(7584):88-91. https://doi.org/10.1038/nature16507

Jahn, R., & Scheller, R. H. (2006). SNAREs - Engines for membrane fusion. *Nature Reviews Molecular Cell Biology*, *7*(9), 631–643. https://doi.org/10.1038/nrm2002

Jorgensen, E. M., Hartwieg, E., Schuske, K., Nonet, M. L., Jin, Y., & Horvitz, H. R. (1995). Defective recycling of synaptic vesicles in synaptotagmin mutants of caenorhabditis elegans. *Nature*, *378*(6553), 196–199. https://doi.org/10.1038/378196a0

Jorquera, R. A., Huntwork-Rodriguez, S., Akbergenova, Y., Cho, R. W., & Troy Littleton, J. (2012). Complexin Controls Spontaneous and Evoked Neurotransmitter Release by Regulating the Timing and Properties of Synaptotagmin Activity. *Journal of Neuroscience*, *32*(50), 18234–18245. https://doi.org/10.1523/JNEUROSCI.3212-12.2012

Kaeser, P. S., & Regehr, W. G. (2014). Molecular mechanisms for synchronous, asynchronous, and spontaneous neurotransmitter release. *Annual Review of*

Physiology, 76:333–363. https://doi.org/10.1146/annurev-physiol-021113-170338

Kaeser, P. S., & Regehr, W. G. (2017). The readily releasable pool of synaptic vesicles. *Current Opinion in Neurobiology*, *43*, 63–70. https://doi.org/10.1016/J.CONB.2016.12.012

Katz, B. (1969). *The release of neural transmitter substances*. Springfield, Ill., Thomas.

Kavalali, E. T. (2015). The mechanisms and functions of spontaneous neurotransmitter release. *Nature Reviews of Neuroscience, 16*(1):5-16. https://doi.org/10.1038/nrn3875

Kochubey, O., Babai, N., & Schneggenburger, R. (2016). A Synaptotagmin Isoform Switch during the Development of an Identified CNS Synapse. *Neuron*, *90*(5), 984–999. https://doi.org/10.1016/j.neuron.2016.04.038

Kozlov, M. M., McMahon, H. T., & Chernomordik, L. V. (2010). Protein-driven membrane stresses in fusion and fission. *Trends in Biochemical Sciences*, *35*(12), 699–706. https://doi.org/10.1016/J.TIBS.2010.06.003

Lee, J., Guan, Z., Akbergenova, Y., & Troy Littleton, J. (2013). Genetic analysis of synaptotagmin C2 domain specificity in regulating spontaneous and evoked neurotransmitter release. *Journal of Neuroscience*, *33*(1), 187–200. https://doi.org/10.1523/JNEUROSCI.3214-12.2013

Li, C., Ullrich, B., Zhang, J. Z., Anderson, R. G. W., Brose, N., & Südhof, T. C. (1995). Ca2 +-dependent and -independent activities of neural and non-neural synaptotagmins. *Nature*, *246*(5429), 170. https://doi.org/10.1038/246170a0

Li, Y. C., Chanaday, N. L., Xu, W., & Kavalali, E. T. (2017). Synaptotagmin-1- and Synaptotagmin-7-Dependent Fusion Mechanisms Target Synaptic Vesicles to Kinetically Distinct Endocytic Pathways. *Neuron*, *93*(3), 616-631.e3. https://doi.org/10.1016/j.neuron.2016.12.010

Liang, K., Wei, L., & Chen, L. (2017). Exocytosis, endocytosis, and their coupling in excitable cells. *Frontiers in Molecular Neuroscience*, *10*:109. https://doi.org/10.3389/fnmol.2017.00109

Lipovsek, M., Bardy, C., Cadwell, C. R., Hadley, K., Kobak, D., & Tripathy, S. J. (2021). Patch-seq: Past, present, and future. *Journal of Neuroscience*, *41*(5), 937–946. https://doi.org/10.1523/JNEUROSCI.1653-20.2020

Lipstein, N., Chang, S., Lin, K. H., López-Murcia, F. J., Neher, E., Taschenberger,

H., & Brose, N. (2021). Munc13-1 is a Ca 2+-phospholipid-dependent vesicle priming hub that shapes synaptic short-term plasticity and enables sustained neurotransmission. *Neuron*, *109*(24), 3980-4000.e7. https://doi.org/10.1016/J.NEURON.2021.09.054

Littleton, J. T., Stern, M., Perin, M., & Bellen, H. J. (1994). Calcium dependence of neurotransmitter release and rate of spontaneous vesicle fusions are altered in Drosophila synaptotagmin mutants. *Proceedings of the National Academy of Sciences of the United States of America*, *91*(23), 10888–10892. https://doi.org/10.1073/pnas.91.23.10888

Liu, H., Bai, H., Hui, E., Yang, L., Evans, C. S., Wang, Z., Kwon, S. E., & Chapman, E. R. (2014). Synaptotagmin 7 functions as a Ca2+-sensor for synaptic vesicle replenishment. *ELife*, *3*, 1–18. https://doi.org/10.7554/elife.01524

Liu, H., Dean, C., Arthur, C. P., Dong, M., & Chapman, E. R. (2009). Autapses and networks of hippocampal neurons exhibit distinct synaptic transmission phenotypes in the absence of synaptotagmin I. *Journal of Neuroscience*, *29*(23), 7395–7403. https://doi.org/10.1523/JNEUROSCI.1341-09.2009

Lynch, K. L., Gerona, R. R. L., Kielar, D. M., Martens, S., McMahon, H. T., & Martin, T. F. J. (2008). Synaptotagmin-1 utilizes membrane bending and SNARE binding to drive fusion pore expansion. *Molecular Biology of the Cell*, *19*(12), 5093–5103. https://doi.org/10.1091/mbc.E08-03-0235

Martens, S., Kozlov, M. M., & McMahon, H. T. (2007). How synaptotagmin promotes membrane fusion. *Science*, *316*(5828), 1205–1208. https://doi.org/10.1126/SCIENCE.1142614

Matthew, W. D., Tsavaler, L., & Reichardt, L. F. (1981). Identification of a synaptic vesicle-specific membrane protein with a wide distribution in neuronal and neurosecretory tissue. *Journal of Cell Biology*, *91*(1), 257–269. https://doi.org/10.1083/jcb.91.1.257

Maximov, A., Lao, Y., Li, H., Chen, X., Rizo, J., Sørensen, J. B., & Südhof, T. C. (2008). Genetic analysis of synaptotagmin-7 function in synaptic vesicle exocytosis. *Proceedings of the National Academy of Sciences of the United States of America*, *105*(10):3986-91. https://doi.org/10.1073/pnas.0712372105

Maximov, A., & Südhof, T. C. (2005). Autonomous function of synaptotagmin 1 in triggering synchronous release independent of asynchronous release. *Neuron*, *48*(4), 547–554. https://doi.org/10.1016/j.neuron.2005.09.006

McTague, A., Howell, K. B., Cross, J. H., Kurian, M. A., & Scheffer, I. E. (2016). The genetic landscape of the epileptic encephalopathies of infancy and childhood. *The Lancet Neurology*, *15*(3), 304–316. https://doi.org/10.1016/S1474-4422(15)00250-1

Nagy, G., Kim, J. H., Pang, Z. P., Matti, U., Rettig, J., Südhof, T. C., & Sørensen, J. B. (2006). Different effects on fast exocytosis induced by synaptotagmin 1 and 2 isoforms and abundance but not by phosphorylation. *Journal of Neuroscience*, *26*(2), 632–643. https://doi.org/10.1523/JNEUROSCI.2589-05.2006

Nishiki, T. I., & Augustine, G. J. (2004a). Dual roles of the C2B domain of synaptotagmin I in synchronizing Ca2+-dependent neurotransmitter release. *Journal of Neuroscience*, *24*(39), 8542–8550. https://doi.org/10.1523/JNEUROSCI.2545-04.2004

Nishiki, T. I., & Augustine, G. J. (2004b). Synaptotagmin I synchronizes transmitter release in mouse hippocampal neurons. *Journal of Neuroscience*, *24*(27), 6127–6132. https://doi.org/10.1523/JNEUROSCI.1563-04.2004

Nonet, M. L., Grundahl, K., Meyer, B. J., & Rand, J. B. (1993). Synaptic function is impaired but not eliminated in C. elegans mutants lacking synaptotagmin. *Cell*, *73*(7), 1291–1305. https://doi.org/10.1016/0092-8674(93)90357-V

Okamoto, T., Tamura, T., Suzuki, K., & Kidokoro, Y. (2005). External Ca2+ dependency of synaptic transmission in Drosophila synaptotagmin I mutants. *Journal of Neurophysiology*, *94*(2), 1574–1586. https://doi.org/10.1152/JN.00205.2005

Pang, Z. P., Sun, J., Rizo, J., Maximov, A., & Südhof, T. C. (2006). Genetic analysis of synaptotagmin 2 in spontaneous and Ca 2+-triggered neurotransmitter release. *EMBO Journal*, *25*(10), 2039–2050. https://doi.org/10.1038/sj.emboj.7601103

Parisotto, D., Malsam, J., Scheutzow, A., Krause, J. M., & Söllner, T. H. (2012). SNAREpin assembly by Munc18-1 requires previous vesicle docking by synaptotagmin 1. *Journal of Biological Chemistry*, *287*(37), 31041–31049. https://doi.org/10.1074/JBC.M112.386805

Park, Y., Hernandez, J. M., Van Den Bogaart, G., Ahmed, S., Holt, M., Riedel, D., & Jahn, R. (2012). Controlling synaptotagmin activity by electrostatic screening. *Nature Structural & Molecular Biology*, *19*. https://doi.org/10.1038/nsmb.2375

Perin, M. S., Brose, N., Jahn, R., & Südhof, T.C. (1991). Domain Structure of

Synaptotagmin (p65). *Journal of Biological Chemistry,* 266(1):623–29. https://doi.org/10.1016/S0021-9258(18)52480-7

Perin, M. S., Fried, V. A., Mignery, G. A., Jahn, R., & Südhof, T. C. (1990). Phospholipid binding by a synaptic vesicle protein homologous to the regulatory region of protein kinase C. *Nature*, *345*(6272), 260–263. https://doi.org/10.1038/345260a0

Popov, S. V., & Poo, M. M. (1993). Synaptotagmin: A calcium-sensitive inhibitor of exocytosis? *Cell*, *73*(7), 1247–1249. https://doi.org/10.1016/0092-8674(93)90352-Q

Poskanzer, K. E., Marek, K. W., Sweeney, S. T., & Davis, G. W. (2003). Synaptotagmin I is necessary for compensatory synaptic vesicle endocytosis in vivo. *Nature*, *426*(6966), 559–563. https://doi.org/10.1038/nature02184

Radhakrishnan, A., Stein, A., Jahn, R., & Fasshauer, D. (2009). The Ca2+ affinity of synaptotagmin 1 is markedly increased by a specific interaction of its C2B domain with phosphatidylinositol 4,5-bisphosphate. *Journal of Biological Chemistry*, *284*(38), 25749–25760. https://doi.org/10.1074/JBC.M109.042499

Ramakrishnan, S., Bera, M., Coleman, J., Rothman, J. E., & Krishnakumar, S. S. (2020). Synergistic roles of synaptotagmin-1 and complexin in calcium-regulated neuronal exocytosis. *ELife*, *9*, 1–18. https://doi.org/10.7554/ELIFE.54506

Rao, T. C., Passmore, D. R., Peleman, A. R., Das, M., Chapman, E. R., & Anantharam, A. (2014). Distinct fusion properties of synaptotagmin-1 and synaptotagmin-7 bearing dense core granules. *Molecular Biology of the Cell*, *25*(16), 2416–2427. https://doi.org/10.1091/mbc.E14-02-0702

Reim, K., Mansour, M., Varoqueaux, F., McMahon, H. T., Südhof, T. C., Brose, N., & Rosenmund, C. (2001). Complexins regulate a late step in Ca2+-dependent neurotransmitter release. *Cell*, *104*(1), 71–81. https://doi.org/10.1016/S0092-8674(01)00192-1

Reist, N. E., Buchanan, J., Li, J., DiAntonio, A., Buxton, E. M., & Schwarz, T. L. (1998). Morphologically docked synaptic vesicles are reduced in synaptotagmin mutants of Drosophila. *Journal of Neuroscience*, *18*(19), 7662–7673. https://doi.org/10.1523/jneurosci.18-19-07662.1998

Rosenmund, C., & Stevens, C. F. (1996). Definition of the readily releasable pool of vesicles at hippocampal synapses. *Neuron*, *16*(6), 1197–1207. https://doi.org/10.1016/S0896-6273(00)80146-4

Rothman, J. E., Krishnakumar, S. S., Grushin, K., & Pincet, F. (2017). Hypothesis – buttressed rings assemble, clamp, and release SNAREpins for synaptic transmission. *FEBS Letters*, *591*(21), 3459–3480. https://doi.org/10.1002/1873-3468.12874

Sabatini, B. L., & Regehr, W. G. (1996). Timing of neurotransmission at fast synapses in the mammalian brain. *Nature*, *384*(6605), 170–172. https://doi.org/10.1038/384170a0

Schikorski, T., & Stevens, C. F. (2001). Morphological correlates of functionally defined synaptic vesicle populations. *Nature Neuroscience*, *4*(4), 391–395. https://doi.org/10.1038/86042

Schonn, J. S., Maximov, A., Lao, Y., Südhof, T. C., & Sørensen, J. B. (2008). Synaptotagmin-1 and -7 are functionally overlapping Ca2+ sensors for exocytosis in adrenal chromaffin cells. *Proceedings of the National Academy of Sciences of the United States of America*, *105*(10), 3998–4003. https://doi.org/10.1073/pnas.0712373105

Schulze, K. L., Broadie, K., Perin, M. S., & Bellen, H. J. (1995). Genetic and electrophysiological studies of drosophila syntaxin-1A demonstrate its role in nonneuronal secretion and neurotransmission. *Cell*, *80*(2), 311–320. https://doi.org/10.1016/0092-8674(95)90414-X

Shao, X., Davletov, B. A., Sutton, R. B., Südhof, T. C., & Rizo, J. (1996). Bipartite Ca2+-binding motif in C2 domains of synaptotagmin and protein kinase C. *Science*, *273*(5272), 248–251. https://doi.org/10.1126/science.273.5272.248

Shao, X., Fernandez, I., Südhof, T. C., & Rizo, J. (1998). Solution structures of the Ca2+-free and Ca2+-bound C2A domain of synaptotagmin I: Does Ca2+ induce a conformational change? *Biochemistry*, *37*(46), 16106–16115. https://doi.org/10.1021/bi981789h

Shin, O. H., Rizo, J., & Südhof, T. C. (2002). Synaptotagmin function in dense core vesicle exocytosis studied in cracked pc12 cells. *Nature Neuroscience*, *5*(7), 649–656. https://doi.org/10.1038/nn869

Silva, M., Tran, V., & Marty, A. (2021). Calcium-dependent docking of synaptic vesicles. *Trends in Neurosciences*, *44*(7):579-592. https://doi.org/10.1016/j.tins.2021.04.003

Söllner, T., Bennett, M. K., Whiteheart, S. W., Scheller, R. H., & Rothman, J. E. (1993). A protein assembly-disassembly pathway in vitro that may correspond to

sequential steps of synaptic vesicle docking, activation, and fusion. *Cell*, *75*(3), 409–418. https://doi.org/10.1016/0092-8674(93)90376-2

Südhof, T. C. (2002). Synaptotagmins: Why so many? *Journal of Biological Chemistry*, *277*(10), 7629–7632. https://doi.org/10.1074/jbc.R100052200

Südhof, T. C. (2012). The presynaptic active zone. *Neuron*, *75*(1), 11–25. https://doi.org/10.1016/J.NEURON.2012.06.012

Südhof, T. C., & Rizo, J. (1996). Synaptotagmins: C2-domain proteins that regulate membrane traffic. *Neuron*, *17*(3), 379–388. https://doi.org/10.1016/S0896-6273(00)80171-3

Südhof, T. C., & Rizo, J. (2011). Synaptic vesicle exocytosis. *Cold Spring Harbor Perspectives in Biology*, *3*(12):a005637. https://doi.org/10.1101/cshperspect.a005637

Sugita, S., Han, W., Butz, S., Liu, X., Fernández-Chacón, R., Lao, Y., Südhof, T. C., (2001). Synaptotagmin VII as a plasma membrane Ca(2+) sensor in exocytosis. *Neuron, 30*(2), 459–473. https://doi.org/10.101016/s0896-6273(01)00290-2

Sun, J., Pang, Z. P., Qin, D., Fahim, A. T., Adachi, R., & Südhof, T. C. (2007). A dual-Ca2+-sensor model for neurotransmitter release in a central synapse. *Nature*, *450*(7170), 676–682. https://doi.org/10.1038/nature06308

Sutton, R. B., Davletov, B. A., Berghuis, A. M., Sudhof, T. C., & Sprang, S. R. (1995). Structure of the first C2 domain of synaptotagmin I: A novel Ca2+/phospholipid-binding fold. *Cell*, *80*(6), 929–938. https://doi.org/10.1016/0092-8674(95)90296-1

Tagliatti, E., Bello, O. D., Mendonça, P. R. F., Kotzadimitriou, D., Nicholson, E., Coleman, J., Timofeeva, Y., Rothman, J. E., Krishnakumar, S. S., & Volynski, K. E. (2020). Synaptotagmin 1 oligomers clamp and regulate different modes of neurotransmitter release. *Proceedings of the National Academy of Sciences of the United States of America*, *117*(7), 3819–3827. https://doi.org/10.1073/pnas.1920403117

Takamori, S., Holt, M., Stenius, K., Lemke, E. A., Grønborg, M., Riedel, D., Urlaub, H., Schenck, S., Brügger, B., Ringler, P., Müller, S. A., Rammner, B., Gräter, F., Hub, J. S., De Groot, B. L., Mieskes, G., Moriyama, Y., Klingauf, J., Grubmüller, H., Heuser, J., Wieland, F., & Jahn, R. (2006). Molecular anatomy of a trafficking organelle. *Cell*, *127*(4), 831–846. https://doi.org/10.1016/j.cell.2006.10.030

Tran, H. T., Anderson, L. H., & Knight, J. D. (2019). Membrane-Binding Cooperativity and Coinsertion by C2AB Tandem Domains of Synaptotagmins 1 and 7. *Biophysical Journal*, *116*(6), 1025–1036. https://doi.org/10.1016/j.bpj.2019.01.035

Trimbuch, T., & Rosenmund, C. (2016). Should I stop or should I go? The role of complexin in neurotransmitter release. *Nature Reviews of Neuroscience, 17*(2):118-25. https://doi.org/10.1038/nrn.2015.16

Turecek, J., Jackman, S. L., & Regehr, W. G. (2017). Synaptotagmin 7 confers frequency invariance onto specialized depressing synapses. *Nature*, *551*(7681), 503–506. https://doi.org/10.1038/nature24474

Turecek, J., & Regehr, W. G. (2018). Synaptotagmin 7 mediates both facilitation and asynchronous release at granule cell synapses. *Journal of Neuroscience*, *38*(13), 3240–3251. https://doi.org/10.1523/JNEUROSCI.3207-17.2018

Ubach, J., Zhang, X., Shao, X., Südhof, T. C., & Rizo, J. (1998). Ca2+ binding to synaptotagmin: How many Ca2+ ions bind to the tip of a C2-domain? *EMBO Journal*, *17*(14), 3921–3930. https://doi.org/10.1093/emboj/17.14.3921

Vardar, G., Salazar-Lázaro, A., Brockmann, M., Weber-Boyvat, M., Zobel, S., Kumbol, V. W. A., Trimbuch, T., & Rosenmund, C. (2021). Reexamination of n-terminal domains of syntaxin-1 in vesicle fusion from central murine synapses. *ELife*, *10:*e69498. https://doi.org/10.7554/ELIFE.69498

Vevea, J. D., Kusick, G. F., Courtney, K. C., Chen, E., Watanabe, S., & Chapman, E. R. (2021). Synaptotagmin 7 is targeted to the axonal plasma membrane through g-secretase processing to promote synaptic vesicle docking in mouse hippocampal neurons. *ELife*, *10:*e67261. https://doi.org/10.7554/ELIFE.67261

Wang, J., Bello, O., Auclair, S. M., Coleman, J., Pincet, F., Krishnakumar, S. S., Sindelar, C. V., & Rothman, J. E. (2014). Calcium sensitive ring-like oligomers formed by synaptotagmin. *Proceedings of the National Academy of Sciences of the United States of America*, *111*(38), 13966–13971. https://doi.org/10.1073/PNAS.1415849111

Wang, J., Li, F., Bello, O. D., Sindelar, C. V., Pincet, F., Krishnakumar, S. S., & Rothman, J. E. (2017). Circular oligomerization is an intrinsic property of synaptotagmin. *ELife*, *6*. https://doi.org/10.7554/ELIFE.27441

Watanabe, S., Trimbuch, T., Camacho-Pérez, M., Rost, B. R., Brokowski, B., Söhl-Kielczynski, B., Felies, A., Davis, M. W., Rosenmund, C., & Jorgensen, E. M.

(2014). Clathrin regenerates synaptic vesicles from endosomes. *Nature*, *515*(7526), 228–233. https://doi.org/10.1038/nature13846

Weber, J. P., Toft-Bertelsen, T. L., Mohrmann, R., Delgado-, I., Delgado-Martinez, I., & Sørensen, J. B. (2014). Synaptotagmin-7 Is an Asynchronous Calcium Sensor for Synaptic Transmission in Neurons Expressing SNAP-23. *PLoS ONE*, *9*(11), 1–22. https://doi.org/10.1371/journal.pone.0114033

Wen, H., Linhoff, M. W., McGinley, M. J., Li, G. L., Corson, G. M., Mandel, G., & Brehm, P. (2010). Distinct roles for two synaptotagmin isoforms in synchronous and asynchronous transmitter release at zebrafish neuromuscular junction. *Proceedings of the National Academy of Sciences of the United States of America*, *107*(31), 13906–13911. https://doi.org/10.1073/pnas.1008598107

Weston, M. C., Nehring, R. B., Wojcik, S. M., & Rosenmund, C. (2011). Article Interplay between VGLUT Isoforms and Endophilin A1 Regulates Neurotransmitter Release and Short-Term Plasticity. *Neuron*, *69*(6), 1147–1159. https://doi.org/10.1016/j.neuron.2011.02.002

Wu, Z., Dharan, N., Mcdargh, Z. A., & Thiyagarajan, S. (2021). The neuronal calcium sensor Synaptotagmin-1 and SNARE proteins cooperate to dilate fusion pores. *Elife, 10*:e68215. https://doi.org/10.7554/eLife.68215

Xu, J., Pang, Z. P., Shin, O. H., & Südhof, T. C. (2009). Synaptotagmin-1 functions as a Ca2+ sensor for spontaneous release. *Nature Neuroscience*, *12*(6), 759–766. https://doi.org/10.1038/nn.2320

Xue, M., Craig, T. K., Shin, O., Li, L., Brautigam, C. A., Tomchick, D.R., Südhof, T.C., Rosenmund, C., Rizo, J. (2010). Structural and Mutational Analysis of Functional Differentiation between Synaptotagmins-1 and -7. *PLoS One, 5*(9):e12544. https://doi.org/10.1371/journal.pone.0012544

Xue, M., Ma, C., Craig, T. K., Rosenmund, C., & Rizo, J. (2008). The Janus-Faced Nature of the C 2 B Domain Is Fundamental for Synaptotagmin-1 Function. *Nature Structural Molecular Biology*, *15*(11), 1160–1168. https://doi.org/10.1038/nsmb.1508

Xue, M., Reim, K., Chen, X., Chao, H. T., Deng, H., Rizo, J., Brose, N., & Rosenmund, C. (2007). Distinct domains of complexin I differentially regulate neurotransmitter release. *Nature Structural and Molecular Biology*, *14*(10), 949–958. https://doi.org/10.1038/nsmb1292

Yao, J., Kwon, S. E., Gaffaney, J. D., Dunning, F. M., & Chapman, E. R. (2012).

Uncoupling the roles of synaptotagmin i during endo-and exocytosis of synaptic vesicles. *Nature Neuroscience*, *15*(2), 243–249. https://doi.org/10.1038/nn.3013

Yoshihara, M., & Littleton, J. T. (2002). Synaptotagmin functions as a calcium sensor to synchronize neurotransmitter release. *Neuron*, *36*(5), 897–908. https://doi.org/10.1016/S0896-6273(02)01065-6

Zanetti, M. N., Bello, O. D., Wang, J., Coleman, J., Cai, Y., Sindelar, C. V., Rothman, J. E., & Krishnakumar, S. S. (2016). Ring-like oligomers of synaptotagmins and related C2 domain proteins. *ELife*, *5*:e17262. https://doi.org/10.7554/ELIFE.17262

Zarebidaki, F., Camacho, M., Brockmann, M. M., Trimbuch, T., Herman, M. A., & Rosenmund, C. (2020). Disentangling the roles of RIM and Munc13 in synaptic vesicle localization and neurotransmission. *Journal of Neuroscience*, *40*(49), 9372–9385. https://doi.org/10.1523/JNEUROSCI.1922-20.2020

Zhou, Q., Lai, Y., Bacaj, T., Zhao, M., Lyubimov, A. Y., Uervirojnangkoorn, M., Zeldin, O. B., Brewster, A. S., Sauter, N. K., Cohen, A. E., Soltis, S. M., Alonso-Mori, R., Chollet, M., Lemke, H. T., Pfuetzner, R. A., Choi, U. B., Weis, W. I., Diao, J., Südhof, T. C., & Brunger, A. T. (2015). Architecture of the synaptotagmin-SNARE machinery for neuronal exocytosis. *Nature*, *525*(7567), 62–67. https://doi.org/10.1038/nature14975

Zhou, Q., Zhou, P., Wang, A. L., Wu, D., Zhao, M., Südhof, T. C., & Brunger, A. T. (2017). The primed SNARE – complexin – synaptotagmin complex for neuronal exocytosis. *Nature, 548*(7668):420-425. https://doi.org/10.1038/nature23484

Zimmermann, J., Trimbuch, T., & Rosenmund, C. (2014). Synaptobrevin 1 mediates vesicle priming and evoked release in a subpopulation of hippocampal neurons. *Journal of Neurophysiology*, *112*(6), 1559–1565. https://doi.org/10.1152/jn.00340.2014

Statutory Declaration

“I, Boris Bouazza Arostegui, by personally signing this document in lieu of an oath, hereby affirm that I prepared the submitted dissertation on the topic “Dissecting the functions of Synaptotagmin-1 and Synaptotagmin-7 in synaptic transmission” / ”Untersuchung der Funktionen von Synaptotagmin-1 und Synaptotagmin-7 in der Synaptischen Transmission”, independently and without the support of third parties, and that I used no other sources and aids than those stated.
All parts which are based on the publications or presentations of other authors, either in letter or in spirit, are specified as such in accordance with the citing guidelines. The sections on methodology (in particular regarding practical work, laboratory regulations, statistical processing) and results (in particular regarding figures, charts and tables) are exclusively my responsibility.

My contributions to any publications to this dissertation correspond to those stated in the below joint declaration made together with the supervisor. All publications created within the scope of the dissertation comply with the guidelines of the ICMJE (International Committee of Medical Journal Editors; http://www.icmje.org) on authorship. In addition, I declare that I shall comply with the regulations of Charité – Universitätsmedizin Berlin on ensuring good scientific practice.

I declare that I have not yet submitted this dissertation in identical or similar form to another Faculty.

The significance of this statutory declaration and the consequences of a false statutory declaration under criminal law (Sections 156, 161 of the German Criminal Code) are known to me.”

Date Signature

Declaration of your own contribution to the top-journal publication

Boris Bouazza Arostegui as the sole first author contributed the following to the below listed publication:

Bouazza-Arostegui B, Camacho M, Brockmann MM, Zobel S, Rosenmund C. Deconstructing Synaptotagmin-1's Distinct Roles in Synaptic Vesicle Priming and Neurotransmitter Release. J Neurosci. 2022 Apr 6;42(14):2856-2871. doi: 10.1523/JNEUROSCI.1945-21.2022. Epub 2022 Feb 22. PMID: 35193927; PMCID: PMC8985867.

Contribution in detail:

Design of research:

B. Bouazza-Arostegui, M. Camacho and C. Rosenmund, conceived the idea and designed the experiments.

Execution of experiments and data analysis:

B. Bouazza-Arostegui performed all hippocampal culture preparation and M. Petzold, and H. Lerch prepared the astrocytic cultures. T. Trimbuch, B. Brokowski, and K. Pötschke prepared the Lentivirus (Figures 1 to 8) and M.M. Brockmann contributed with analytic tools and initial assessment of lentiviral infection with *shRNA(syt7)* in Figure 4. B. Bouazza-Arostegui performed electrophysiological recordings of Figures 1, 2, 4, 5, 6, 7 and 8. S. Zobel and M. Camacho contributed with electrophysiological recordings in Figure 4 and Figure 5, respectively. B. Bouazza-Arostegui performed confocal microscopy and B. Söhl-Kielczynski helped with immunostainings (Figures 2, 3, 5, 6, 7 and 8). B. Bouazza-Arostegui performed data analysis, data visualization, and the statistical tests for all experiments (Figure 1 to 8 and Extended data Figure 7-1). B. Bouazza-Arostegui prepared all figures and tables (Figure 1 to 8 and Extended data Figure 7-1).

Manuscript preparation:

B. Bouazza-Arostegui wrote the draft of the manuscript. B. Bouazza-Arostegui, M. Camacho and C. Rosenmund edited the manuscript.

_____

Signature, date, and stamp of first supervising university professor

_____

Signature of doctoral candidate

Excerpt from the Journal Summary List (ISI Web of Knowledge)

Journal Data Filtered By: **Selected JCR Year: 2020** Selected Editions: SCIE,SSCI
Selected Categories: **"NEUROSCIENCES"** Selected Category Scheme: WoS
Gesamtanzahl: 273 Journale

Rank	Full Journal Title	Total Cites	Journal Impact Factor	Eigenfactor Score
1	NATURE REVIEWS NEUROSCIENCE	49,897	34.870	0.048890
2	NATURE NEUROSCIENCE	73,709	24.884	0.128020
3	TRENDS IN COGNITIVE SCIENCES	33,482	20.229	0.036270
4	NEURON	111,115	17.173	0.175220
5	ACTA NEUROPATHOLOGICA	28,031	17.088	0.036970
6	MOLECULAR PSYCHIATRY	28,622	15.992	0.046220
7	Molecular Neurodegeneration	6,772	14.195	0.011650
8	TRENDS IN NEUROSCIENCES	22,858	13.837	0.019470
9	Nature Human Behaviour	5,549	13.663	0.023120
10	BRAIN	64,627	13.501	0.061550
11	BIOLOGICAL PSYCHIATRY	50,155	13.382	0.045540
12	JOURNAL OF PINEAL RESEARCH	12,492	13.007	0.008170
13	BEHAVIORAL AND BRAIN SCIENCES	11,610	12.579	0.007760
14	Annual Review of Neuroscience	14,699	12.449	0.010490
15	PROGRESS IN NEUROBIOLOGY	15,161	11.685	0.010300
16	SLEEP MEDICINE REVIEWS	11,218	11.609	0.014840
17	ANNALS OF NEUROLOGY	43,728	10.422	0.039960
18	NEUROSCIENCE AND BIOBEHAVIORAL REVIEWS	36,525	8.989	0.048970
19	Brain Stimulation	9,206	8.955	0.015960
20	npj Parkinsons Disease	1,093	8.651	0.003040
21	FRONTIERS IN NEUROENDOCRINOLOGY	5,338	8.606	0.005050

Rank	Full Journal Title	Total Cites	Journal Impact Factor	Eigenfactor Score
22	Neurology-Neuroimmunology & Neuroinflammation	3,863	8.485	0.008390
23	Journal of Neuroinflammation	19,657	8.322	0.027070
24	NEUROPATHOLOGY AND APPLIED NEUROBIOLOGY	4,791	8.090	0.004640
25	NEURAL NETWORKS	18,837	8.050	0.019420
26	Translational Neurodegeneration	1,759	8.014	0.003160
27	NEUROPSYCHOPHARMACOLOGY	30,856	7.853	0.034600
28	Acta Neuropathologica Communications	6,580	7.801	0.016320
29	Fluids and Barriers of the CNS	1,956	7.662	0.002170
30	Neurotherapeutics	6,764	7.620	0.009400
31	NEUROSCIENTIST	5,949	7.519	0.005010
32	Molecular Autism	3,579	7.509	0.007400
33	GLIA	17,858	7.452	0.016000
34	NEUROPSYCHOLOGY REVIEW	3,941	7.444	0.003460
35	Current Neuropharmacology	6,080	7.363	0.007730
36	JOURNAL OF HEADACHE AND PAIN	5,400	7.277	0.008140
37	BRAIN BEHAVIOR AND IMMUNITY	24,161	7.217	0.026930
38	Alzheimers Research & Therapy	5,593	6.982	0.011680
39	PAIN	45,325	6.961	0.031030
40	Translational Stroke Research	3,377	6.829	0.003920
41	BIPOLAR DISORDERS	6,185	6.744	0.007510
42	CURRENT OPINION IN NEUROBIOLOGY	17,009	6.627	0.025180
43	NEUROIMAGE	119,618	6.556	0.105820

Selected JCR Year: 2020; Selected Categories: "NEUROSCIENCES"

Rank	Full Journal Title	Total Cites	Journal Impact Factor	Eigenfactor Score
22	Neurology-Neuroimmunology & Neuroinflammation	3,863	8.485	0.008390
23	Journal of Neuroinflammation	19,657	8.322	0.027070
24	NEUROPATHOLOGY AND APPLIED NEUROBIOLOGY	4,791	8.090	0.004640
25	NEURAL NETWORKS	18,837	8.050	0.019420
26	Translational Neurodegeneration	1,759	8.014	0.003160
27	NEUROPSYCHOPHARMACOLOGY	30,856	7.853	0.034600
28	Acta Neuropathologica Communications	6,580	7.801	0.016320
29	Fluids and Barriers of the CNS	1,956	7.662	0.002170
30	Neurotherapeutics	6,764	7.620	0.009400
31	NEUROSCIENTIST	5,949	7.519	0.005010
32	Molecular Autism	3,579	7.509	0.007400
33	GLIA	17,858	7.452	0.016000
34	NEUROPSYCHOLOGY REVIEW	3,941	7.444	0.003460
35	Current Neuropharmacology	6,080	7.363	0.007730
36	JOURNAL OF HEADACHE AND PAIN	5,400	7.277	0.008140
37	BRAIN BEHAVIOR AND IMMUNITY	24,161	7.217	0.026930
38	Alzheimers Research & Therapy	5,593	6.982	0.011680
39	PAIN	45,325	6.961	0.031030
40	Translational Stroke Research	3,377	6.829	0.003920
41	BIPOLAR DISORDERS	6,185	6.744	0.007510
42	CURRENT OPINION IN NEUROBIOLOGY	17,009	6.627	0.025180
43	NEUROIMAGE	119,618	6.556	0.105820

Selected JCR Year: 2020; Selected Categories: "NEUROSCIENCES"

Rank	Full Journal Title	Total Cites	Journal Impact Factor	Eigenfactor Score
44	BRAIN PATHOLOGY	6,559	6.508	0.006220
45	Developmental Cognitive Neuroscience	4,477	6.464	0.011160
46	Annual Review of Vision Science	935	6.422	0.004560
47	Multiple Sclerosis Journal	15,551	6.312	0.016680
48	CEPHALALGIA	12,756	6.292	0.011940
49	Biological Psychiatry-Cognitive Neuroscience and Neuroimaging	2,193	6.204	0.007120
50	JOURNAL OF CEREBRAL BLOOD FLOW AND METABOLISM	22,732	6.200	0.019640
51	JOURNAL OF PSYCHIATRY & NEUROSCIENCE	4,100	6.186	0.004200
52	JOURNAL OF NEUROSCIENCE	186,015	6.167	0.130970
53	EUROPEAN JOURNAL OF NEUROLOGY	14,490	6.089	0.016730
54	NEUROBIOLOGY OF DISEASE	21,360	5.996	0.020680
55	Dialogues in Clinical Neuroscience	5,272	5.986	0.005200
56	SLEEP	28,688	5.849	0.023920
57	JOURNAL OF PAIN	13,655	5.820	0.014690
58	Frontiers in Aging Neuroscience	13,654	5.750	0.025540
59	CURRENT OPINION IN NEUROLOGY	6,723	5.710	0.008480
60	Frontiers in Molecular Neuroscience	10,570	5.639	0.022450
61	MOLECULAR NEUROBIOLOGY	20,795	5.590	0.033020
62	Journal of Parkinsons Disease	3,562	5.568	0.006390
63	Frontiers in Cellular Neuroscience	17,299	5.505	0.033870
64	Neurobiology of Stress	1,628	5.441	0.004280
65	Cognitive Computation	2,407	5.418	0.002870

Selected JCR Year: 2020; Selected Categories: "NEUROSCIENCES"

Printed copy of selected publication

Bouazza-Arostegui B, Camacho M, Brockmann MM, Zobel S, Rosenmund C. Deconstructing Synaptotagmin-1's Distinct Roles in Synaptic Vesicle Priming and Neurotransmitter Release. J Neurosci. 2022 Apr 6;42(14):2856-2871. doi: 10.1523/JNEUROSCI.1945-21.2022. Epub 2022 Feb 22. PMID: 35193927; PMCID: PMC8985867.

Cellular/Molecular

Deconstructing Synaptotagmin-1's Distinct Roles in Synaptic Vesicle Priming and Neurotransmitter Release

Boris Bouazza-Arostegui,[1,2] Marcial Camacho,[1,2] Marisa M. Brockmann,[1,2] Sina Zobel,[1,2] and Christian Rosenmund[1,2]

[1]Institute of Neurophysiology, Charité–Universitätsmedizin Berlin, corporate member of Freie Universität Berlin and Humboldt-Universität zu Berlin, 10117 Berlin, Germany, and [2]NeuroCure Cluster of Excellence, Charité–Universitätsmedizin Berlin, 10117 Berlin, Germany

Synaptotagmin-1 (SYT1) is a synaptic vesicle resident protein that interacts via its C2 domain with anionic lipids from the plasma membrane in a calcium-dependent manner to efficiently trigger rapid neurotransmitter (NT) release. In addition, SYT1 acts as a negative regulator of spontaneous NT release and regulates synaptic vesicle (SV) priming. How these functions relate to each other mechanistically and what role other synaptotagmin (SYT) isoforms play in supporting and complementing the role of SYT1 is still under intensive investigation. In this work, we analyzed three putative functions of SYT1 in exocytosis by systematically varying its expression in autaptic hippocampal glutamatergic neurons from mice of either sex. We find that regulation of release probability is most sensitive to variation of expression levels, whereas its impact on vesicle priming is least sensitive. Also, loss of SYT1 phenotypes on spontaneous release and vesicle priming is compensated in less mature synaptic cultures by redundant support from SYT7. Overall, our data help in resolving some controversies in SYT1 functions in exocytosis and in our understanding of how SYT1 contributes to the pathophysiology underlying SYT1-related human neurologic disorders.

Key words: **autaptic culture; development; synaptic transmission; synaptic vesicle priming; Synaptotagmin**

Significance Statement

Our work clarifies the functions of SYT1 protein in synaptic vesicle priming and spontaneous and calcium-evoked neurotransmitter release and analyzes whether these occur at different stages of synaptic responses by examining their relative sensitivity to protein concentration at the synaptic terminal. We demonstrate that these synaptic functions are unequally sensitive to both protein levels and neuronal stage, indicating that they operate under distinct molecular mechanisms. Furthermore, we analyze how these functions are modulated by another synaptotagmin isoform expression. We show that to understand the phenotype displayed by SYT1 knock-out neurons ($Syt1^{-/-}$) is necessary to consider the interplay between SYT1 and SYT7 molecules at the presynaptic terminal.

Received Sep. 27, 2021; revised Jan. 18, 2022; accepted Jan. 23, 2022.

Author contributions: C.R., B.B.-A., and M.C. designed research; B.B.-A., M.C., and S.Z. performed research; M.M.B. /analytic tools; B.B.-A. analyzed data; C.R. and B.B.-A. wrote the paper.

This work was supported by grants from the German Research Council (Collaborative Research Center 958 and Reinhart Koselleck Projects). B.B.-A. was supported by the Deutsche Forschungsgemeinschaft (DFG, German Research Foundation) under Germany's Excellence Initiative – EXC-257. We thank Berit Söhl-Kielczynski, Bettina Brokowski, Katja Pötschke, Sabine Lenz, and Heike Lerch for technical support; Dr. Melissa Herman for comments and discussion; the services of the Charité Viral Core Facility for virus production and characterization; and the services of Advanced Medical Bioimaging Core Facility, Nikon imaging core facilities, at the Charité Campus Mitte (Berlin, Germany).

The authors declare no competing financial interests.

M. Camacho's present address: Unidad de Farmacología, Facultad de Medicina, Universidad de La Laguna, 38200 La Laguna, Tenerife, Spain.

M. M. Brockmann's present address: Center of Molecular Neurobiology Hamburg, 2051 Hamburg, Germany.

Correspondence should be addressed to Christian Rosenmund at christian.rosenmund@charite.de.

https://doi.org/10.1523/JNEUROSCI.1945-21.2022

Copyright © 2022 Bouazza-Arostegui et al.

This is an open-access article distributed under the terms of the Creative Commons Attribution 4.0 International license, which permits unrestricted use, distribution and reproduction in any medium provided that the original work is properly attributed.

Introduction

Calcium-evoked neurotransmitter (NT) release from the presynaptic nerve terminal occurs in less than 1 ms following the activation of voltage-gated calcium channels triggered by the arrival of an action potential (AP; Katz, 1969; Sabatini and Regehr, 1999). A key element in orchestrating the rapid and efficient presynaptic Ca^{2+}-evoked NT release is the synaptic vesicular protein Synaptotagmin-1 (SYT1; DiAntonio and Schwarz, 1994; Fernández-Chacón et al., 2001; Rizo and Xu, 2015). Biochemical studies have demonstrated that SYT1 is a phospholipid-binding machine that acts in a calcium-dependent manner via its C2A and C2B cytoplasmic domains to trigger NT release (Perin et al., 1990; Brose et al., 1992; Sutton et al., 1995; Chapman and Davis, 1998; Fernandez et al., 2001).

In *Drosophila* and mammalian synapses in the absence of *Syt1*, AP-evoked synchronous release is drastically impaired (Broadie et al., 1994; Geppert et al., 1994; Yoshihara and Littleton, 2002; Nishiki and Augustine, 2004; Maximov and

Südhof, 2005; Xue et al., 2008), but structure/function analysis of the C2B domain reveals that SYT1 is involved in two additional functions. SYT1 also acts as a clamping factor, suppressing spontaneous release of synaptic vesicles (SVs; DiAntonio and Schwarz, 1994; Littleton et al., 1994; Chicka et al., 2008; Xu et al., 2009), and different research groups have shown a role for SYT1 in SV docking/priming, mediating the recruitment of vesicles to the plasma membrane (PM) by the interaction with phosphatidylserine and phosphatidylinositol 4, 5-bisphosphate (Reist et al., 1998; Liu et al., 2009; Bacaj et al., 2015; Chang et al., 2018). However, how these functions of SYT1 mechanistically interact is currently unclear.

In addition to the different roles of SYT1 in the process of neurotransmitter release, other synaptotagmin isoforms have been implicated in distinct and overlapping roles. For example, the SYT7 isoform has been claimed to be a high-affinity calcium sensor for asynchronous release (Bacaj et al., 2013; Chen and Jonas, 2017), a regulator of short-term plasticity (STP; Wen et al., 2010; Jackman et al., 2016; Chen et al., 2017b; Fujii et al., 2021), and to act redundantly with SYT1 in the maintenance of the ready releasable pool (RRP) of SVs (Bacaj et al., 2015). Furthermore, the expression of synaptotagmin isoforms is regulated in a cell-type-specific manner. At the calyx of Held synapse and in some GABAergic neurons, the vesicular SYT2 protein, the closest relative isoform of SYT1 (Geppert et al., 1991; Marquèze et al., 1995), regulates neurotransmission redundantly with SYT1 (Pang et al., 2006; Chen et al., 2017a). Synaptic transmission depends on SYT1 in the early postnatal calyx of Held synapses but later switches to SYT2 (Kochubey et al., 2016), suggesting that dynamic changes in synaptotagmin content at synapses during development and their redundant functions in priming and release have an impact in synaptic function. Consistent with this idea, heterozygotic *de novo* mutations in the *syt1* gene detected in patients have been shown to be associated with a neurodevelopmental disorder (Baker et al., 2015, 2018; Bradberry et al., 2020).

In this study, we therefore aim to analyze the proposed distinct roles of SYT1 in vesicle priming and spontaneous and evoked release, and investigate these functions in the context of development, its interplay with SYT7, and the relative contribution of SYT1 expression levels on these functions. We found that the loss of function phenotype of SYT1 depends on the maturation stage of neurons, where immature neurons can compensate the loss of SYT1 with expression of SYT7 in two of the three SYT1 functions. Furthermore, by systematically investigating the three key functions of SYT1 as a function of protein levels, we define distinct sensitivity of these processes, arguing a distinct role of SYT1 in these different functions.

Materials and Methods

Animals. In this study, we used embryonic day (E)18–19 $Syt1^{+/+}$, $Syt1^{+/-}$, and $Syt1^{-/-}$ embryos on C57BL/6 background of either sex generated by interbreeding *Syt1* heterozygous mice as described previously (Xue et al., 2008). All procedures and animals used were handled according to the regulations of Directive 2010/63/EU of the European Parliament on the protection of animals used for scientific purposes and were approved by the Berlin state authorities under the license number G-Project 106/20 and the animal welfare committee of Charité–Universitätsmedizin Berlin.

Lentiviral constructs and production. Lentiviruses were generated by the Viral Core Facility of the Charité–Universitätsmedizin Berlin. All lentiviral particles were produced as described previously (Lois et al., 2002). Lentiviral *Syt1* construct used for rescue and overexpression experiments was generated from mouse *Syt1* cDNA (National Center for Biotechnology Information reference sequence NM_001252341). The cDNA was cloned into a lentiviral vector (FUGW) with a human synapsin1 promoter and following a nuclear localization signal (NLS)-RFP-P2A expression cassette for identification of infected cells. A lentivirus expressing only NLS-RFP-P2A controlled by the human synapsin1 promoter served as control. For short hairpin RNA (shRNA)-mediated knockdown experiments of SYT1 protein, an shRNA cassette containing a 19 bp target sequence of *Syt1* (5′AGTCTTCCTGCTGCCCGAC-3′) was cloned downstream of a U6 promoter that also contained a ubiquitin promoter-driven RFP expression cassette (f(U6)shRNA-Syt1.Ubi-RFP.WPRE). For shRNA mediated knockdown of SYT7 a 21 bp targeting sequence KD607 from Bacaj et al. (2013) was used under the control of U6 promoter expression cassette within a lentivirus that also contained a human synapsin1 promoter to control the nuclear RFP expression cassette (f(U6) shRNA-Syt7.Syn-NLS-RFP.WPRE). A scramble RNA (*scRNA*) sequence served in both shRNA constructs as control (Watanabe et al., 2014). The lentiviral titer for all generated constructs was estimated by quantification of hippocampal neurons in mass culture expressing a fluorescent marker after day *in vitro* (DIV)7.

Autaptic neuronal culture and viral infection. For electrophysiology recordings and immunocytochemistry experiments, autaptic glutamatergic hippocampal neurons were prepared as previously reported by Bekkers and Stevens (1991). Briefly, hippocampal neurons derived from $Syt1^{+/+}$, $Syt1^{+/-}$, and $Syt1^{-/-}$ embryonic mice (E18–19) of either sex were used and plated at a density of 300 cells/cm^2 on 30 mm coverslips containing astrocytic microislands. Astrocytes were obtained from cerebral cortices of postnatal day (P)0–2 C57BL/6N mice and plated at a density of 5000 cells/cm^2 on the micropattern coverslips 1 week before of the preparation of the neurons. Autaptic neuronal cultures were infected with the appropriate viral construct 24–48 h after plating and maintained at 37°C and 5% CO_2.

Electrophysiology. Whole-cell patch-clamp recordings in autaptic neurons were performed at DIV11–21. All electrophysiological recordings were done at room temperature with a MultiClamp 700B amplifier (Molecular Devices) controlled by Clampex 10 software (Molecular Devices). Data were digitally sampled at 10 kHz and were filtered using a low-pass Bessel filter at 3 kHz. Series resistance was compensated up to 70%. Autaptic cultures during recordings were immersed in an extracellular solution that contained the following (in mM): 140 NaCl, 2.4 KCl, 10 HEPES, 10 glucose, 2 $CaCl_2$ and 4 $MgCl_2$. Borosilicate glass patch pipettes were pulled using a multistep puller (model P-1000, Sutter Instruments). Pipettes with resistance (3–5 MOhms) were filled with KCl-based intracellular solution containing the following (in mM): 136 KCl, 17.8 HEPES, 1 EGTA, 4.6 $MgCl_2$, 4 ATP-Na_2, 0.3 GTP-Na_2, 12 creatine phosphate, and 50 U/ml phosphocreatine kinase. Both internal and extracellular solutions were adjusted to 300 mOsm, pH 7.4. Neurons were clamped at −70 mV during recordings. Exclusion criteria were stablished for patched cells with a leak current higher than −200 pA. Single APs were evoked by a 2 ms depolarization step to 0 mV and EPSCs were recorded. To measure the synchronicity of synaptic responses we inverted the EPSC charge and integrated the signal. Then, we fitted a two-components function provided by AxoGraph X (AxoGraph Scientific), from which we calculated their relative contribution to the total charge released. The first component represents the fast and synchronous release part of the EPSC charge and the second component the slow and asynchronous release part of the EPSC charge.

The RRP of synaptic vesicles was assessed by the application for 5 s of external solution containing 500 mM sucrose (Rosenmund and Stevens, 1996). Evoked-sucrose currents were recorded, and the RRP size was estimated by integrating the area of the evoked-sucrose current with the steady-state current set as the baseline. Vesicular release probability (Pvr) was calculated as the ratio between the charge of the EPSC and the evoked-sucrose charge.

We calculated the paired-pulsed ratio (PPR) by dividing the second EPSC (EPSC2) amplitude by the first (EPSC1). A train of AP stimulation at 20 Hz for 5 s was recorded to assess short-term plasticity. The synaptic responses from the train of AP were normalized to the first EPSC peak amplitude.

To analyze mini EPSCs (mEPSCs), electrophysiological traces were filtered at 1 kHz, and the range of parameters for inclusion of selected events using a conventionally defined template algorithm in AxoGraph X (AxoGraph Scientific) were 5–200 pA, 0.15–1.5 ms rise time, and 0.5–5 ms half-width. False-positive events were excluded by subtracting events detected from traces in the presence of AMPA receptor antagonist, NBQX (3 μM). Spontaneous release rate was calculated by dividing the mEPSC frequency by the number of synaptic vesicles in the RRP. The number of synaptic vesicles in the RRP was calculated by dividing the RRP size by the mEPSC charge. Off-line analysis was performed using AxoGraph X (AxoGraph Scientific).

Immunocytochemistry and image acquisition. Autaptic hippocampal neurons were immunostained as previously reported by Xue et al. (2007). Briefly, neurons were fixed with 4% paraformaldehyde (PFA; Sigma-Aldrich) for 10 min at DIV11 and DIV16 (see Fig. 3; see Figs. 2, 5, 6, 7 and 8 for 15–21 DIV). Primary antibodies monoclonal mouse anti-Synaptotagmin-1 (1:1000; Synaptic Systems), polyclonal guinea pig anti-VGLUT1 (1:4000; Synaptic Systems), and polyclonal rabbit anti-Synaptogamin 7 (1:500; Synaptic Systems) were used. Secondary antibodies (1:500) conjugated with Alexa Fluor 405, 488, or 647 (Jackson ImmunoResearch) were used to visualize fluorescence. For quantitative assessment, all groups compared in one experiment were processed in parallel using identical antibodies solutions and other reagents.

Single neurons on the astrocytic micro islands were imaged by using a Nikon Scanning Confocal A1Rsi+ with a 60×, 1.4 NA oil-immersion objective. For acquiring all the images, we used the same microscope and camera with identical acquisition settings for all experimental groups. Overexposure and photobleaching were avoided by checking the fluorescence signal saturation in synaptic boutons. Z stacks of neurons were set with a 0.3 μm interstack interval and total z axis range of 5–6 μm, and a sum of intensity projection was further used for analyses. The images were obtained at 1024 × 1024 pixels resolution and at the pixel size of 0.2 μm. During acquisition, laser settings were applied identically to all coverslips quantified in all experimental groups compared.

The analysis was performed using ImageJ software (National Institutes of Health) by drawing regions of interst (ROIs) of 50 synapses per neuron. Excitatory synapses (ROIs) were defined by staining for the SV marker VGLUT1. SYT1 or SYT7 fluorescence intensity signal for each synapse was measured within the defined ROI. Five to 10 autaptic neurons were collected per condition per culture, and at least three independent cultures were analyzed per experiment. Relative expression level of SYT1 among groups was calculated by normalizing the measured intensities of SYT1 to that of VGLUT1. The data were normalized to the control of each experiment.

Experimental design and statistics. For electrophysiology and immunocytochemistry experiments, we recorded and imaged approximately the same number of autaptic neurons from each experimental group each day to reduce data variability. For each parameter analyzed, the number of neurons used (n) and the number of independent cultures (N) are indicated in the figures, specifically within the bar graphs (n/N).

Data were acquired from at least three independent hippocampal autaptic cultures generated from three different animals ($N = 3$) to minimize culture–culture variation. We chose the nonlinear regression model standard Hill equation (see Fig. 7). We did not constrain any parameter of the model to a constant value. We performed a global nonlinear regression; we specify that parameters are shared to fit all datasets. All data points are weighted equally in the model.

Data from each experimental group were pooled except for those that were normalized to the mean value of the control group (see Figs. 2, 7, 8). Statistical analyses were performed using Prism 8 (GraphPad). All data were first subjected to Pearson omnibus K2 normality testing. Two-tailed unpaired t test or one-way ANOVA test for normally distributed data and Mann–Whitney test or Kruskal–Wallis ANOVA test for non-normally distributed data were then conducted. *Post hoc* multiple-comparison methods were used following ANOVA tests. Significance and p values were calculated and are shown in the corresponding figures or Table 1.

Results

Phenotype of synaptotagmin-1 loss in synaptic vesicle priming and spontaneous release is sensitive to neuronal maturation state

Given the controversy over SYT1 involvement in clamping and priming SVs, the observation of developmentally dependent effects of SYT2 in the calyx of Held (Kochubey et al., 2016), and the discovery of new point mutations in *SYT1* gene associated with a neurodevelopmental disorder (Baker et al., 2018), we aimed to reanalyze the roles of Synaptotagmin-1 in SV priming, synchronized and spontaneous release as a function of neuronal culture age. We recorded from autaptic hippocampal neurons derived from $Syt1^{+/+}$ or $Syt1^{-/-}$ mice across a 10 d time period (DIV11–21), and subsequently grouped our results into three different classes (DIV11–12, 15–16 and 20–21).

To assess SV priming, we measured the RRP of SVs using 5 s application of 500 mOsm hypertonic solution (Rosenmund and Stevens, 1996) and integrated the transient component of the evoked inward current. Although the RRP charge of $Syt1^{+/+}$ and $Syt1^{-/-}$ autaptic neurons at DIV11–12 was indistinguishable, at both later culturing stages (DIV15–16) and (DIV20–21) we detected a significant (~40–50%) reduction in RRP charge in the $Syt1^{-/-}$ group (Fig. 1*A*; RRP, pC: DIV11–12, $Syt1^{+/+}$ 135 ± 18, $n = 60/3$, and $Syt1^{-/-}$ 148 ± 17, $n = 57/3$, $p = 0.26$; DIV15–16, $Syt1^{+/+}$ 477 ± 54, $n = 58/3$, and $Syt1^{-/-}$ 247 ± 33, $n = 47/3$, $p = 0.0004$; DIV20–21, $Syt1^{+/+}$ 759 ± 89, $n = 44/3$, and $Syt1^{-/-}$ 360 ± 54, $n = 44/3$, $p < 0.0001$; Mann–Whitney test). Next, we analyzed spontaneous neurotransmitter release. We observed that loss of SYT1 led to no significant changes in spontaneous release rates for the early DIV group, whereas spontaneous release rate was enhanced in the two older DIV groups (Fig. 1*B*; Spontaneous rate, s^{-1}: DIV11–12, $Syt1^{+/+}$ 0.0028 ± 0.0003, $n = 56/3$, and $Syt1^{-/-}$ 0.0034 ± 0.0003, $n = 48/3$, $p = 0.0544$; DIV15–16, $Syt1^{+/+}$ 0.0029 ± 0.0005, $n = 42/3$, and $Syt1^{-/-}$ 0.0065 ± 0.0009, $n = 43/3$, $p < 0.0001$; DIV20-21, $Syt1^{+/+}$ 0.0019 ± 0.0004, $n = 44/3$, and $Syt1^{-/-}$ 0.0052±0.0012, $n = 44/3$, $p < 0.0001$; Mann–Whitney test), emphasizing that the impact of SYT1 loss on spontaneous release, like the impact on RRP size, is dependent on the maturation state of the neuron.

In contrast, Ca^{2+}-evoked release was massively affected regardless of culture age as indicated by the reduction in EPSC amplitude and charge in all three DIV groups (Fig. 1*C*; EPSC amplitude, nA: DIV11–12, $Syt1^{+/+}$ −1.17 ± 0.19, $n = 60/3$, and $Syt1^{-/-}$ −0.069 ± 0.007, $n = 58/3$, $p < 0.0001$; DIV15–16, $Syt1^{+/+}$ −3.2 ± 0.5, $n = 47/3$, and $Syt1^{-/-}$ −0.097 ± 0.012, $n = 43/3$, $p < 0.0001$; DIV20–21, $Syt1^{+/+}$ −4.19 ± 0.58, $n = 44/3$, and $Syt1^{-/-}$ −0.085 ± 0.012, $n = 44/3$, $p < 0.0001$; Mann–Whitney test). Moreover, the Pvr, as calculated by dividing the EPSC charge by the RRP charge, was similarly reduced by ~60% in all three DIV groups measured (Fig. 1D; Pvr, %: DIV11–12, $Syt1^{+/+}$ 7.7 ± 0.7, $n = 60/3$, and $Syt1^{-/-}$ 2.6 ± 0.3, $n = 57/3$, $p < 0.0001$; DIV15–16, $Syt1^{+/+}$ 7.4 ± 0.9, $n = 46/3$, and $Syt1^{-/-}$ 2.9 ± 0.6, $n = 43/3$, $p < 0.0001$; DIV20–21, $Syt1^{+/+}$ 6.7 ± 0.7, $n = 44/3$, and $Syt1^{-/-}$ 2.3 ± 0.3, $n = 44/3$, $p < 0.0001$; Mann–Whitney test).

Lentiviral-mediated SYT1 rescue experiments showed fully restored SV priming and spontaneous and AP-induced release efficacy in stages DIV15–21 (Fig. 2; RRP normalized (norm.): $Syt1^{+/+}$ 1 ± 0.11, $n = 39/3$, $Syt1^{-/-}$ 0.40 ± 0.05, $n = 31/3$, $p < 0.001$, and $Syt1^{-/-}{}_{+SYT1}$ 0.93 ± 0.15, $n = 29/3$, p = n.s. or <0.05; Spontaneous rate norm.: $Syt1^{+/+}$ 1 ± 0.13, $n = 37/3$, $Syt1^{-/-}$ 2.53 ± 0.53, $n = 30/3$, $p < 0.01$, and $Syt1^{-/-}{}_{+SYT1}$ 0.96 ± 0.12, $n = 26/3$, p = n.s. or <0.05; EPSC charge norm.: $Syt1^{+/+}$ 1 ±

Table 1. Summary table with the electrophysiological parameters measured in autaptic hippocampal glutamatergic neurons related to the culture stage

		$SYT1^{-/-}$			$SYT1^{-/-}$ +SYT7KD				
		DIV			DIV		SYT1 expression (DIV15–21)		
		11–12	15–16	20–21	11–12	15–16	<50%	50–100%	>100%
Synaptic transmission parameter	RRP	=	Reduced	Reduced	Reduced	Reduced	Reduced	=	=
	Spontaneous release	=	Increased	Increased	Increased	Increased	Increased	Increased	=
	Evoked release	Reduced	Reduced	Reduced	Reduced	Reduced	Reduced	=	=
	Pvr	Reduced	Reduced	Reduced	=	=	Reduced	Reduced	*Increased

*The Pvr endency toward an increased value, confirmed by STP experiment. The "=" symbol is "not significant differences detected when compared to control group".

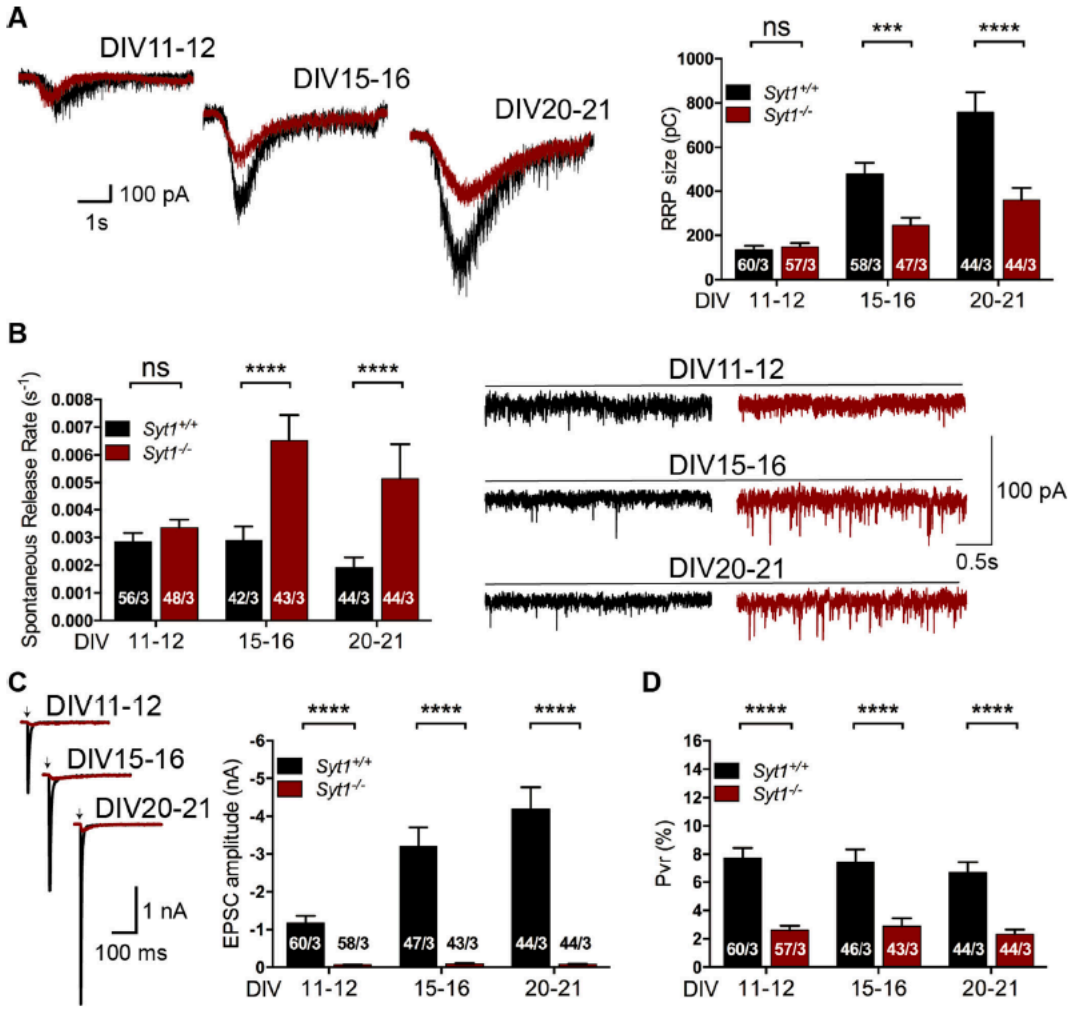

Figure 1. Electrophysiological characterization of *Synaptotagmin-1* knock-out hippocampal glutamatergic autaptic neurons at different time points. ***A***, Representative sucrose-evoked current traces (left) and summary bar graphs (right) of total current charge of $Syt1^{+/+}$ (black) and $Syt1^{-/-}$ (red) neurons evoked by 0.5 M sucrose solution for 5 s at early (DIV11–12), intermediate (DIV15–16), and late (DIV20–21) culture stages. ***B***, Example traces of spontaneous release events (right) and summary bar graphs of spontaneous release rate (left) calculated by dividing the mEPSC frequency by the number of primed synaptic vesicles at different neuronal culture stages. ***C***, Representative EPSC traces (left) and summary bar graphs of EPSC amplitudes (right) evoked by a 2 ms depolarization in 2 mM extracellular Ca^{2+} from autaptic neurons at the three neuronal stages from $Syt1^{+/+}$ (black) and $Syt1^{-/-}$ (red). Action potentials were blanked for better EPSC illustration and substituted by arrows. ***D***, Plot of Pvr in percentage calculated by dividing the evoked EPSC charge by the sucrose charge at the different neuronal stages. Data are mean ± SEM. Statistical significance and *p* values were calculated using the Mann–Whitney *U* test (***$p \leq 0.001$, ****$p \leq 0.0001$). ns, Not significant.

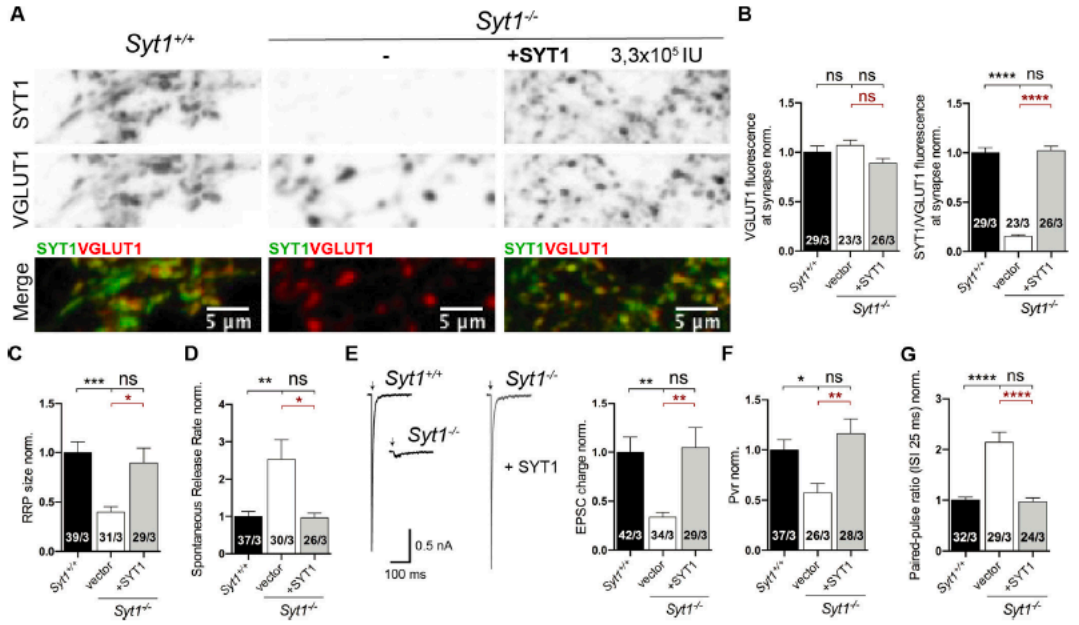

Figure 2. Evaluation of the synaptic SYT1 functions in $Syt1^{-/-}$ neurons rescued with SYT1. All immunocytochemistry and electrophysiological experiments were done from $Syt1^{+/+}$ and $Syt1^{-/-}$ hippocampal glutamatergic autaptic neurons at DIV15–21. ***A***, Representative images of hippocampal glutamatergic autaptic neurons of $Syt1^{-/-}$ infected with a lentivirus containing a nuclear GFP vector (−) or *Syt1*. ***B***, Right, Summary bar graph showing SYT1/VGLUT1 fluorescence normalized to $Syt1^{+/+}$. Summary bar plot of VGLUT1 fluorescence (left) and normalized summary bar plot of SYT1/VGLUT1 fluorescence intensity. ***C***, Bar plot of RRP size estimated by application of a hypertonic solution of $Syt1^{-/-}$ neurons rescued with SYT1 normalized to the $Syt1^{+/+}$control. ***D***, Summary bar plot of spontaneous release rate from $Syt1^{-/-}$ neurons rescued with SYT1 normalized to the $Syt1^{+/+}$ control. ***E***, Sample traces of EPSCs (right) and summary bar plot of the quantification of total EPSC charge transfer (left) from $Syt1^{-/-}$ neurons rescued with SYT1 normalized to the $Syt1^{+/+}$ control. Artifacts and/or action potentials were blanked and substituted with arrows. ***F***, Bar plot of Pvr from $Syt1^{-/-}$ neurons rescued with SYT1 normalized to $Syt1^{+/+}$ control. ***G***, Graph of the paired-pulse ratio. All data shown indicate mean ± SEM. Statistical analysis was applied by Kruskal–Wallis test (*$p < 0.05$, **$p < 0.01$, ***$p < 0.001$, ****$p < 0.0001$. ns, Not significant. Scale bars: 5 μm.

0.16, n = 42/3, $Syt1^{-/-}$ 0.34 ± 0.05, n = 34/3, $p < 0.01$, and $Syt1^{-/-}{}_{+SYT1}$ 1.05 ± 0.2, n = 29/3, p = n.s. or <0.01; Pvr norm.: $Syt1^{+/+}$ 1 ± 0.10, n = 37/3, $Syt1^{-/-}$ 0.57 ± 0.09, n = 26/3, $p <$ 0.05, and $Syt1^{-/-}{}_{+SYT1}$ 1.16 ± 0.15, n = 28/3, p = n.s. or <0.01; PPR 40 Hz, norm.: $Syt1^{+/+}$ 1 ± 0.06, n = 32/3, $Syt1^{-/-}$ 2.15 ± 0.20, n = 29/3, $p < 0.0001$, and $Syt1^{-/-}{}_{+SYT1}$ 0.97 ± 0.07, n = 24/3, p = n.s. or <0.0001; Kruskal–Wallis test), indicating that the loss of function phenotype of SYT1 at older cultures was because of the loss of the protein and not because of developmental processes. Expression levels of exogenously expressed SYT1 were near wild-type levels as indicated by relative SYT1 immunofluorescence intensity from VGLUT1 marker positive compartments (Fig. 2*A*,*B*; VGLUT1 norm.: $Syt1^{+/+}$ 1 ± 0.06, n = 29/3, $Syt1^{-/-}$ 1.07 ± 0.06, n = 23/3, p = n.s., and $Syt1^{-/-}{}_{+SYT1}$ 0.89 ± 0.04, n = 26/3, p = n.s./n.s.; SYT1/VGLUT1 norm.: $Syt1^{+/+}$ 1 ± 0.05, n = 29/3, $Syt1^{-/-}$ 0.16 ± 0.01, n = 23/3, $p < 0.0001$, and $Syt1^{-/-}{}_{+SYT1}$ 1.02 ± 0.05, n = 26/3, p = n.s. or <0.0001; Kruskal–Wallis test).

Overall, our data confirm that loss of SYT1 leads to loss of synchronized and efficient AP-triggered release but also that the impairment of RRP and clamping of spontaneous release only appears in more mature neurons. One possible explanation could be that the loss of SYT1 at early maturation stages may be compensated by other synaptotagmin isoform, which would be downregulated over neuronal development as similarly shown at the calyx of Held synapses (Kochubey et al., 2016). These findings may provide an explanation for findings in autaptic glutamatergic neurons where no significant changes in RRP size were reported when recordings were pooled over extended times *in vitro* (e.g., Liu et al., 2009; DIV12–17). Therefore, in the remaining part of the experiments, we limited our experiments to neurons that were DIV15 or older.

Partial functional redundancy between synaptotagmin-1 and synaptotagmin-7

Recent genetic and functional analysis indicates that SYT7 plays a redundant role in SV priming function (Bacaj et al., 2015). Moreover, the expression of the Synaptotagmin1/2 paralogs are developmentally regulated at a murine auditory synapse, contributing to maturation-dependent variation in synaptic phenotypes in synaptotagmin loss of function mouse models (Kochubey et al., 2016). We therefore explored whether SYT7 expression in less mature hippocampal neurons contributes to the milder phenotype of SYT1 loss by knocking down SYT7 protein expression in $Syt1^{-/-}$ neurons. First, we examined SYT1 and SYT7 protein levels in presynaptic compartments at early (DIV11–12) or intermediate stages (DIV15–16) in $Syt1^{+/+}$ and $Syt1^{-/-}$ neurons and subsequently measured at both stages the presynaptic SYT7 reduction affected by lentiviral expression of a SYT7 *shRNA* construct in $Syt1^{-/-}$ autaptic neurons (Fig. 3). We used VGLUT1 protein expression to spatially define presynaptic compartments and to serve as a reference signal for SYT1 and SYT7 expression levels. In $Syt1^{+/+}$ neurons, SYT1 protein levels gradually increased with time of DIV but stayed relatively

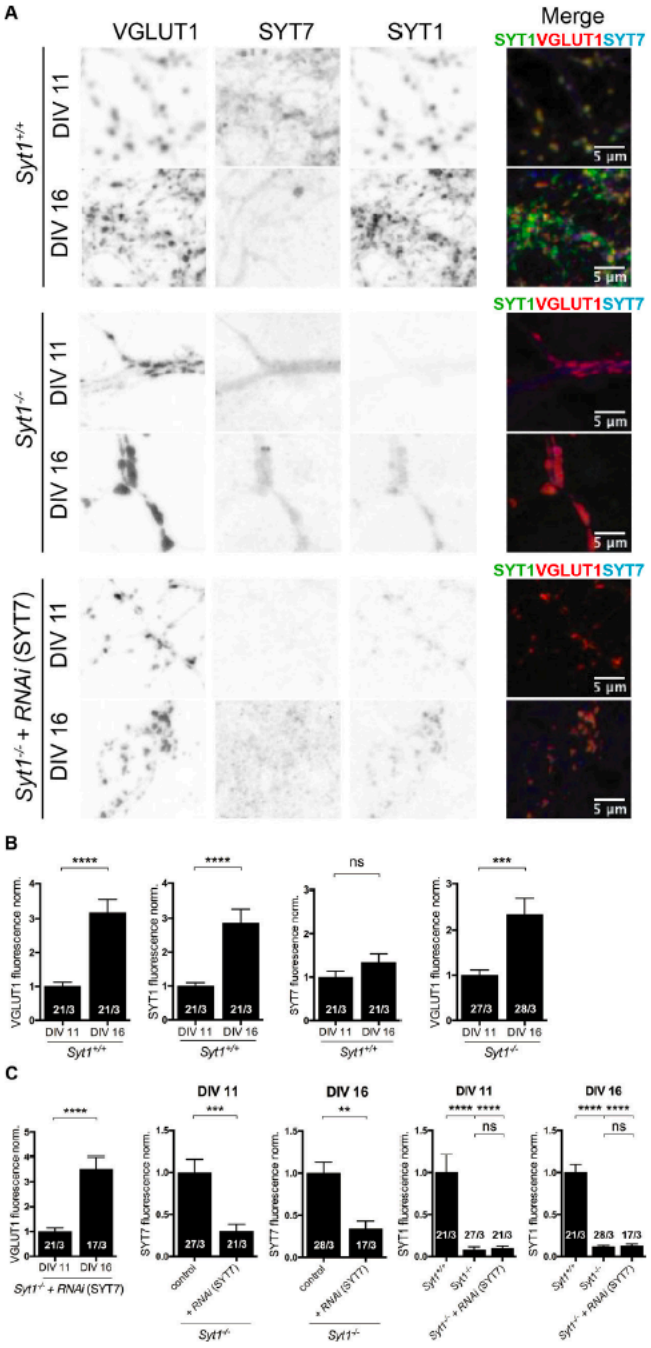

Figure 3. Presynaptic SYT7 quantification of Synaptotagmin-7 in presence and absence of SYT1 and its silencing effect in $Syt1^{-/-}$ hippocampal glutamatergic neurons at different neuronal stages. ***A***, ***B***, Representative images (***A***) and (***B***) quantification of SYT1 (green) and SYT7 (blue) protein levels at VGLUT1 (red) positive regions at DIV11 and DIV16 of $Syt1^{+/+}$ and $Syt1^{-/-}$ neurons. ***C***, Quantification of SYT1, SYT7, and VLGUT1 from $Syt1^{-/-}$ autaptic neurons infected with lentivirus carrying either an empty vector or RNA interference (*RNAi*) for SYT7 at early and mature stages. Data are mean ± SEM. Statistical significance and p values were calculated using the Mann–Whitney U test (**$p \leq 0.01$,***$p \leq 0.001$, ****$p \leq 0.0001$). ns, Not significant. Scale bars: 5 μm.

constant in comparison to VGLUT1. In contrast, SYT7 protein expression levels remained constant and, consequently, SYT7/VGLUT1 signal decreased over time in culture (Fig. 3*A*,*B*; VGLUT1 norm.: $Syt1^{+/+}{}_{DIV11}$ 1 ± 0.12, n = 21/3, and $Syt1^{+/+}{}_{DIV16}$ 3.2 ± 0.4, n = 21/3, $p <$ 0.0001; two-tailed unpaired t test; SYT1 norm.: $Syt1^{+/+}{}_{DIV11}$ 1 ± 0.10, n = 21/3, and $Syt1^{+/+}{}_{DIV16}$ 2.9 ± 0.4, n = 21/3, $p <$ 0.0001; two-tailed unpaired t test; SYT7 norm.: $Syt1^{+/+}{}_{DIV11}$ 1 ± 0.14, n = 21/3, and $Syt1^{+/+}{}_{DIV16}$ 1.3 ± 0.2, n = 21/3, p = n.s.; Mann–Whitney test; VGLUT1 norm.: $Syt1^{-/-}{}_{DIV11}$ 1 ± 0.12, n = 27/3, and $Syt1^{+/+}{}_{DIV16}$ 2.3 ± 0.36, n = 28/3, $p <$ 0.001; Mann–Whitney test). We tested how effective the SYT7 *shRNA* reduced the presynaptic SYT7 protein expression and found an average reduction of ~75% across all DIVs tested using $Syt1^{-/-}$ autaptic neurons (Fig. 3*C*; VGLUT1 norm.: $Syt1^{-/-}{}_{+RNAi(Syt7)DIV11}$ 1 ± 0.14, n = 21/3, and $Syt1^{-/-}{}_{+RNAi(Syt7)DIV16}$ 3.5 ± 0.47, n = 17/3, $p <$ 0.0001; Mann–Whitney test; SYT7DIV11 norm.: $Syt1^{-/-}$ 1 ± 0.21, n = 27/3, and $Syt1^{-/-}{}_{+RNAi(Syt7)}$ 0.30 ± 0.15, n = 21/3, $p <$ 0.001; Mann–Whitney test; SYT7DIV16 norm.: $Syt1^{-/-}$ 1 ± 0.13, n = 28/3, and $Syt1^{-/-}{}_{+RNAi(Syt7)}$ 0.34 ± 0.09, n = 17/3, $p <$ 0.001; Mann–Whitney test; SYT1DIV11 norm.: $Syt1^{+/+}$ 1 ± 0.20, n = 21/3, $Syt1^{-/-}$ 0.08 ± 0.04, n = 27/3, $p <$ 0.0001, and $Syt1^{-/-}{}_{+RNAi(Syt7)}$ 0.1 ± 0.096, n = 21/3, $p <$ 0.0001; Kruskal–Wallis test; SYT1DIV16 norm.: $Syt1^{+/+}$ 1 ± 0.096, n = 21/3, $Syt1^{-/-}$ 0.11 ± 0.02, n = 28/3, $p <$ 0.0001, and $Syt1^{-/-}{}_{+RNAi(Syt7)}$ 0.07 ± 0.06, n = 17/3, $p <$ 0.0001; Kruskal–Wallis test).

Reduction of SYT7 protein expression in $Syt1^{-/-}$ autaptic neurons reduced RRP size and increased mEPSC rates at DIV11–12 and DIV15–16 (Fig. 4*A*,*B*; RRP, pC: DIV11–12, $Syt1^{+/+}$ 165 ± 23, n = 48/4, $Syt1^{-/-}$ 170 ± 21, n = 40/4, p = n.s., and $Syt1^{-/-}{}_{+iRNA(Syt7)}$ 34 ± 6, n = 40/4, $p <$ 0.0001/0.0001; DIV15–16, $Syt1^{+/+}$ 567 ± 69, n = 44/4, $Syt1^{-/-}$ 279 ± 43, n = 41/4, $p <$ 0.01, and $Syt1^{-/-}{}_{+iRNA(Syt7)}$ 50 ± 9, n = 30/4, $p <$ 0.0001/0.0001; Kruskal–Wallis test; Spontaneous rate, s^{-1}: DIV11–12, $Syt1^{+/+}$ 0.003 ± 0.0004, n = 48/4, $Syt1^{-/-}$ 0.0043 ± 0.0005, n = 33/4, p = n.s., and $Syt1^{-/-}{}_{+iRNA(Syt7)}$ 0.012 ± 0.0015, n = 38/4, $p <$ 0.0001/0.01; DIV15–16, $Syt1^{+/+}$ 0.0016 ± 0.0002, n = 44/4, $Syt1^{-/-}$

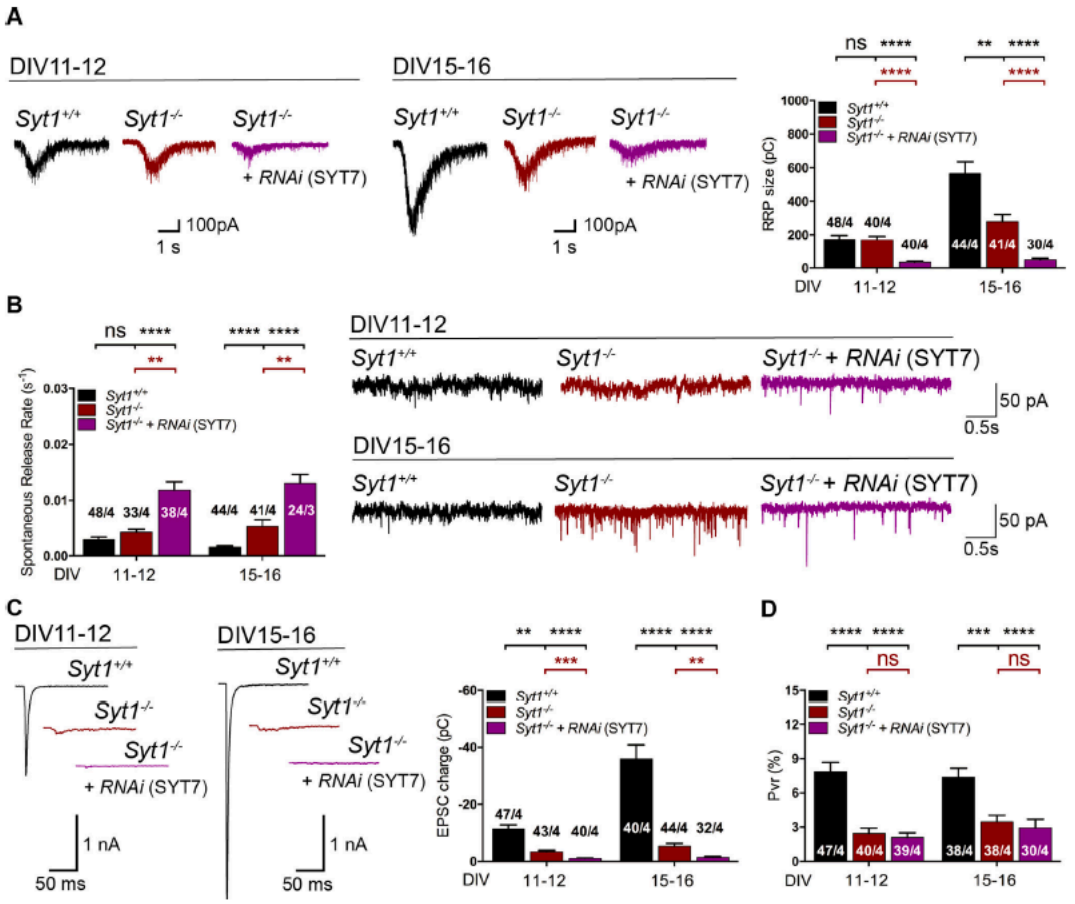

Figure 4. Knockdown of Synaptotagmin-7 in $Syt1^{-/-}$ hippocampal glutamatergic neurons at different neuronal stages. ***A***, Representative traces at early (DIV11–12) and intermediate (DIV15–16) autaptic neuronal stages (right) and summary bar graphs (left) of the charge of sucrose-evoked release of $Syt1^{+/+}$ (black), $Syt1^{-/-}$ (red), and $Syt1^{-/-}$ neurons infected with lentivirus containing RNAi for silencing SYT7 (purple). ***B***, Example traces of spontaneous release events (right) and summary bar graphs of spontaneous release rate (left) at the two different neuronal stages as ***A***. ***C***, Representative EPSC traces (right) and summary bar graphs of total EPSC charge measured over an interval of 1 s (left). ***D***, Summary bar graphs of vesicular release probability. Data indicate mean ± SEM. Statistical significance and *p* values were estimated by a Kruskal–Wallis test (*$p \leq 0.05$, **$p \leq 0.01$, ***$p \leq 0.001$, ****$p \leq 0.0001$). ns, Not significant.

0.0054 ± 0.0012, $n = 41/4$, $p < 0.01$, and $Syt1^{-/-}{}_{+iRNA(Syt7)}$ 0.013 ± 0.001, $n = 24/4$, $p < 0.0001/0.01$; Kruskal–Wallis test). These results suggest that SYT7 compensates for the loss of SYT1-dependent synaptic vesicle priming and clamp of spontaneous release (Fig. 4*A*,*B*). Next, we examined whether SYT7 expression contributes evoked NT release and the probability of vesicle fusion of $Syt1^{-/-}$ neurons. Although knocking down SYT7 expression levels in $Syt1^{-/-}$ neurons had an impact on the amplitude and charge of the Ca^{2+}-evoked release at both stages, the changes were proportional to those observed for the RRP size and thus did not lead to a further significant effect in the Pvr (Fig. 4*C*,*D*; EPSC charge, pC: DIV11–12, $Syt1^{+/+}$ −11.1 ± 1.5, $n = 47/4$, $Syt1^{-/-}$ −3.8 ± 0.5, $n = 43/4$, $p < 0.01$, and $Syt1^{-/-}{}_{+iRNA(Syt7)}$ −1.1 ± 0.2, $n = 40/4$, $p < 0.0001/0.001$; DIV15–16, $Syt1^{+/+}$ −36 ± 5, $n = 40/4$, $Syt1^{-/-}$ −5.3 ± 1, $n = 44/4$, $p < 0.0001$, and $Syt1^{-/-}{}_{+iRNA(Syt7)}$ −1.4 ± 0.3, $n = 32/4$, $p < 0.0001/0.01$; Pvr, %, DIV11–12: $Syt1^{+/+}$ 8.5 ± 1, $n = 47/4$, $Syt1^{-/-}$ 3.2 ± 0.5, $n = 40/4$, $p < 0.0001$, and $Syt1^{-/-}{}_{+iRNA(Syt7)}$ 3.3± 0.6, $n = 39/4$, $p < 0.0001$/n.s.; DIV15–16, $Syt1^{+/+}$ 7.4 ± 0.8, $n = 38/4$, $Syt1^{-/-}$ 3.5 ± 0.6, $n = 38/4$, $p < 0.001$, and $Syt1^{-/-}{}_{+iRNA(Syt7)}$ 2.9 ± 0.8, $n = 30/4$, $p < 0.0001$/n.s.; Kruskal–Wallis test) of $Syt1^{-/-}$ autaptic neurons in any stages tested.

Altogether these results suggest that although SYT1 is essential for evoked neurotransmitter release, SYT7 is well capable of substituting in the role of SYT1 in clamping spontaneous release and enabling SV priming, which results in the weakening of SYT1 deficiency of these two phenotypes in less mature neurons.

Synaptotagmin-1 haploinsufficiency affects release efficiency and spontaneous release rate

Our results on SV priming and spontaneous clamping suggest that the underlying phenotypes are dependent on both SYT1 and

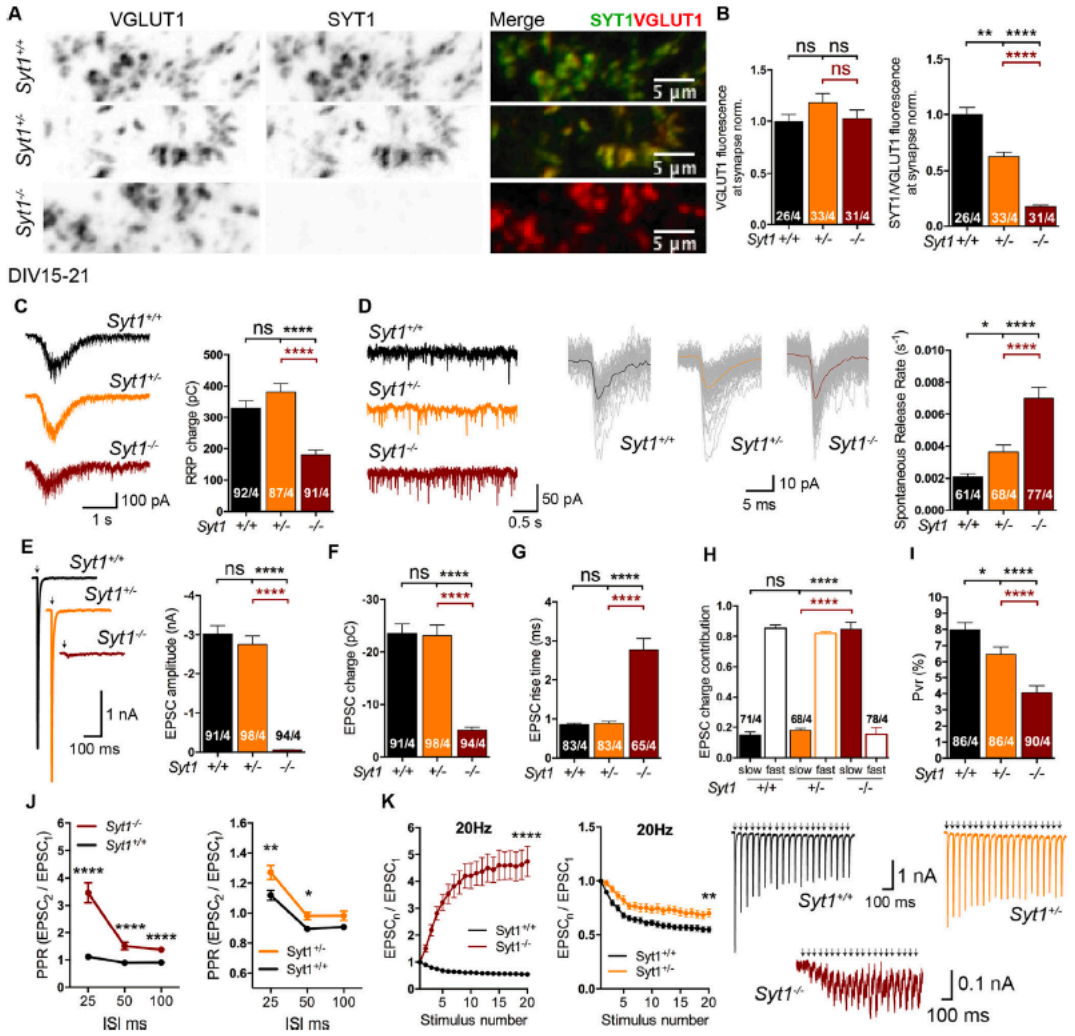

Figure 5. Evaluation of SV priming and neurotransmitter release in Synaptotagmin-1 heterozygous neurons. All immunocytochemistry and electrophysiological experiments were done from $Syt1^{+/+}$, $Syt1^{+/-}$, and $Syt1^{-/-}$ hippocampal glutamatergic autaptic neurons at DIV15-21. ***A***, Sample images from $Syt1^{+/+}$, $Syt1^{+/-}$ and $Syt1^{-/-}$ hippocampal glutamatergic autaptic neurons double labeled with VGLUT1 (left, black puncta), SYT1 (middle, black puncta), antibodies and colocalization image of SYT1 in green and VLGUT1 in red (right, Merge), demonstrating the presence of Synaptotagmin-1 at the presynaptic terminals. Scale bar, 5 µm. ***B***, Bar plot of VGLUT1 average fluorescence intensities at presynaptic terminal for the three *Syt-1* genotypes (left), normalized to SYT1 expression levels of the $Syt1^{+/+}$ neurons. Summary bar plot of SYT1 average fluorescence intensity at VGLUT1-positive puncta normalized to SYT1 average fluorescence intensity of $Syt1^{+/+}$ (right). ***C***, Left, Sample traces of sucrose responses for the three *Syt-1* genotypes. Right, Bar graph of sucrose-evoked current charges of $Syt1^{+/+}$ (black), $Syt1^{+/-}$ (orange), and $Syt1^{-/-}$ (cayenne) autaptic neurons. ***D***, Left, Example traces of spontaneous release events and 106 mEPSC events superimposed from $Syt1^{+/+}$, 198 mEPSC events superimposed from $Syt1^{+/-}$, and 257 mEPSC events superimposed from $Syt1^{-/-}$ of a recording time period of 3 s in a 15 ms time window (center). Right, Summary bar graph of the spontaneous release rate of mEPSC events. ***E***, Representative EPSC traces (left) and summary bar graphs (right) of EPSC amplitudes. ***F***, Summary bar graph of total EPSC charge transfer. ***G***, Summary bar plot of the rise time (20–80%) of EPSCs. ***H***, Bar graphs of the relative contribution of the synchronic and asynchronic components to the EPSC charge. ***I***, Bar plot of the average vesicular release probability of $Syt1^{+/+}$, $Syt1^{+/-}$ and $Syt1^{-/-}$. ***J***, Summary graph of the average paired-pulse ratio plotted against interpulse interval from 25 to 100 ms corresponding to 40, 20, and 10 Hz of $Syt1^{+/+}$ (black), $Syt1^{+/-}$ (orange), and $Syt1^{-/-}$ (cayenne) autaptic neurons. ***K***, Short-term plasticity response during high-frequency (20 Hz) stimulation. Representative sample traces of EPSCs resulted from the stimulation of 20 consecutives APs separated by 50 ms (right) and plots of mean EPSC amplitudes normalized to the first EPSC of $Syt1^{+/+}$ (black), $Syt1^{+/-}$ (orange), and $Syt1^{-/-}$ (cayenne) during train stimulation. Artifacts and action potentials were blanked from the traces and substituted by arrows in ***E*** and ***K***. Data are mean ± SEM. Statistical significances and *p* values were obtained by Kruskal–Wallis test (*$p \leq 0.05$, **$p \leq 0.01$, ***$p \leq 0.001$, ****$p \leq 0.0001$). ns, Not significant. Scale bars: 5 µm.

SYT7 protein expression levels. Because monoallelic mutations in *SYT1* lead to neurologic disorders (Baker et al., 2015, 2018), it raises the question of whether and which of the three SYT1 functions in NT release is impaired by reduced SYT1 protein amount. We first quantified SV priming, clamping, and calcium-evoked release in $Syt1^{+/+}$, $Syt1^{+/-}$, and $Syt1^{-/-}$ at a maturation stage where SYT1 dominates the synaptic phenotype (DIV15–21).

Immunocytochemistry experiments showed that the amount of SYT1 protein at presynaptic terminals of $Syt1^{+/-}$ neurons was ~50% reduced compared with $Syt1^{+/+}$ neurons (Fig. 5*A*,*B*; *VGLUT1* norm.: $Syt1^{+/+}$ 1 ± 0.07, n = 26/4, $Syt1^{+/-}$ 1.18 ± 0.09, n = 33/4, p = n.s., and $Syt1^{-/-}$ 1.03 ± 0.09, n = 31/4, p = n.s./n.s.; *SYT1/VGLUT1* norm.: $Syt1^{+/+}$ 1 ± 0.06, n = 26/4, $Syt1^{+/-}$ 0.62 ± 0.04, n = 33/4, $p < 0.01$, and $Syt1^{-/-}$ 0.18 ± 0.02, n = 31/4, $p < 0.0001/< 0.0001$; Kruskal–Wallis test). As expected, the complete absence of SYT1 in $Syt1^{-/-}$ neurons resulted in a ~40% reduction in the pool size (Fig. 5*C*). However, we found no significant differences in the RRP size between $Syt1^{+/+}$ and $Syt1^{+/-}$ neurons (Fig. 5*C*; RRP, pC: $Syt1^{+/+}$ 330 ± 24, n = 92/4, $Syt1^{+/-}$ 382 ± 26, n = 87/4, p = n.s., and $Syt1^{-/-}$ 180 ± 15, n = 91/4, $p < 0.0001/<0.0001$; Kruskal–Wallis test). This indicates that loss of >50% of SYT1 protein is required to impair the role of SYT1 in SV priming. A significant increase in the spontaneous release rate of synaptic vesicles was observed in $Syt1^{+/-}$ autaptic neurons (Fig. 5*D*; Spontaneous rate, s^{-1}: $Syt1^{+/+}$ 0.002 ± 0.0002, n = 61/4, $Syt1^{+/-}$ 0.004 ± 0.0004, n = 68/4, $p < 0.05$, and $Syt1^{-/-}$ 0.007 ± 0.0007, n = 77/4, $p < 0.0001/< 0.0001$; Kruskal–Wallis test).

In agreement with previous work (Geppert et al., 1994; Nishiki and Augustine, 2004; Xue et al., 2008), autaptic $Syt1^{-/-}$ neurons showed severe desynchronization of evoked release, which is reflected in the drastic reduction in peak EPSC amplitude (Fig. 5*E*). Furthermore, integrating the charge of the EPSC over 1 s past AP triggering, we also observed an ~75% decrease in the EPSC charge (Fig. 5*F*). In contrast, we detected no significant difference in $Syt1^{+/-}$ EPSC amplitude and charge when compared with $Syt1^{+/+}$ autaptic neurons (Fig. 5*E*,*F*; EPSC amplitude, nA: $Syt1^{+/+}$ −3.0 ± 0.2, n = 91/4, $Syt1^{+/-}$ −2.8 ± 0.2, n = 98/4, p = n.s., and $Syt1^{-/-}$ −0.06 ± 0.006, n = 94/4, $p < 0.0001/<0.0001$; Kruskal–Wallis test; EPSC charge, pC: $Syt1^{+/+}$ −24 ± 2, n = 91/4, $Syt1^{+/-}$ −23 ± 2, n = 98/4, p = n.s., and $Syt1^{-/-}$ −5 ± 0.5, n = 94/4, $p < 0.0001/<0.0001$; Kruskal–Wallis test). We then examined whether 50% loss of SYT1 protein leads to some changes in EPSC kinetics in the $Syt1^{+/-}$ neurons. The EPSC rise time of $Syt1^{+/-}$ neurons was like wild type, whereas the rise time was about threefold slower for $Syt1^{-/-}$ neurons (Fig. 5*G*; EPSC rise time, ms: $Syt1^{+/+}$ 0.9 ± 0.04, n = 83/4, $Syt1^{+/-}$ 0.9 ± 0.04, n = 83/4, p = n.s., and $Syt1^{-/-}$ *2.8±0.3*, n = 65/4, $p < 0.0001/< 0.0001$; Kruskal–Wallis test). The decay time of EPSC was analyzed by a two-exponential fit, and we found that between the $Syt1^{+/+}$ and $Syt1^{+/-}$ neurons, both the fast and slow components were unaltered in their relative amplitudes and time constants (Fig. 5*H*). In contrast, in $Syt1^{-/-}$ neurons, time constant increased, and the fractional contribution of the slow component increased from ~20% to 80% (Fig. 5*H*; EPSC components: $Syt1^{+/+}$, slow 0.15 ± 0.02, fast 0.85 ± 0.02, n = 71/4, $Syt1^{+/-}$, slow 0.18 ± 0.01, fast 0.82 ± 0.01, n = 68/4, p = 0.1705, and $Syt1^{-/-}$, slow 0.85 ± 0.05, fast 0.15 ± 0.05, n = 78/4, $p < 0.0001/< 0.0001$; Kruskal–Wallis test).

The reduction of EPSC charge in $Syt1^{-/-}$ exceeds the reduction in RRP size, indicating that complete loss of SYT1 leads to a reduction in vesicular release probability. We thus measured vesicular release probability in $Syt1^{+/-}$ neurons and surprisingly found a significant reduction in Pvr when compared with $Syt1^{+/+}$ autaptic neurons (Fig. 5*I*; Pvr, %: $Syt1^{+/+}$ 8.6 ± 0.4, n = 86/4, $Syt1^{+/-}$ 7.5 ± 0.6, n = 86/4, $p < 0.05$, and $Syt1^{-/-}$ 4.4 ± 0.5, n = 90/4, $p <0.0001/< 0.0001$; Kruskal–Wallis test). The reduced release probability was corroborated by analysis of short-term plasticity experiments, in which we applied sequential pairs of action potentials with an interpulse interval of 25, 50, or 100 ms. Consistent with the Pvr results, $Syt1^{-/-}$ neurons displayed a significant increase of the PPR at 10, 20, and 40 Hz compared with $Syt1^{+/+}$ and a significant increase of the PPR at 20 and 40 Hz compared with $Syt1^{+/-}$ (Fig. 5*J*; 10 Hz: $Syt1^{+/+}$ 0.91 ± 0.02, n = 47/4, $Syt1^{+/-}$ 0.98 ± 0.03, n = 62/4, p = n.s., and $Syt1^{-/-}$ 1.38 ± 0.09, n = 41/4, $p < 0.0001/< 0.0001$; Kruskal–Wallis test; 20 Hz: $Syt1^{+/+}$ 0.90 ± 0.02, n = 53/4, $Syt1^{+/-}$ 0.99 ± 0.02, n = 50/4, $p < 0.05$, and $Syt1^{-/-}$ 1.51 ± 0.13, n = 20/4, $p < 0.0001/< 0.0001$; Kruskal–Wallis test; 40 Hz: $Syt1^{+/+}$ 1.09 ± 0.03, n = 86/4, $Syt1^{+/-}$ 1.28 ± 0.05, n = 81/4, $p < 0.01$, and $Syt1^{-/-}$ 3.46 ± 0.37, n = 78/4, $p < 0.0001/< 0.0001$; Kruskal–Wallis test). In addition, we performed a 20 AP at 20 Hz train pulses experiment. $Syt1^{-/-}$ neurons strongly facilitated, and even $Syt1^{+/-}$ neurons showed significantly less depression compared with $Syt1^{+/+}$ neurons (Fig. 5*K*; $Syt1^{+/+}$ 0.55 ± 0.03, n = 53/4, $Syt1^{+/-}$ 0.70 ± 0.04, n = 50/4, $p < 0.01$, and $Syt1^{-/-}$ 4.7 ± 0.6, n = 20/4, $p < 0.0001$; Kruskal–Wallis test).

Together, these results demonstrate that the 50% reduced SYT1 protein at $Syt1^{+/-}$ presynaptic terminals did not affect the RRP size but modestly impaired release efficiency and the rate of spontaneous release. Although it isn't clear whether the patients carrying a heterozygous mutation in the *SYT1* gene may have an altered SYT1 presence at the glutamatergic synapses, these findings may be relevant to understand how a 50% deficiency in SYT1 expression could contribute to develop an aberrant neurologic phenotype.

Synaptotagmin-1 is a limiting factor for vesicle fusion release efficiency during high-frequency stimulation

Our analysis with the $Syt1^{+/-}$ neurons showed that 50% reduced STY1 expression affects synaptic properties such as spontaneous release rate and efficiency of the release, indicating the relative sensitivity of SYT1 protein levels on release efficacy. We extended this analysis to overexpression of the SYT1. We used a dose of lentivirus to mediate SYT1 overexpression in $Syt1^{+/+}$ autaptic neurons (DIV15–21), which led to an overexpression of ~75% of WT levels in SYT1 content in presynaptic terminals (Fig. 6*A*; *VGLUT1* norm.: $Syt1^{+/+}$ 1 ± 0.04, n = 30/3, and $Syt1^{+/+}{}_{+SYT1}$ 1.06 ± 0.04, n = 30/3, p = 0.29; *SYT1/VGLUT1* norm.: $Syt1^{+/+}$ 1 ± 0.05, n = 30/3, and $Syt1^{+/+}{}_{+SYT1}$ 1.78 ± 0.06, n = 30/3, p < 0.0001; two-tailed unpaired t test). RRP size (Fig. 6*B*; RRP, pC: $Syt1^{+/+}$ 549 ± 85, n = 33/3, and $Syt1^{+/+}{}_{+SYT1}$ 500 ± 57, n = 36/3, p = 0.67; Mann–Whitney test), spontaneous release rate (Fig. 6*C*; Spontaneous rate, s^{-1}: $Syt1^{+/+}$ 0.003 ± 0.0005, n = 31/3, and $Syt1^{+/+}{}_{+SYT1}$ 0.0017 ± 0.0002, n = 34/3, p = 0.45; Mann–Whitney test), and the EPSC amplitude (Fig. 6*D*; EPSC amplitude, nA: $Syt1^{+/+}$ −2.99 ± 0.43, n = 34/3, and $Syt1^{+/+}{}_{+SYT1}$ −4.10 ± 0.47, n = 37/3, p = 0.084; Mann–Whitney test) were statistically not significant compared with $Syt1^{+/+}$ neurons (DIV15–21). Also computing Pvr in the SYT1 overexpressing neurons did not show any significant change (Fig. 6*E*; Pvr, %: $Syt1^{+/+}$ 7.0 ± 1.1, n = 33/3, and $Syt1^{+/+}{}_{+SYT1}$ 8.4 ± 1.0, n = 35/3, p = 0.19; Mann–Whitney test). However, SYT1 overexpression caused more depression of the second response during paired-pulse experiments (Fig. 6*F*; 40 Hz: $Syt1^{+/+}$ 1.26 ± 0.06, n = 34/3, and $Syt1^{+/+}{}_{+SYT1}$ 0.98 ± 0.04, n = 33/3, p = 0.0005; Mann–Whitney test) compared with $Syt1^{+/+}$, emphasizing that release efficacy is more sensitive to changes in SYT1 levels than its function in regulating RRP size.

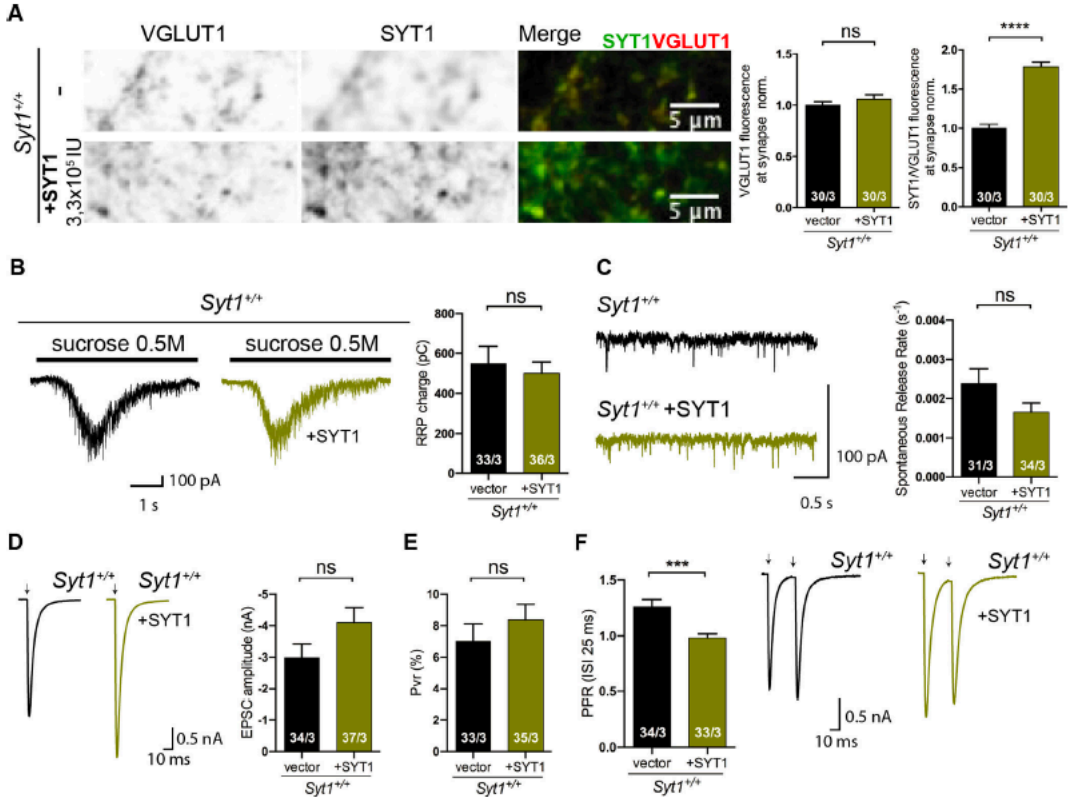

Figure 6. Impact of Synaptotagmin-1 overexpression on synaptic properties. All immunocytochemistry and electrophysiological experiments were done from $Syt1^{+/+}$ hippocampal glutamatergic autaptic neurons at DIV15–21. ***A***, Representative images of $Syt1^{+/+}$ autaptic neurons with and without overexpression of SYT1, co-immunolabeled for VGLUT1 (left), SYT1 (middle), and Merge image (right), showing the presence of VGLUT1 in red and SYT1 in green. Scale bar, 5 µm. Quantification graphs of normalized VGLUT1 fluorescence intensities and SYT1/VGLUT1 fluorescence intensity ratios of $Syt1^{+/+}$ hippocampal neurons overexpressing GFP vector (black) or SYT1 (right, olive green). ***B***, Representative sucrose-evoked current traces (left) and summary bar plot of RRP size (right). ***C***, Example traces of spontaneous release events (left) and summary bar graph (right) of spontaneous release rate. ***D***, Sample EPSC traces (left) and bar plot of EPSC amplitude (right). ***E***, Summary bar graph of average probability of vesicle release. ***F***, Left, Bar graph of PPR at 40 Hz. Right, Representative sample traces of EPSCs resulted from the stimulation of two consecutives APs separated by 25 ms. Artifacts and/or action potentials are blanked and substituted with arrows in ***D*** and ***F***. All data shown are mean ± SEM. Statistical analysis was applied Mann–Whitney *U test* (*$p \leq 0.05$, **$p \leq 0.01$, ***$p \leq 0.001$, ****$p \leq 0.0001$). ns, Not significant. Scale bars, 5 µm.

Manipulation of endogenous expression levels of synaptotagmin-1 reveals different functional thresholds

Does SYT1 regulate NT release and recruitment of SVs to the presynaptic PM in a protein concentration-dependent manner? To address this question, we examined the impact of titrating endogenous SYT1 protein expression in autaptic neurons at DIV15–21 using RNA interference (RNAi) technology, which led to a graded reduction of SYT1 levels in presynaptic terminals down to 10–25% of $Syt1^{+/+}$ SYT1 expression levels (Fig. 7*A*; *VGLUT1* norm.: $Syt1^{+/+}$ 1 ± 0.06, n = 19/3, $Syt1^{+/+}{}_{1xRNA(Syt1)}$ 1.32 ± 0.1, n = 20/3, p = n.s., $Syt1^{+/+}{}_{2xRNA(Syt1)}$ 1.26 ± 0.09, n = 24/3, p = n.s., and $Syt1^{+/+}{}_{4xRNA(Syt1)}$ 1.33 ± 0.10, n = 27/3, p = n.s.; *SYT1/VGLUT1* norm.: $Syt1^{+/+}$ 1 ± 0.05, n = 19/3, $Syt1^{+/+}{}_{1xRNA(Syt1)}$ 0.25 ± 0.04, n = 20/3, $p < 0.001$, $Syt1^{+/+}{}_{2xRNA(Syt1)}$ 0.13 ± 0.02, n = 24/3, $p < 0.0001$, and $Syt1^{+/+}{}_{4xRNA(Syt1)}$ 0.096 ± 0.01, n = 27/3, $p < 0.0001$; Kruskal–Wallis test).

We found that the number of fusion-competent vesicles, as measured by sucrose application, was only significantly reduced when the SYT1 protein expression level was below 10% (Fig. 7*B*; RRP norm.: $Syt1^{+/+}$ 1 ± 0.11, n = 51/4, $Syt1^{+/+}{}_{1xRNA(Syt1)}$ 0.97 ± 0.13, n = 35/4, p = n.s., $Syt1^{+/+}{}_{2xRNA(Syt1)}$ 0.83 ± 0.11, n = 37/4, p = n.s., and $Syt1^{+/+}{}_{4xRNA(Syt1)}$ 0.61 ± 0.08, n = 39/4, $p < 0.05$; Kruskal–Wallis test). On the other hand, the spontaneous release rate was affected by the gradual reduction in SYT1 expression levels, showing progressive unclamping with reduction of SYT1 expression, reaching about a threefold increase when SYT1 levels were close to those of $Syt1^{-/-}$ (Fig. 7*C*; Spontaneous rate norm.: $Syt1^{+/+}$ 1 ± 0.11, n = 55/4, $Syt1^{+/+}{}_{1xRNA(Syt1)}$ 1.54 ± 0.16, n = 40/4, $p < 0.05$, $Syt1^{+/+}{}_{2xRNA(Syt1)}$ 1.67 ± 0.23, n = 35/4, $p < 0.05$, and $Syt1^{+/+}{}_{4xRNA(Syt1)}$ 2.4 ± 0.47, n = 41/4, $p < 0.0001$; Kruskal–Wallis test). Processes involved in evoked release showed an even higher sensitivity to SYT1 expression levels (Fig. 7*D–G*). The EPSC charge as well as the fast synchronous component of release was significantly reduced with all levels of SYT1 knock down tested (Fig. 7*D,E*; EPSC charge norm.: $Syt1^{+/+}$ 1 ± 0.11, n = 57/4, $Syt1^{+/+}{}_{1xRNA(Syt1)}$ 0.58 ± 0.1, n = 36/4, $p < 0.01$, $Syt1^{+/+}{}_{2xRNA(Syt1)}$ 0.36 ± 0.06, n = 39/4, $p < 0.0001$, and $Syt1^{+/+}{}_{4xRNA(Syt1)}$ 0.32 ± 0.05, n = 43/4, $p < 0.0001$; Kruskal–Wallis test; EPSC components: $Syt1^{+/+}$, slow 0.28 ± 0.02, fast 0.72 ± 0.02, n = 56/4, $Syt1^{+/+}{}_{1xRNA(Syt1)}$, slow 0.61 ± 0.06, fast 0.39 ± 0.06, n = 29/4, $p < 0.0001$,

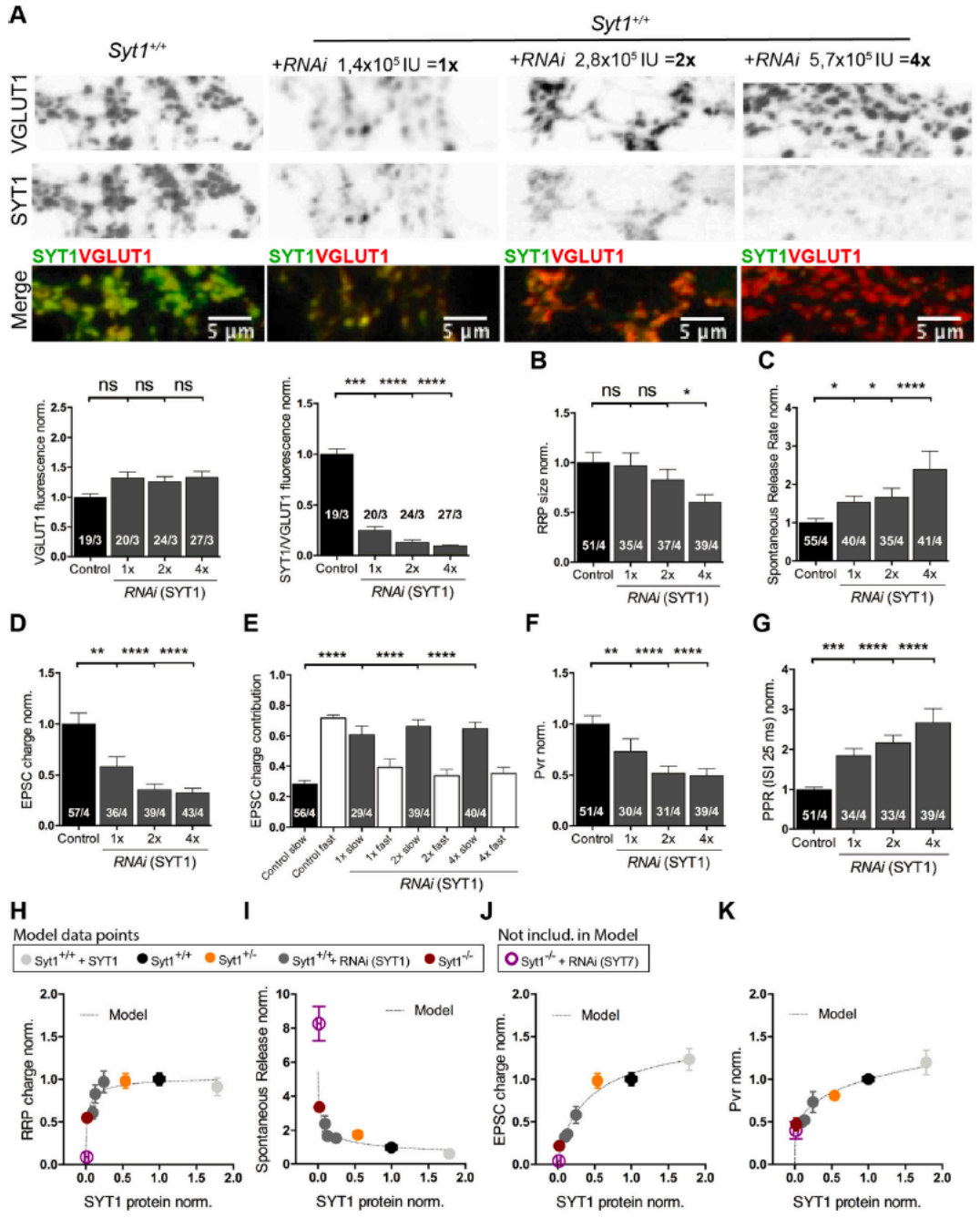

Figure 7. Dose dependence of Synaptotagmin-1 on neurotransmitter release functions. All immunocytochemistry and electrophysiological experiments were done from *Syt1*$^{+/+}$ hippocampal glutamatergic autaptic neurons at DIV15–21. ***A***, Representative images immunolabeled for VGLUT and SYT1, as in Figure 6, from *Syt1*$^{+/+}$ hippocampal glutamatergic autaptic neurons infected with a lentiviral vector expressing a scramble RNA (control) or increasing amounts of a *Syt1 RNAi*. Scale bar, 5 µm. Summary bar graphs of VGLUT1 fluorescence intensities at presynaptic terminal (left) and SYT1/VGLUT1 fluorescence intensities ratios normalized to *Syt1*$^{+/+}$ (right). ***B***, Plot of sucrose charges of Syt1$^{+/+}$ control and increasingly knock-down SYT1 autaptic neurons normalized to the average Syt1$^{+/+}$ control sucrose charge. ***C***, Summary bar graph of spontaneous release rate normalized to control *Syt1*$^{+/+}$. ***D***, Normalized bar graphs of the effect on evoked EPSC charge of titration of SYT1. ***E***, Bar graphs of the relative contribution of the synchronic and asynchronic components to the EPSC total charge transfer with different amount of

$Syt1^{+/+}{}_{2xRNA(Syt1)}$, slow 0.66 ± 0.04, fast 0.34 ± 0.04, $n = 39/4$, $p < 0.0001$, and $Syt1^{+/+}{}_{4xRNA(Syt1)}$, slow 0.65 ± 0.04, fast 0.35 ± 0.04, $n = 40/4$, $p < 0.0001$; one-way ANOVA test). Additionally, the release efficacy was significantly reduced in all knocked-down groups, demonstrated by a reduced Pvr and increased paired-pulse ratio compared with $Syt1^{+/+}$ (Fig. 7*F*,*G*; Pvr norm.: $Syt1^{+/+}$ 1 ± 0.08, $n = 51/4$, $Syt1^{+/+}{}_{1xRNA(Syt1)}$ 0.73 ± 0.12, $n = 30/4$, $p < 0.01$, $Syt1^{+/+}{}_{2xRNA(Syt1)}$ 0.52 ± 0.07, $n = 31/4$, $p < 0.0001$, and $Syt1^{+/+}{}_{4xRNA(Syt1)}$ 0.5 ± 0.07, $n = 39/4$, $p < 0.0001$; PPR40Hz, norm.: $Syt1^{+/+}$ 1 ± 0.05, $n = 51/4$, $Syt1^{+/+}{}_{1xRNA(Syt1)}$ 1.84 ± 0.18, $n = 34/4$, $p < 0.001$, $Syt1^{+/+}{}_{2xRNA(Syt1)}$ 2.16 ± 0.19, $n = 33/4$, $p < 0.0001$, and $Syt1^{+/+}{}_{4xRNA(Syt1)}$ 2.67 ± 0.35, $n = 39/4$, $p < 0.0001$; Kruskal–Wallis test). To exclude that these results might be because of the number of viral particles used, we manipulated SYT1 endogenous protein expression in $Syt1^{+/-}$ neurons (DIV15–21) using the same *Syt1 RNAi* construct (Fig. 8). We used half of the amount of viral infection units to reduce the expression to approximately the same levels as in the titration experiments in the $Syt1^{+/+}$ neurons (Fig. 8*A*; *VGLUT1* norm.: $Syt1^{+/-}$ 1 ± 0.08, $n = 20/3$, $Syt1^{+/-}{}_{1xRNA(Syt1)}$ 1.2 ± 0.16, $n = 17/3$, p = n.s., and $Syt1^{+/-}{}_{2xRNA(Syt1)}$ 0.93 ± 0.14, $n = 15/3$, p = n.s.; *SYT1/VGLUT1* norm.: $Syt1^{+/-}$ 1 ± 0.07, $n = 20/3$, $Syt1^{+/-}{}_{1xRNA(Syt1)}$ 0.32 ±0 .03, $n = 17/3$, $p < 0.0001$, and $Syt1^{+/-}{}_{2xRNA(Syt1)}$ 0.22 ± 0.02, $n = 15/3$, $p < 0.0001$; Kruskal–Wallis test). All electrophysiological parameters measured showed the same trend as our experiments performed on $Syt1^{+/+}$ neurons (Fig. 8*B*–*G*; RRP norm.: $Syt1^{+/+}$ 1 ± 0.16, $n = 21/3$, $Syt1^{+/+}{}_{1xRNA(Syt1)}$ 0.72 ± 0.14, $n = 22/3$, p = n.s., and $Syt1^{+/+}{}_{2xRNA(Syt1)}$ 0.5 ± 0.08, $n = 19/3$, $p < 0.05$; Spontaneous rate norm.: $Syt1^{+/+}$ 1 ± 0.25, $n = 15/3$, $Syt1^{+/+}{}_{1xRNA(Syt1)}$ 1.70 ± 0.39, $n = 18/3$, p = n.s., and $Syt1^{+/+}{}_{2xRNA(Syt1)}$ 3.21 ± 1.09, $n = 15/4$, $p < 0.05$; EPSC charge norm.: $Syt1^{+/+}$ 1 ± 0.15, $n = 29/3$, $Syt1^{+/+}{}_{1xRNA(Syt1)}$ 0.35 ± 0.06, $n = 23/3$, $p < 0.001$, and $Syt1^{+/+}{}_{2xRNA(Syt1)}$ 0.29 ± 0.05, $n = 21/4$, $p < 0.0001$; EPSC components: $Syt1^{+/+}$, slow 0.27 ± 0.04, fast 0.73 ± 0.04, $n = 21/3$, $Syt1^{+/+}{}_{1xRNA(Syt1)}$, slow 0.62 ± 0.08, fast 0.38 ± 0.08, $n = 18/3$, $p < 0.01$, and $Syt1^{+/+}{}_{2xRNA(Syt1)}$, slow 0.64 ± 0.07, fast 0.36 ± 0.07, $n = 20/3$, $p < 0.001$; Pvr norm.: $Syt1^{+/+}$ 1 ± 0.12, $n = 22/3$, $Syt1^{+/+}{}_{1xRNA(Syt1)}$ 0.62 ± 0.11, $n = 21/3$, $p < 0.05$, and $Syt1^{+/+}{}_{2xRNA(Syt1)}$ 0.57 ± 0.09, $n = 20/3$, $p < 0.01$; PPR40Hz, norm.: $Syt1^{+/+}$ 1 ± 0.09, $n = 27/3$, $Syt1^{+/+}{}_{1xRNA(Syt1)}$ 2.47 ± 0.28, $n = 22/3$, $p < 0.0001$, and $Syt1^{+/+}{}_{2xRNA(Syt1)}$ 2.41 ± 0.2, $n = 17/3$, $p < 0.0001$; Kruskal–Wallis test).

Our previous results suggest different relationships between synaptic functions and SYT1 expression levels. To understand these relationships in greater detail, we used our wide range of SYT1 protein level measurements at the presynaptic terminals of glutamatergic neurons (DIV15–21) to construct dose–response curves for the following different release properties: RRP size, spontaneous release rate, EPSC charge, and Pvr (Fig. 7*H*–*K*) and fitted our experimental data with a standard Hill equation (see above, Materials and Methods). To illustrate how SYT7 may potentially modulate the synaptic functions of SYT1 and to illustrate putative redundant function between SYT1 and SYT7, we included the normalized data from the SYT7 knock-down experiments performed on $Syt1^{-/-}$ neurons from Figure 4 (DIV15–16). However, the SYT7 data point was excluded from the curve fitting of the SYT1 expression–function relation.

First, the function of SYT1 in synaptic vesicle priming was least sensitive to protein loss (Fig. 7*H*) because even an 85% decrease in SYT1 protein expression at the synapse still displayed normal priming function. The best-fit value Kd for this parameter of 0.02 demonstrates that only when SYT1 is almost absent from the synapse, RRP size decreases (Fig. 7*H*). The function of SYT1 as a regulator of spontaneous NT release (Fig. 7*I*) showed a higher sensitivity to protein levels, leading to increased spontaneous release activity when the expression levels were reduced by 50% or more. Evoked release was the most sensitive to the variations of SYT1 expression, as reflected both by assessing EPSC charge and Pvr (Fig. 7*J*,*K*). The similarity of the EPSC charge and Pvr functions is not surprising as both reflect the role of SYT1 as calcium sensor for evoked release. The Kd value (0.47) for the EPSC charge fit indicates that genetic modification of SYT1 expression associated with allelic loss or gene duplication may lead to a more pronounced impact on evoked neurotransmitter release compared with SYT1 functions in vesicle priming or suppression of spontaneous release. The difference in the sensitivity and shape of the dose–function relationships (Fig. 7*H*,*I*) may also indicate that SYT1 performs its distinct functions with different molecular stoichiometries.

Discussion

In this study, we iterated the existence of three different synaptic functions performed by SYT1 using an autaptic primary neuronal culture model. Previous results concerning the ability of SYT1 to promote SV docking/priming (Geppert et al., 1994; Jorgensen et al., 1995; Reist et al., 1998; Nagy et al., 2006; Liu et al., 2009; Bacaj et al., 2013, 2015; Imig et al., 2014; Chang et al., 2018; Huson et al., 2020) and spontaneous release clamping (DiAntonio and Schwarz, 1994; Geppert et al., 1994; Littleton et al., 1994; Mackler et al., 2002; Yoshihara and Littleton, 2002; Chicka et al., 2008; Liu et al., 2009; Xu et al., 2009; Bacaj et al., 2013; Wierda and Sørensen, 2014) have been contradictory. Here, we demonstrated that SYT1 has a role in SV priming and clamping spontaneous release, which becomes essential over neuronal maturation. More mature SYT1-lacking hippocampal glutamatergic neurons showed a deficit in the RRP size and an increase in the spontaneous release rate, whereas early autaptic cultures did not (Table 1). Therefore, the time point and neuronal maturation stage at which experiments were performed could explain some discrepancies in previous work. What factor could compensate for SYT1 loss at early stages? We found that SYT7 has partially overlapping functions to SYT1 (Figs. 4, 7), largely consistent with previous results (Bacaj et al., 2013, 2015), and we conclude that at an early neuronal stage endogenous SYT7 protein could compensate for the loss of SYT1 in calcium-

←

SYT1 expression levels. ***F***, Vesicular release probability (Pvr) normalized to $Syt1^{+/+}$. ***G***, Normalized summary graph of the paired-pulse stimulation at 40 Hz. Statistical analysis was applied by Kruskal–Wallis test (*$p \leq 0.05$, **$p \leq 0.01$, ***$p \leq 0.001$, ****$p \leq 0.0001$). ns, Not significant. ***H–K***, Plots of RRP size (***H***), spontaneous release rate (***I***), EPSC charge (***J***), and Pvr (***K***) normalized to $Syt1^{+/+}$ against the SYT1/VGLUT1 fluorescence intensity ratios, obtained from the titration of SYT1 in autaptic neuronal cultures. To calculate SYT1 expression at the following synapses: $Syt1^{+/+}$ (black), $Syt1^{+/-}$ (orange), and $Syt1^{-/-}$ (burgundy), data (Fig. 5) and $Syt1^{-/-}$+ *RNAi* (SYT7, purple) data (Fig. 4, DIV16) were normalized to $Syt1^{+/+}$, subtracting the $Syt1^{-/-}$ expression levels in the different experiments. For $Syt1^{+/+}$ with the different amounts of *Syt1 RNAi* (dark gray) and $Syt1^{+/+}$ plus SYT1 (light gray) data (Figs. 6, 7) SYT1 expression levels were normalized to $Syt1^{+/+}$. All cells used for the model were from DIV15–21. $Syt1^{-/-}$ + *RNAi* (SYT7) cells were excluded from the model, but the group is represented in the plot to illustrate its functional relevance. The discontinuous gray line represent the curve fitting of the Hill function. All data shown represent mean ± SEM. Scale bars, 5 μm. For ***H–K*** data point values, see the table in Extended Data Figure 7-1.

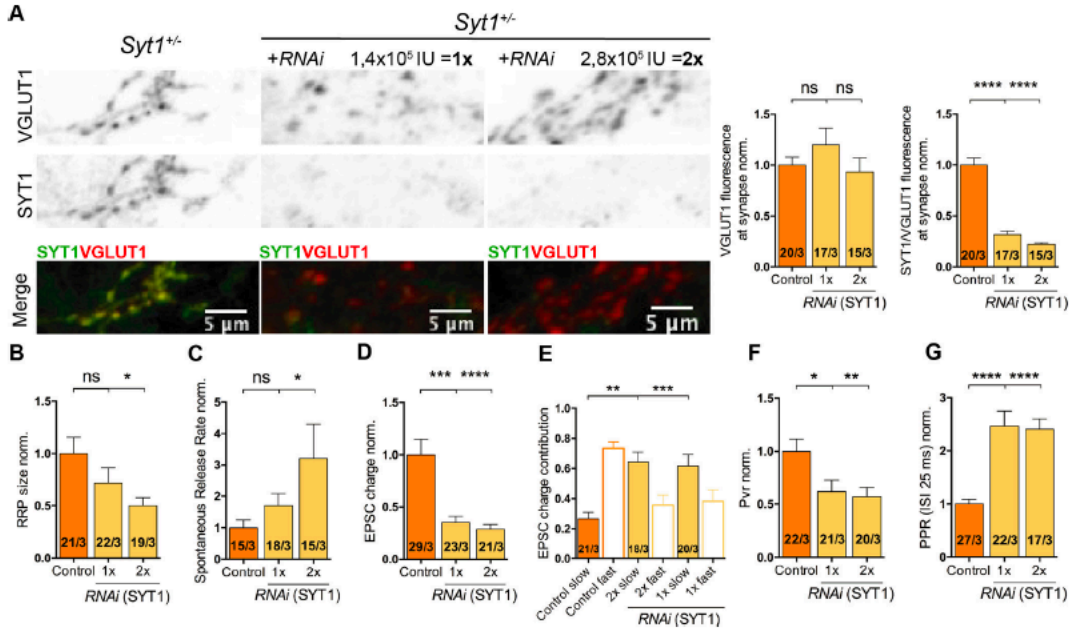

Figure 8. Impact of SYT1 RNAi viral titer on synaptic function in Synaptotagmin-$1^{+/-}$ neurons. All immunocytochemistry and electrophysiological experiments were done from $Syt1^{+/-}$ hippocampal glutamatergic autaptic neurons at DIV15–21. ***A***, Representative images of $Syt1^{+/-}$ cultured hippocampal glutamatergic neurons infected with a lentiviral vector expressing either RNAi or scramble RNA as control. Scale bar, 5 µm. Left, Summary bar graph of VGLUT1 fluorescence at synaptic terminal. Right, Summary bar graph showing SYT1/VGLUT1 fluorescence at the synaptic terminal normalized to $Syt1^{+/+}$. ***B***, Normalized bar graph of sucrose charge currents from autaptic cultures of $Syt1^{+/+}$ neurons with *scRNA* (control) or RNA interference. ***C***, Summary bar graph of spontaneous release rate. ***D***, Normalized bar graphs of the effect of RNA interference on evoked EPSC charge. ***E***, Bar graphs of the relative contribution of the synchronic and asynchronic components to the EPSC total charge transfer after a single AP with different amount of SYT1 levels. ***F***, Vesicular release probability (Pvr) was calculated by the ratio of evoked EPSC charge and RRP size and normalized to $Syt1^{+/+}$. ***G***, Normalized summary graph of the paired-pulse stimulation at 40 Hz. Statistical analysis was applied by Kruskal–Wallis test (*$p \leq 0.05$, **$p \leq 0.01$, ***$p \leq 0.001$, ****$p \leq 0.0001$). ns, Not significant. All data shown indicate mean ± SEM. Scale bars: 5 µm.

independent SV functions, such as priming and clamping of spontaneous release. When both proteins were missing at the presynaptic terminal, regardless of the culture stage, the pool of SVs was consistently reduced, and spontaneous release was significantly increased.

To dissect the specific interaction of the different mechanisms of NT release and to better understand the functions of SYT1 beyond that in synchronous release, we investigated the impact of systematically varying SYT1 expression levels on SV priming, clamping, and evoked release. SV priming was impaired only after a major drop in SYT1 concentration, suggesting that this process, although ultimately affected by the presence of SYT1, was relatively insensitive to changes in the number of SYT1 molecules. Varying SYT1 protein concentration also had a rather moderate impact on spontaneous release compared with the graded impact of varying SYT1 concentration on calcium-triggered release processes. Accordingly, heterozygotic $Syt1^{+/-}$ excitatory hippocampal neurons with a 50% reduction in SYT1 protein expression in the presynaptic terminal showed no effect on RRP size compared with WT SYT1 protein levels, whereas calcium-dependent release efficacy was impaired by the 50% SYT1 protein reduction in $Syt1^{+/-}$ neurons. Hence, when we applied a dose–response model to illustrate the sensitivity of the priming function to SYT1 expression, the curve described has a hyperbolic-like shape, where small amounts of SYT1 protein expression are sufficient to preserve maximum priming activity. Our overall analysis of the sensitivity of synaptic processes to SYT1 protein levels renders a rank where the least sensitive function is SV priming, followed by clamping of spontaneous and, finally, calcium-evoked release. Do the differences in sensitivity to SYT1 protein levels of these three synaptic processes indicate that SYT1 is involved in three consecutive and independent pathways? Because of the clear difference in sensitivity to expression levels for priming compare to evoked release, we think that SYT1 is affecting at least two pathways, in addition to its possible roles in endocytosis (Poskanzer et al., 2003; Yao et al., 2011; Liang et al., 2017). One hypothesis is that SYT1 undergoes different conformational stages to regulate different synaptic processes. Indeed, it has been suggested that SYT1 C2B domain-dependent oligomerization provides the molecular basis for SYT1 control of spontaneous and asynchronous release, and on influx of calcium SYT1 oligomers undergoes a conformational change from an SV clamping mode to a mode that allows the triggering of synchronous release (Bello et al., 2018; Tagliatti et al., 2020).

SYT1 protein level titration experiments not only revealed to us the distinct roles of SYT1 but may also could contribute to the understanding of the pathophysiological mechanisms underlying SYT1-associated neurodevelopmental disorders (Baker et al., 2015, 2018; Bradberry et al., 2020). In our study, we show that haploinsufficiency of SYT1 resulted in an aberrant spontaneous release phenotype and decreased release probability with additional consequences in short-term plasticity characteristics. If in patients with heterozygous SYT1 mutations, that have been

described to produce a SYT1 loss of function (Bradberry et al., 2020), a reduced SYT1 protein level occurs, this could lead to an enhanced spontaneous release or a decreased release probability and, ultimately, contribute to network disfunction. It has been reported that at least one of the *de novo SYT1* mutations ($SYT1_{M303K}$) is expressed at lower level than the endogenous wild-type protein and failed to localize at nerve terminals (Baker et al., 2018). Furthermore, two of the variants ($SYT1_{D304G}$ and $SYT1_{D366E}$) failed to efficiently relocalize to nerve terminals following stimulation (Baker et al., 2018). Although allelic expressivity may not explain the whole pathophysiology of the SYT1-associated neurodevelopmental disorder, it could exacerbate synaptic manifestations of individual SYT1 variants (Baker et al., 2018; Bradberry et al., 2020). In fact, a recent article revealed aberrant spontaneous NT release with some mutations from SNAP25-associated encephalopathies, indicating that when this form of release is affected it could result in developmental and epileptic encephalopathies (Alten et al., 2021). Conversely, our findings may indicate that the patient's pathophysiology that could derive from changes in the SYT1 expression levels are unlikely to be related to the priming of synaptic vesicles function at the presynaptic terminal.

Although the function of SYT1 as a calcium sensor for NT release has been extensively proven, the role for SYT7 is less clear. SYT7 has been suggested as the calcium sensor for asynchronous release (Maximov et al., 2008; Bacaj et al., 2013; Luo et al., 2015; Turecek and Regehr, 2018). SYT7 has also been proposed as a mediator of short-term facilitation of transmission during repetitive stimulation (Wen et al., 2010; Jackman et al., 2016; Chen et al., 2017b; Fujii et al., 2021), involving a mechanism of the concerted action of SYT7 with SYT1 on the fusion energy barrier (Schotten et al., 2015; Jackman and Regehr, 2017; Chen et al., 2017b; Huson et al., 2020). Supporting its role as a calcium sensor, SYT7 contributes to regulated exocytosis in chromaffin and pancreatic cells (Sugita et al., 2001; Shin et al., 2002; Schonn et al., 2008; Bendahmane et al., 2020). Additionally, it has been reported that SYT7 functions as a Ca^{2+} sensor for synaptic vesicle replenishment (Liu et al., 2014; Silva et al., 2021). In our study, we found no direct evidence that SYT7 is involved in regulating calcium-dependent release. However, we showed that suppressing SYT7 expression on $Syt1^{-/-}$ neurons further decreased evoked neurotransmitter release, and the analysis of RRP size reveals that the reduction in evoked response is rather because of the priming action of SYT7 and not because of an effect on calcium-triggered release. It is quite possible that putative competition between SYT1 and SYT7 may contribute to the observed modulation of calcium-triggered NT release.

This study could be framed within a series of works that aim to understand how synapses respond to the relative changes in the expression of different presynaptic components and to study the consequences on neurotransmission (Arancillo et al., 2013; Zarebidaki et al., 2020). Although mammalian and invertebrate loss-of-function mutants of presynaptic proteins continue to provide deep insights into their role in neurotransmitter release (Geppert et al., 1994; Schulze et al., 1995; Deng et al., 2011), a more sophisticated model where there is a control of protein amount has been proven to be a powerful approach. For instance, examining the Munc13-1 concentration dependency of priming showed that the Rab3-interacting molecule boosts the priming function of Munc13-1 (Zarebidaki et al., 2020). Another example comes from the study of Syntaxin-1 (Stx1), where to titrate down protein expression levels of Stx1 revealed that priming and vesicle fusion are likely governed by highly related mechanisms (Arancillo et al., 2013). Here, therefore, we advocate for this experimental approach as a useful way to obtain a quantitative understanding of how the different elements of the presynaptic release machinery differently regulate the steps involved in the process of synaptic transmission.

Overall, to precisely understand the distinct functions of SYT1, variations in the expression and balance between SYT1 and SYT7 at SVs and the PM over neuronal stages should be taken into consideration. Also, our data demonstrated that both SYT1 and SYT7 are capable of SV priming and clamping. Likely the efficient execution of these functions relies on their intermolecular interactions with both SNAREs and phospholipids from the PM (Perin et al., 1990; Chapman et al., 1995; Li et al., 1995; Sugita et al., 2002; Zhou et al., 2017). Further study on how the interplay between these proteins affects the intrinsic speed of neurotransmitter release is needed. Moreover, we emphasize that when studying disorders associated with presynaptic protein mutations, all these parameters could be conditioning the quantitative aspects of the cellular phenotype and, in turn, the pathophysiology that derives from it.

References

Alten B, Zhou Q, Shin OH, Esquivies L, Lin PY, White KI, Sun R, Chung WK, Monteggia LM, Brunger AT, Kavalali ET (2021) Role of aberrant spontaneous neurotransmission in SNAP25-associated encephalopathies. Neuron 109:59–72.e5.

Arancillo M, Min S-W, Gerber S, Münster-Wandowski A, Wu Y-J, Herman M, Trimbuch T, Rah J-C, Ahnert-Hilger G, Riedel D, Südhof TC, Rosenmund C (2013) Titration of Syntaxin1 in mammalian synapses reveals multiple roles in vesicle docking, priming, and release probability. J Neurosci 33:16698–16714.

Bacaj T, Wu D, Yang X, Morishita W, Zhou P, Xu W, Malenka RC, Südhof TC (2013) Asynchronous phases of neurotransmitter release. Neuron 80:947–959.

Bacaj T, Wu D, Burré J, Malenka RC, Liu X, Südhof TC (2015) Synaptotagmin-1 and -7 are redundantly essential for maintaining the capacity of the readily-releasable pool of synaptic vesicles. PLoS Biol 13: e1002267.

Baker K, Gordon SL, Grozeva D, Van Kogelenberg M, Roberts NY, Pike M, Blair E, Hurles ME, Chong WK, Baldeweg T, Kurian MA, Boyd SG, Cousin MA, Raymond FL (2015) Identification of a human synaptotagmin-1 mutation that perturbs synaptic vesicle cycling. J Clin Invest 125:1670–1678.

Baker K, Gordon SL, Melland H, Bumbak F, Scott DJ, Jiang TJ, Owen D, Turner BJ, Boyd SG, Rossi M, Al-Raqad M, Elpeleg O, Peck D, Mancini GMS, Wilke M, Zollino M, Marangi G, Weigand H, Borggraefe I, Haack T, et al. (2018) SYT1-associated neurodevelopmental disorder: a case series. Brain 141:2576–2591.

Bekkers JM, Stevens CF (1991) Excitatory and inhibitory autaptic currents in isolated hippocampal neurons maintained in cell culture. Proc Natl Acad Sci U S A 88:7834–7838.

Bello OD, Jouannot O, Chaudhuri A, Stroeva E, Coleman J, Volynski KE, Rothman JE, Krishnakumar SS (2018) Synaptotagmin oligomerization is essential for calcium control of regulated exocytosis. Proc Natl Acad Sci U S A 115:E7624–E7631.

Bendahmane M, Morales A, Kreutzberger AJB, Schenk NA, Mohan R, Bakshi S, Philippe JM, Zhang S, Kiessling V, Tamm LK, Giovannucci DR, Jenkins PM, Anantharam A (2020) Synaptotagmin-7 enhances calcium-sensing of chromaffin cell granules and slows discharge of granule cargos. J Neurochem 154:598–617.

Bradberry MM, Courtney NA, Dominguez MJ, Lofquist SM, Knox AT, Sutton RB, Chapman ER (2020) Molecular basis for synaptotagmin-1-associated neurodevelopmental disorder. Neuron 107:52–64.

Broadie K, Bellen HJ, DiAntonio A, Littleton JT, Schwarz TL (1994) Absence of synaptotagmin disrupts excitation-secretion coupling during synaptic transmission. Proc Natl Acad Sci U S A 91:10727–10731.

Brose N, Petrenko AG, Südhof TC, Jahn R (1992) Synaptotagmin: a calcium sensor on the synaptic vesicle surface. Science 256:1021–1025.
Chang S, Trimbuch T, Rosenmund C (2018) Synaptotagmin-1 drives synchronous Ca 2+ -triggered fusion by C 2 B-domain-mediated synaptic-vesicle-membrane attachment. Nat Neurosci 21:33–42.
Chapman ER, Davis AF (1998) Direct interaction of a Ca2+-binding loop of synaptotagmin with lipid bilayers. J Biol Chem 273:13995–14001.
Chapman ER, Hanson PI, An S, Jahn R (1995) Ca2+ regulates the interaction between synaptotagmin and syntaxin 1. J Biol Chem 270:23667–23671.
Chen C, Jonas P (2017) Synaptotagmins: that's why so many. Neuron 94:694–696.
Chen C, Arai I, Satterfield R, Young SM, Jonas P (2017a) Synaptotagmin 2 is the fast Ca2+ sensor at a central inhibitory synapse. Cell Rep 18:723–736.
Chen C, Satterfield R, Young SM, Jonas P (2017b) Triple function of Synaptotagmin 7 ensures efficiency of high-frequency transmission at central GABAergic synapses. Cell Rep 21:2082–2089.
Chicka MC, Hui E, Liu H, Chapman ER (2008) Synaptotagmin arrests the SNARE complex before triggering fast, efficient membrane fusion in response to Ca2+. Nat Struct Mol Biol 15:827–835.
Deng L, Kaeser PS, Xu W, Südhof TC (2011) RIM proteins activate vesicle priming by reversing autoinhibitory homodimerization of munc13. Neuron 69:317–331.
DiAntonio A, Schwarz TL (1994) The effect on synaptic physiology of synaptotagmin mutations in *Drosophila*. Neuron 12:909–920.
Fernandez I, Araç D, Ubach J, Gerber SH, Shin OH, Gao Y, Anderson RGW, Südhof TC, Rizo J (2001) Three-dimensional structure of the synaptotagmin 1 C2B-domain: synaptotagmin 1 as a phospholipid binding machine. Neuron 32:1057–1069.
Fernández-Chacón R, Königstorfer A, Gerber SH, García J, Matos MF, Stevens CF, Brose N, Rizo J, Rosenmund C, Südhof TC (2001) Synaptotagmin I functions as a calcium regulator of release probability. Nature 410:41–49.
Fujii T, Sakurai A, Littleton JT, Yoshihara M (2021) Synaptotagmin 7 switches short-term synaptic plasticity from depression to facilitation by suppressing synaptic transmission. Sci Rep 11:4059.
Geppert M, Archer BT, Südhof TC (1991) Synaptotagmin II: a novel differentially distributed form of synaptotagmin. J Biol Chem 266:13548–13552.
Geppert M, Goda Y, Hammer RE, Li C, Rosahl TW, Stevens CF, Südhof TC (1994) Synaptotagmin I: a major Ca2+ sensor for transmitter release at a central synapse. Cell 79:717–727.
Huson V, Meijer M, Dekker R, Veer MT, Ruiter M, van Weering J, Verhage M, Cornelisse LN (2020) Post-tetanic potentiation lowers the energy barrier for synaptic vesicle fusion independently of synaptotagmin-1. Elife 9:e55713.
Imig C, Min SW, Krinner S, Arancillo M, Rosenmund C, Südhof TC, Rhee JS, Brose N, Cooper BH (2014) The morphological and molecular nature of synaptic vesicle priming at presynaptic active zones. Neuron 84:416–431.
Jackman SL, Regehr WG (2017) The mechanisms and functions of synaptic facilitation. Neuron 94:447–464.
Jackman SL, Turecek J, Belinsky JE, Regehr WG (2016) The calcium sensor synaptotagmin 7 is required for synaptic facilitation. Nature 529:88–91.
Jorgensen EM, Hartwieg E, Schuske K, Nonet ML, Jin Y, Horvitz HR (1995) Defective recycling of synaptic vesicles in synaptotagmin mutants of *Caenorhabditis elegans*. Nature 378:196–199.
Katz B (1969) The release of neural transmitter substances. Springfield, IL: Thomas.
Kochubey O, Babai N, Schneggenburger R (2016) A synaptotagmin isoform switch during the development of an identified CNS synapse. Neuron 90:984–999.
Li C, Ullrich B, Zhang JZ, Anderson RGW, Brose N, Südhof TC (1995) Ca2+-dependent and -independent activities of neural and non-neural synaptotagmins. Nature 375:594–599.
Liang K, Wei L, Chen L (2017) Exocytosis, endocytosis, and their coupling in excitable cells. Front Mol Neurosci 10:109.
Littleton JT, Stern M, Perin M, Bellen HJ (1994) Calcium dependence of neurotransmitter release and rate of spontaneous vesicle fusions are altered in *Drosophila* synaptotagmin mutants. Proc Natl Acad Sci U S A 91:10888–10892.
Liu H, Dean C, Arthur CP, Dong M, Chapman ER (2009) Autapses and networks of hippocampal neurons exhibit distinct synaptic transmission phenotypes in the absence of synaptotagmin I. J Neurosci 29:7395–7403.
Liu H, Bai H, Hui E, Yang L, Evans CS, Wang Z, Kwon SE, Chapman ER (2014) Synaptotagmin 7 functions as a Ca2+-sensor for synaptic vesicle replenishment. Elife 3:e0152.
Lois C, Hong EJ, Pease S, Brown EJ, Baltimore D (2002) Germline transmission and tissue-specific expression of transgenes delivered by lentiviral vectors. Science 295:868–872.
Luo F, Bacaj T, Südhof TC (2015) Synaptotagmin-7 is essential for Ca2+-triggered delayed asynchronous release but not for Ca2+-dependent vesicle priming in retinal ribbon synapses. J Neurosci 35:11024–11033.
Mackler J, Drummond J, Loewen C, Robinson I, Reist N (2002) The C(2)B Ca(2+)-binding motif of synaptotagmin is required for synaptic transmission *in vivo*. Nature 418:340–344.
Marquèze B, Boudier JA, Mizuta M, Inagaki N, Seino S, Seagar M (1995) Cellular localization of synaptotagmin I, II, and III mRNAs in the central nervous system and pituitary and adrenal glands of the rat. J Neurosci 15:4906–4917.
Maximov A, Südhof TC (2005) Autonomous function of synaptotagmin 1 in triggering synchronous release independent of asynchronous release. Neuron 48:547–554.
Maximov A, Lao Y, Li H, Chen X, Rizo J, Sørensen JB, Südhof TC (2008) Genetic analysis of synaptotagmin-7 function in synaptic vesicle exocytosis. Proc Natl Acad Sci U S A 105:3986–3991.
Nagy G, Kim JH, Pang ZP, Matti U, Rettig J, Südhof TC, Sørensen JB (2006) Different effects on fast exocytosis induced by synaptotagmin 1 and 2 isoforms and abundance but not by phosphorylation. J Neurosci 26:632–643.
Nishiki TI, Augustine GJ (2004) Synaptotagmin I synchronizes transmitter release in mouse hippocampal neurons. J Neurosci 24:6127–6132.
Pang ZP, Sun J, Rizo J, Maximov A, Südhof TC (2006) Genetic analysis of synaptotagmin 2 in spontaneous and Ca 2+-triggered neurotransmitter release. EMBO J 25:2039–2050.
Perin MS, Fried VA, Mignery GA, Jahn R, Südhof TC (1990) Phospholipid binding by a synaptic vesicle protein homologous to the regulatory region of protein kinase C. Nature 345:260–263.
Poskanzer KE, Marek KW, Sweeney ST, Davis GW (2003) Synaptotagmin I is necessary for compensatory synaptic vesicle endocytosis *in vivo*. Nature 426:559–563.
Reist NE, Buchanan J, Li J, DiAntonio A, Buxton EM, Schwarz TL (1998) Morphologically docked synaptic vesicles are reduced in synaptotagmin mutants of *Drosophila*. J Neurosci 18:7662–7673.
Rizo J, Xu J (2015) The Synaptic vesicle release machinery. Annu Rev Biophys 44:339–367.
Rosenmund C, Stevens CF (1996) Definition of the readily releasable pool of vesicles at hippocampal synapses. Neuron 16:1197–1207.
Sabatini BL, Regehr WG (1999) Timing of synaptic transmission. Annu Rev Physiol 61:521–542.
Schonn JS, Maximov A, Lao Y, Südhof TC, Sørensen JB (2008) Synaptotagmin-1 and -7 are functionally overlapping Ca2+ sensors for exocytosis in adrenal chromaffin cells. Proc Natl Acad Sci U S A 105:3998–4003.
Schotten S, Meijer M, Walter AM, Huson V, Mamer L, Kalogreades L, Ter Veer M, Ruiter M, Brose N, Rosenmund C, Sørensen JB, Verhage M, Cornelisse LN (2015) Additive effects on the energy barrier for synaptic vesicle fusion cause supralinear effects on the vesicle fusion rate. Elife 2015:e05531.
Schulze KL, Broadie K, Perin MS, Bellen HJ (1995) Genetic and electrophysiological studies of drosophila syntaxin-1A demonstrate its role in non-neuronal secretion and neurotransmission. Cell 80:311–320.
Shin OH, Rizo J, Südhof TC (2002) Synaptotagmin function in dense core vesicle exocytosis studied in cracked PC12 cells. Nat Neurosci 5:649–656.
Silva M, Tran V, Marty A (2021) Calcium-dependent docking of synaptic vesicles. Trends Neurosci 44:579–592.
Sugita S, Han W, Butz S, Lao Y, Liu X, Ferna R, Su TC, Hines H, Na B (2001) Synaptotagmin VII as a plasma membrane Ca(2+) sensor in exocytosis. Neuron 30:459–473.
Sugita S, Shin OH, Han W, Lao Y, Südhof TC (2002) Synaptotagmins form a hierarchy of exocytotic Ca(2+) sensors with distinct Ca(2+) affinities. EMBO J 21:270–280.

Sutton RB, Davletov BA, Berghuis AM, Südhof TC, Sprang SR (1995) Structure of the first C2 domain of synaptotagmin I: a novel Ca2+/phospholipid-binding fold. Cell 80:929–938.

Tagliatti E, Bello OD, Mendonça PRF, Kotzadimitriou D, Nicholson E, Coleman J, Timofeeva Y, Rothman JE, Krishnakumar SS, Volynski KE (2020) Synaptotagmin 1 oligomers clamp and regulate different modes of neurotransmitter release. Proc Natl Acad Sci U S A 117:3819–3827.

Turecek J, Regehr WG (2018) Synaptotagmin 7 mediates both facilitation and asynchronous release at granule cell synapses. J Neurosci 38:3240–3251.

Watanabe S, Trimbuch T, Camacho-Pérez M, Rost BR, Brokowski B, Söhl-Kielczynski B, Felies A, Davis MW, Rosenmund C, Jorgensen EM (2014) Clathrin regenerates synaptic vesicles from endosomes. Nature 515:228–233.

Wen H, Linhoff MW, McGinley MJ, Li GL, Corson GM, Mandel G, Brehm P (2010) Distinct roles for two synaptotagmin isoforms in synchronous and asynchronous transmitter release at zebrafish neuromuscular junction. Proc Natl Acad Sci U S A 107:13906–13911.

Wierda KDB, Sørensen JB (2014) Innervation by a GABAergic neuron depresses spontaneous release in glutamatergic neurons and unveils the clamping phenotype of synaptotagmin-1. J Neurosci 34:2100–2110.

Xu J, Pang ZP, Shin OH, Südhof TC (2009) Synaptotagmin-1 functions as a Ca2+ sensor for spontaneous release. Nat Neurosci 12:759–766.

Xue M, Ma C, Craig TK, Rosenmund C, Rizo J (2008) The Janus-faced nature of the C(2)B domain is fundamental for synaptotagmin-1 function. Nat Struct Mol Biol 15:1160–1168.

Xue M, Reim K, Chen X, Chao H, Deng H, Rizo J, Brose N, Rosenmund C (2007) Distinct domains of complexin I differentially regulate neurotransmitter release. Nat Struct Mol Biol 14:949–958.

Yao J, Kwon SE, Gaffaney JD, Dunning FM, Chapman ER (2011) Uncoupling the roles of synaptotagmin I during endo-and exocytosis of synaptic vesicles. Nat Neurosci 15:243–249.

Yoshihara M, Littleton JT (2002) Synaptotagmin functions as a calcium sensor to synchronize neurotransmitter release. Neuron 36:897–908.

Zarebidaki F, Camacho M, Brockmann MM, Trimbuch T, Herman MA, Rosenmund C (2020) Disentangling the roles of RIM and Munc13 in synaptic vesicle localization and neurotransmission. J Neurosci 40:9372–9385.

Zhou Q, Zhou P, Wang AL, Wu D, Zhao M, Südhof TC, Brunger AT (2017) The primed SNARE–complexin–synaptotagmin complex for neuronal exocytosis. Nature 548:420–425.

Figure 7-1. Values corresponding to Figure 7H-K.

H		SYT1 expression norm.		RRP norm.			I	SYT1 expression norm.		Spontaneous Release norm.	
Syt1+/+		1,00	0,08	1	0,072	Syt1+/+		1,00	0,08	1,000	0,079
Syt1+/-		0,54	0,04	0,9808	0,087	Syt1+/-		0,54	0,04	1,749	0,205
Syt1-/-		0,02	0,02	0,5469	0,047	Syt1-/-		0,02	0,02	3,363	0,326
Syt1+/+	1x *RNAi (SYT1)*	0,25	0,04	0,9697	0,127	Syt1+/+	1x *RNAi (SYT1)*	0,25	0,04	1,539	0,163
	2x *RNAi (SYT1)*	0,13	0,02	0,8282	0,107		2x *RNAi (SYT1)*	0,13	0,02	1,666	0,230
	4x *RNAi (SYT1)*	0,10	0,01	0,6067	0,075		4x *RNAi (SYT1)*	0,10	0,01	2,391	0,474
Syt1+/+	1x SYT1 *iRNA (SYT7)*	1,78	0,06	0,9109	0,103	Syt1+/+	1x SYT1 *iRNA (SYT7)*	1,78	0,06	0,622	0,088
Syt1-/-		0,01	0,03	0,08801	0,016	Syt1-/-		0,01	0,03	8,260	1,008

J		SYT1 expression norm.		EPSC charge norm.			K	SYT1 expression norm.		Pvr norm.	
Syt1+/+		1,00	0,08	1	0,076	Syt1+/+		1,00	0,08	1,000	0,054
Syt1+/-		0,54	0,04	0,9808	0,087	Syt1+/-		0,54	0,04	0,808	0,059
Syt1-/-		0,02	0,02	0,2176	0,023	Syt1-/-		0,02	0,02	0,470	0,078
Syt1+/+	1x *RNAi (SYT1)*	0,25	0,04	0,5809	0,099	Syt1+/+	1x *RNAi (SYT1)*	0,25	0,04	0,731	0,124
	2x *RNAi (SYT1)*	0,13	0,02	0,3553	0,056		2x *RNAi (SYT1)*	0,13	0,02	0,520	0,065
	4x *RNAi (SYT1)*	0,10	0,01	0,3208	0,05		4x *RNAi (SYT1)*	0,10	0,01	0,495	0,066
Syt1+/+	1x SYT1 *iRNA (SYT7)*	1,78	0,06	1,23	0,129	Syt1+/+	1x SYT1 *iRNA (SYT7)*	1,78	0,06	1,196	0,144
Syt1-/-		0,01	0,03	0,03991	0,007	Syt1-/-		0,01	0,03	0,399	0,102

My curriculum vitae does not appear in the electronic version of my paper for reasons of data protection.

My curriculum vitae does not appear in the electronic version of my paper for reasons of data protection.

List of Publications

2022

- **Bouazza-Arostegui B**, Camacho M, Brockmann MM, Zobel S, Rosenmund C. Deconstructing Synaptotagmin-1's Distinct Roles in Synaptic Vesicle Priming and Neurotransmitter Release. J Neurosci. 2022 Apr 6;42(14):2856-2871. doi: 10.1523/JNEUROSCI.1945-21.2022. Epub 2022 Feb 22. PMID: 35193927.

2019

- Brockmann MM, Maglione M, Willmes CG, Stumpf A, **Bouazza BA**, Velasquez LM, Grauel MK, Beed P, Lehmann M, Gimber N, Schmoranzer J, Sigrist SJ, Rosenmund C, Schmitz D. RIM-BP2 primes synaptic vesicles *via* recruitment of Munc13-1 at hippocampal mossy fiber synapses. Elife. 2019 Sep 19;8:e43243. doi: 10.7554/eLife.43243. PMID: 31535974; PMCID: PMC6752948.
- Manrique-Castano D, van Casteren A, **Bouazza-Arostegui B**, MacDonald DI, Pfeiffer P. ENCODS: A novel initiative to inspire young neuroscientists. Eur J Neurosci. 2019 May;49(9):1077-1083. doi: 10.1111/ejn.14428. PMID: 31038241.

2016

- Richter F, Fonfara I, **Bouazza B**, Schumacher CH, Bratovič M, Charpentier E, Möglich A. Engineering of temperature- and light-switchable Cas9 variants. Nucleic Acids Res. 2016 Nov 16;44(20):10003-10014. doi: 10.1093/nar/gkw930. Epub 2016 Oct 15. PMID: 27744350; PMCID: PMC5175372.

Acknowledgments

I would like to express my deepest gratitude to my doctoral supervisor Prof. Christian Rosenmund for his invaluable mentoring, support, and accepting me as a PhD student in his laboratory. I am deeply indebted to my co-supervisor Dr. Marcial Camacho for his guidance and unparalleled support. I am also grateful to my co-supervisor Dr. Marisa Brockmann for her constructive advice and support. I would like to extend my sincere thanks to all of my colleagues and friends in the Rosenmund laboratory for their insightful suggestions during the lab meetings. I would like to acknowledge the technical assistance of Berit Söhl-Kielczynski, Bettina Brokowski, Katja Pötschke, Heike Lerch and Anne Hahmann. Special thanks to my partner for her encouragement. Finally, the completion of my dissertation would not have been possible without the love and unconditional support of my mother and father.